ON THE CONTROL OF COLLAGEN FIBRIL ORGANIZATION AND MORPHOLOGY

A dissertation presented

by

Nima Saeidi

to

The Graduate School of Engineering

in partial fulfillment of the requirements
for the degree of

Doctor of Philosophy

in the field of

Mechanical Engineering

Northeastern University
Boston, Massachusetts

August 2009

ABSTRACT

ON THE CONTROL OF COLLAGEN FIBRIL ORGANIZATION AND MORPHOLOGY

Nima Saeidi

Department of Mechanical and Industrial Engineering

Doctor of Philosophy

Despite the extensive research on the *in vitro* engineering of load-bearing tissues (i.e. ligament, tendon and cornea) there has been only limited clinical success. Load-bearing biological structures in vertebrate animals have high mechanical strength which is generally the result of their highly-organized extracellular matrix (ECM). Due to its biocompatibility and ability to form polymerized gels around cells in culture, collagen is an attractive candidate for both *de novo* tissue engineering and as a scaffolding material. 2 or 3D networks of collagen (most possessing little organization) have been extensively used in tissue engineering applications but have not performed well when the target tissue possesses highly-organized ECM. To overcome this limitation, investigators have employed physical or chemical manipulations of collagen molecules to produce 2D aligned arrays of collagen fibrils for use as guiding templates to influence cell behavior and to control subsequent matrix organization. Unfortunately, the organization of the cells and the synthesized ECM is only influenced over short distances from the organized template. Thus there is a need for scaffolds which are organized in 3-dimensions.

The goal this thesis was to investigate the methods to gain control over organization and ultrastructure of collagen fibrils during self-assembly *de novo*. In chapter two, the real time dynamics of shear-induced collagen self-assembly was investigated. Thin layers of collagen fibrils were produced by subjecting the solution of collagen molecules to shearing flow. The effects of both simple shear flow and confined shear flow on the organization of the collagen fibrils were studied. In the next chapter, by taking advantage of the "liquid crystalline" properties of collagen molecules, highly-organized lamellae of collagen fibrils were produced from a highly-concentrated solution of collagen molecules. Lastly, the mutability of collagen fibrils subsequent to their association with proteoglycans (PGs) and the results of the chemical interaction on matrix stability were investigated.

The driving hypothesis behind this thesis is that ECM is a dynamic, energy driven system. The interactions between collagen molecules and collagen aggregates with other ECM macromolecules (e.g. proteoglycans) progresses such that the energy landscape of the system decreases, resulting in more stable structures. Through gaining control over these interactions we could produce lamellae of collagen fibrils with organization similar to load-bearing tissues.

Acknowledgement

This thesis is the last chapter of my 22 years of academic study book. Many have supported me during this long journey to whom I will always remain deeply grateful forever. At the top of this stand my parents, my wife Pegah and my brother. Their constant support and encouragement has been a great source of energy for during all these years. They never stopped believing me and my successes has always been their wish. I love you guys and I will never forget what you have done for me. I am especially grateful to Pegah for completely supporting me in the last six years. For managing our life single handed and putting up with all working weekends and my working late hours.

My greatest appreciation goes to my advisor Dr. Jeffrey Ruberti for giving me an opportunity to pursuit my studies passionately in his laboratory. Thank you for believing in me, a Thermofluid engineer, and letting me into your lab. I have enjoyed every minute of our scientific discussions and I didn't learn from anything else as much as my discussions with you. Thank you for teaching me how to do research and how to be a good scientist. How to be a good man and how to be a good advisor. And, thank you for showing me what is a good science (although it made my job for finding a postdoc very difficult!). You will always be my mentor.

I am also grateful to my labmates for making my research fruitful and enjoyable. Among them, to Suzi for listing to all my complaints and for all your sympathies. Our morning coffees were the highlight of my days and I will miss them. And I would like to acknowledge my current or past labmates with whom I collaborated on projects and I enjoyed working with them: Ramin, Katie, Anirudha, Amit, Ericja, and JJ.

And at the end, I acknowledge every single person who taught me something including all my teachers and my friends, especially Shervin, Kaveh, and Hamid.

Nima
August 2009

Table of Contents

List of Figures

Chapter 1

Introduction and Background

Introduction

Cells in metazoans are embedded in a complex network of macromolecules known as the extracellular matrix (ECM). The ECM provides a framework within which cells can attach and spread. Cell signaling, communication and motility may be achieved through cell-matrix adhesion and interaction (Giancotti 1997; Rosso, Giordano et al. 2004). For *in vitro* tissue engineering, mounting evidence suggests that it is necessary to provide the cells with structural environments (topology/rigidity/organization) similar to that which is experienced *in vivo*.

In animal tissues, load-bearing ECM typically comprises 3D arrangements of collagen fibrils in which, the collagen organization reflects the tissue's mechanical function. For example, to carry the tensile load in tendon, collagen fibrils are arranged into long and parallel fascicles. In anulus fibrosus in the spine, aligned arrays of collagen fibrils are arranged in a nematic stack where the angle between lamellae is ~60° (Cassidy, Hiltner et al. 1989; Wagner and Lotz 2004). The stack of lamellae wrap concentrically to form nested cylindrical sections with their central axis oriented in the superior/inferior direction. Such an arrangement is optimized to carry both torsional and circumferential (tensile) loads (Cassidy, Hiltner et al. 1989). In the cornea, which is one of the most highly-organized tissues in vertebrate animals, aligned fibrillar arrays of monodisperse

diameter collagen fibrils are arranged in a nematic stack of alternating lamellae. The lamellae form a series of nested spherical shells which resist the biaxial tension produced by pressure within the ocular globe. In humans, adjacent nested lamellae are typically oriented at right angles.

To date, 28 genetically different types of collagen are known (Kadler, Baldock et al. 2007). Fibril forming collagens (i.e. I-III, V, XI) are the main load-bearing components of the ECM which self-assemble into 67 nm cross striated (D-banding) fibrils. *In vivo*, fibril forming collagens are synthesized as soluble procollagen. To start the fibrillogenesis, the globular N- and C- terminus of procollagen undergo an enzymatic cleavage (for review (Kadler, Holmes et al. 1996; Kadler 2004)). It should be mentioned that fibril formation could also proceed with the N- terminus intact. The members of this group spontaneously assemble into fibers, fibrils, and bundles: bundles are eventually assembled into the higher order lamellae (Birk and Trelstad 1984). *In vitro*, increasing the temperature of a neutralized solution of acid or pepsin extracted type I collagen molecules results in the self-assembly of the monomers into an isotropic fibrillar network. *In vitro* studies have shown that collagen self-assembly is an entropy-driven process in which the molecules reach a lower energy state by loss of solvent molecules from their surface (Kadler, Hojima et al. 1987). As early as the 1950's, the ability of extracted collagen monomers to self-assemble into native-like fibrils was investigated extensively (Highberger, Gross et al. 1951; Gross, Highberger et al. 1954; Gross 1958; Gross 1958). These initial studies were both quantitatively and morphologically advanced and have provided the basis for numerous investigations which have probed the assembly

kinetics and resulting morphology of collagen assembled *ex vivo*. This rather large body of work is summarized by Prockop and Hulmes 1994 (Prockop and Hulmes 1994).

The use of self-assembled, reconstituted fibrillar collagen as a scaffold for tissue engineering (principally due to its natural biocompatibility *in vivo*) first began in the 1960s (Konigsberg 1963; Hauschka and Konigsberg 1966). Since then reconstituted type I collagen has been extensively used as a substrate for cell culture with the results of these studies indicating that collagen substrates enhance cell signaling, proliferation, and further collagen synthesis (Hauschka and Konigsberg 1966; Martin and Kleinman 1981; Kleinman, Luckenbill-Edds et al. 1987). In tissue engineering investigations, researchers typically seed the cells of interest into either 2D or 3D networks of randomly assembled collagen fibrils. Although promising results have been obtained for the engineering of structures which possess a low level of ECM organization (e.g. skin) (Naughton 2002), there has been only limited success when the target tissues comprise highly-organized ECMs (e.g. tendon, ligament, cornea and bone). This has lead to the realization that *a priori* organizational cues (such as preorganized scaffold) may be critical to the engineering of load-bearing tissue (Ruberti and Zieske 2008).

Compared to the investigations on the random assembly of collagen, methods designed to "influence" organization of self-assembling collagen fibrils have received much less attention. Gravity derived drainage (Elsdale and Bard 1972), electro-spinning (Matthews, Wnek et al. 2002), strong magnetic fields (Dickinson, Guido et al. 1994; Dubey, Letourneau et al. 1999; Dubey, Letourneau et al. 2001), electrical gradients (Benjamin, Pawlowski et al. 1964), flows through a microfluidic channel (Lee, Lin et al. 2006; Lanfer, Freudenberg et al. 2008), a combination of fluid flow and magnetic field

(Guo and Kaufman 2007), dip-pen nanolithography (Wilson, Martin et al. 2001), and even freezing and thawing (Faraj, van Kuppevelt et al. 2007) were among the methods employed to influence collagen fibril organization during self-assembly. Though great progress has been made in controlling collagen organization, most of these methods are performed in a non physiological and harsh environment (except magnetic field) to influence collagen self-assembly. In addition, they are not capable of producing highly organized arrays of collagen fibrils with ultra-structures similar to native collagen fibrils. In general, the kinetics of collagen polymerization during influenced assembly has been neglected.

The interaction of collagen molecules with proteoglycans and its effects on the morphology of the resulting collagen fibrils has been widely investigated. Both *in vivo* and *in vitro* studies have revealed that when proteoglycans are introduced to the collagen molecules prior to fibrillogenesis, they influence the diameter and D-banding of the resulting fibrils. There is also mounting evidence that proteoglycans are able to interact with collagen molecules after the fibrils are formed. This could be potentially a very significant concept that reintroduces the ECM as an active, dynamic, and mutable energy driven system.

The focus of this thesis is to explore methods to gain control over the organization and morphology of the collagen fibrils during the self-assembly process. In addition the mutability and energetic interactions of collagen fibrils with proteoglycans and glycosaminoglycans has been investigated. Due to the large number of topics covered in this thesis, this chapter only covers the background for the topics and concepts that are

common in all the chapters. In addition, there is an introduction at the beginning of each chapter that provides a detailed background related to the topic covered in the chapter.

Background

1.1. Collagen Significance and Structure

1.1.1. Collagen Structure

In vivo, collagen molecules are secreted by fibroblasts in the form of soluble procollagen. Procollagen is mostly composed of a linear helical domain (300nm length and 1.5nm diameter) flanked by two globular regions (N- and C- propeptides, Figure 1-1). The molecular structure of collagen which was first explained by Ramachandran and Kartha (Ramachandran and Kartha 1954; Ramachandran and Kartha 1955; Ramachandran 1956; Ramachandran and Sasisekharan 1961) is composed of three left handed polypeptide (α chains) that are wound together to form a right handed helix. The amino acid backbone of the α-chains have a repeating form of Gly-X-Y in which X and Y in most cases are tertiary amides of L-proline and 4(R)-hydroxy-L-proline, respectively (van der Rest and Garrone 1991). Glycine, the smallest amino acid in nature, is essential for collagen stability. It is small enough to fit in the space between proline and hydroxyproline enabling it to form a hydrogen bond (through its NH- group) with the CO- group of the proline (or any amino acid in the X- position) in the neighboring α-chains (Engel and Bächinger 2005).

The globular N- and C- propeptides attached to each end of tropocollagen occupy a large space around the molecules preventing the self-assembly of the molecules. It has been shown that the cleavage of these regions is necessary for the self-assembly of the molecules into the fibrils with morphologies similar to the native collagen fibril

(Kuznetsova and Leikin 1999). The N- and C- propeptidases which are members of a group of zinc metalloproteinases enzymes moderate cleavage of the propeptides (Leung, Fessler et al. 1979; Hulmes 2008).

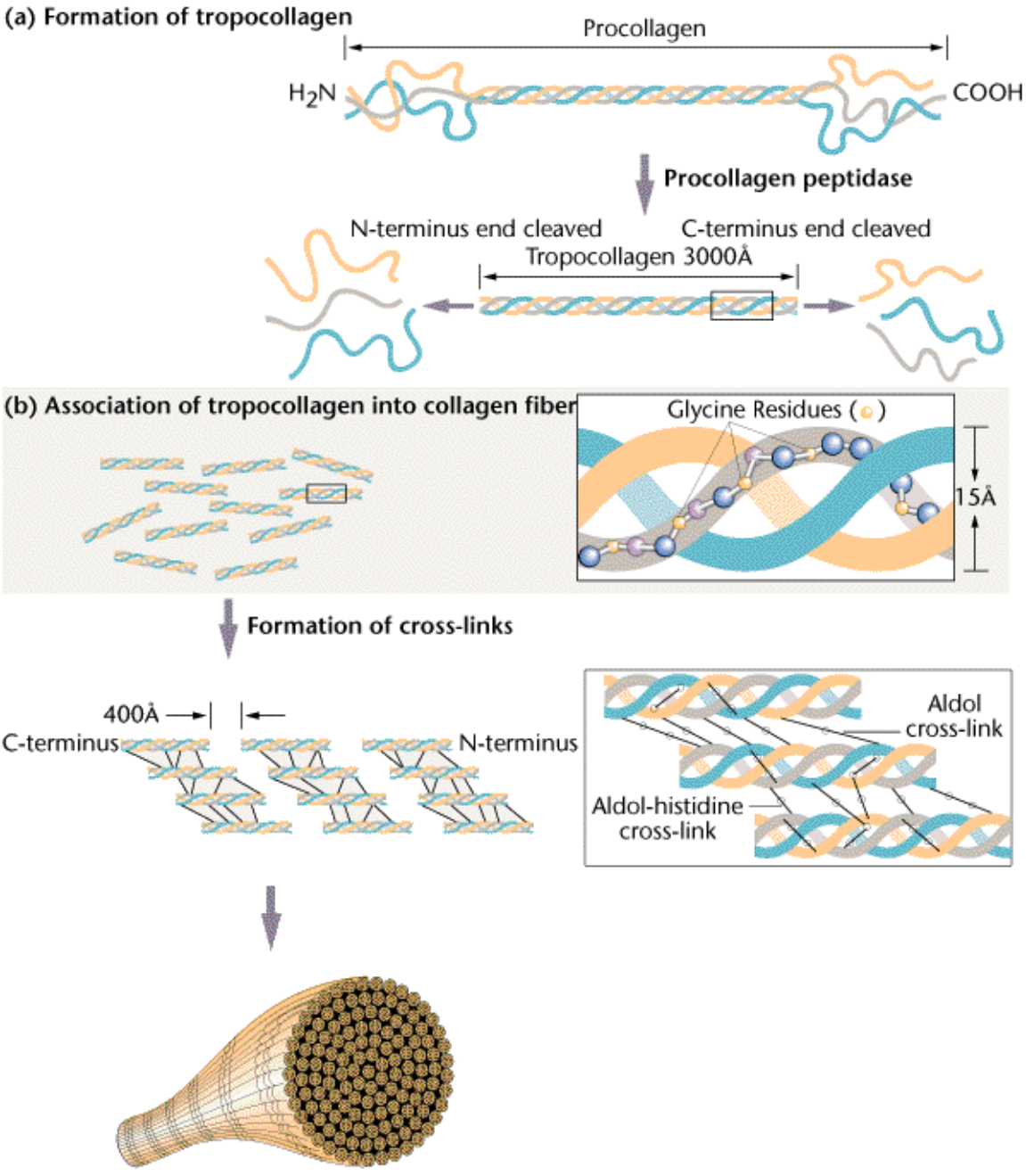

Figure 1-1: Collagen molecules secretion and self-assembly into fibrils (Klug, Cummings et al. 1997)

In vitro studies of the enzymatic cleavage of procollagen and self-assembly have shown that removal of the C-terminal is necessary for self-assembly. In contrast, pC-collagen (procollagen with its N- terminal removed) can still form fibrils. However, the diameter of fibrils formed from pC-collagens is significantly smaller than the diameter of the fibrils formed from collagen molecules (Fleischmajer, Timpl et al. 1981; Fleischmajer, Perlish et al. 1987; Mellor, Atkins et al. 1990). It is possible that the presence of the N- terminals prevents the excessive lateral self-assembly of the molecules, resulting in the smaller collagen fibrils (Kadler, Holmes et al. 1996). Evolutionary studies of collagen molecules have revealed that the C-terminal has been present in the collagen structure since the formation of this molecule. In contrast, the N-terminal is formed in the later stages of evolution (Exposito, Cluzel et al. 2002). Therefore, it has been suggested that the formation of N-propeptide is one of the methods that evolution uses to control fibril diameter. The enzymatic cleavage of propeptide domains of a procollagen exposes the telo-peptide regions of the molecules (i.e. telo-collagen). Due to the existence of C- and N- telo-peptides collagen molecules are bipolar. The telo-peptides contain the residues capable of forming irreversible covalent bonds with the helical domains of neighboring collagen molecules within a fibril (Eyre, Paz et al. 1984) resulting in a more stable fibril.

1.1.2. Origin of Fibrillar Striation

Native collagen fibrils are best characterized by their ~67 nm striations (D-banding, Figure 1-2) which are the result of the precise lateral arrangement of the molecules within a fibril. Figure 1-3 is a schematic of the radial packing of the molecules in a fibril's cross-section. The width of the D-band and its existence is due to the gap-overlap patterns between head-to-end arrangement of the lateral fibrils. Since the patterns were first observed using electron microscopy, it was initially believed that the D-banding is the result of the change in the molecular structure of the collagen monomers at the N- and C- terminal (existence of electron dense residues) and hence the patterns are only a chemical pattern. However, the situations are also seen in the quick-freeze/deep-etch microscopy (a non staining EM method), which indicates that the D-banding is the result of a change in the geometry of the fibrils (e.g. diameter) in the length of the molecules.

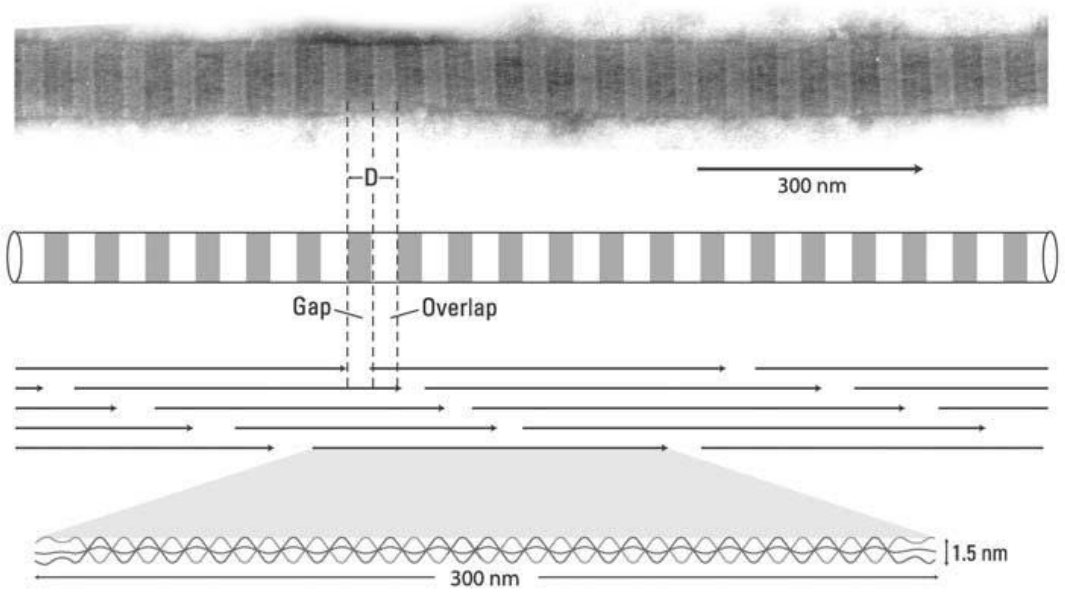

Figure 1-2: Longitudinal arrangement of the molecules in a collagen fibril. TEM micrograph of a negatively stained collagen fibril from fowl tendon and axial arrangement of the molecules in 2D (Birk and Bruckner 2005)

The explanation of the molecular arrangement in 3D (e.g. lateral arrangement of the molecules perpendicular to the long axis of a fibril) which gives rise to the formation of D-banding has proven to be very difficult and has been the topic of extensive research for the last few decades (for review (Ottani, Martini et al. 2002; Wess 2008)). The models were first developed based on the patterns observed in positive or negative staining TEM, which gave rise to the positional resolution of the individual residues. However, this method relies on the arrangement of molecules within a few outer layers of the fibrils stained and imaged with the TEM techniques, which provides very little information about the inner core of the fibrils. These models are mostly based on a crystalline arrangement of the molecules in the cross section of a fibril. Development of the X-ray diffraction methods and the diffuse equatorial scattering perpendicular to the long axis of the fibrils, which is an indication of liquid-like short-range order in the lateral packing did not agree with the solid crystalline structure. In addition, the data from Nuclear Magnetic Resonance (NMR) indicate that there is a considerable azimuthal mobility of the molecules within fibrils. In an elegant study Hulmes et. al. simulated different molecular packing structures previously proposed for collagen fibrils based on an energy minimization method (Hulmes, Wess et al. 1995). Furthermore, they produced the Fourier transform of the resulting hypothetical fibril and compared it with the X-ray diffraction patterns from native collagen fibrils. Their results indicate that most of the models account for only one of the long –range (axial crystalline order) or short-range (liquid-like order) and therefore, they are not completely accurate. Therefore, they proposed a new model based on the concentric ring and spiral arrangement with radial nearest-neighbor contacts. This molecular arrangement which features both liquid-like

and crystalline arrangment demonstrates a Fourier transform pattern similar to the observed equatorial x-ray diffraction data from native collagen fibrils (Figure 1-3).

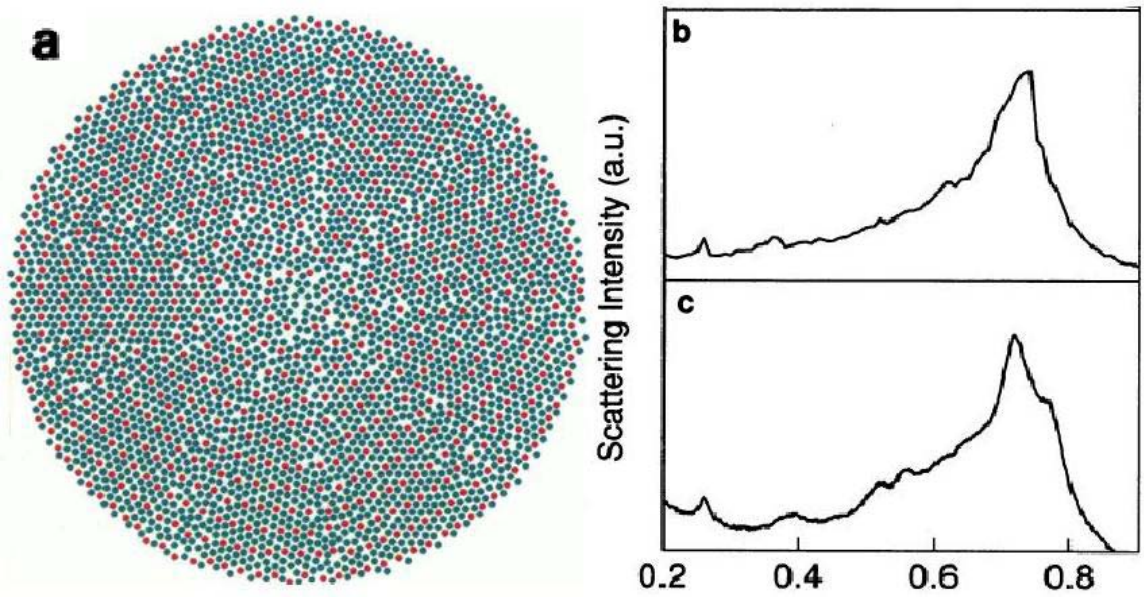

Figure 1-3: Monomer packing in a collagen fibril in a cross-section. (a) arrangement of the molecules and resulting Fourier transform from the model proposed by Hulmes et. al. (Hulmes, Wess et al. 1995). Red indicates one of the molecules in the overlap region. (b), Fourier transform of the structure perpendicular to the axis of the fibril, which is in great agreement with the X-ray scattering from a rat tail tendon (b) (Hulmes, Wess et al. 1995).

1.2. Collagen Self-assembly and Organization

1.2.1. Control of Collagen Organization in Vivo

As mentioned before, *in vivo,* collagen fibrils are assembled into matrices with a variety of organizations and ultrastructures (Figure 1-4). Despite the extensive amount of research on the details of collagen self-assembly, the process through which the higher order of organization is produced *in vivo* and during development is still not clear.

Two theories have been proposed to explain the process. The first theory, known

as the fibripositor theory, is based on the role that fibroblasts play in organizing collagen fibrils (Trelstad and Hayashi 1979; Birk and Trelstad 1984). According to this theory, fibroblast cells divide the extracellular matrix into several compartments, called fibripositors (Figure 1-5 and Figure 1-6). Using these compartments, cells exert control over the assembly of the molecules into fibrils and transformation of the fibers into bundles and eventually organized lamellae. Also, cells use the fibripositors to physically position and align bundles in the extracellular matrix. Therefore, this theory suggests that

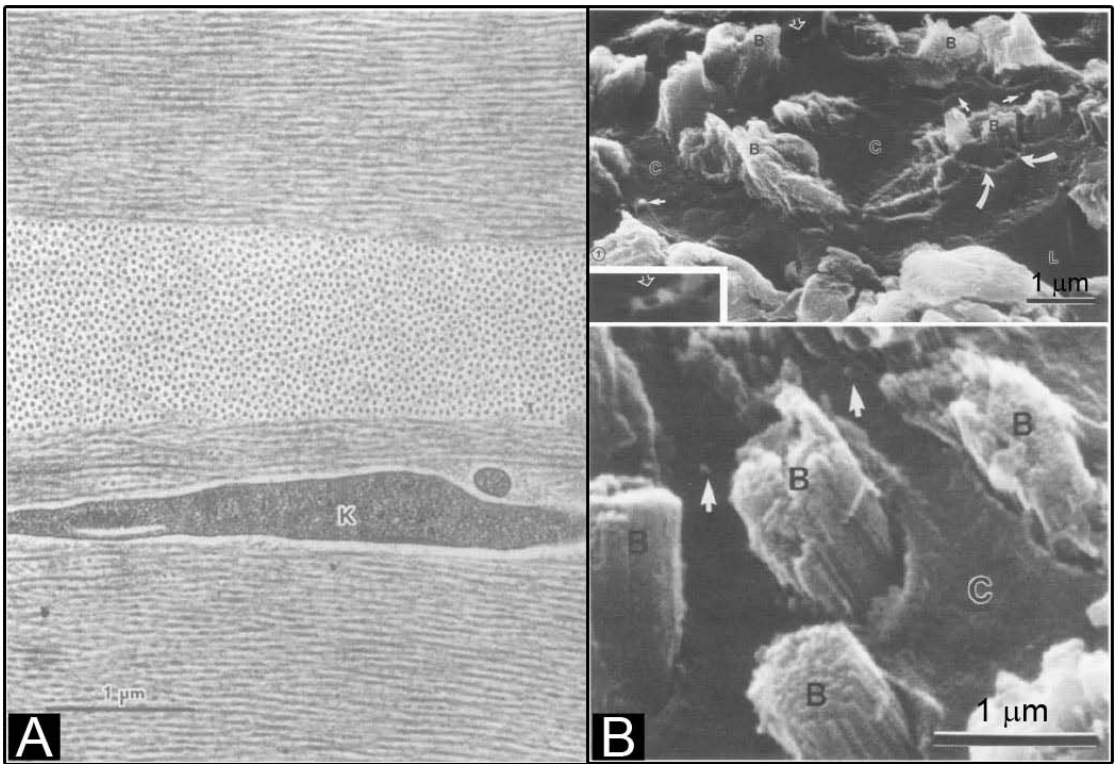

Figure 1-4: Fine macroscale organization of the collagen fibrils in cornea and tendon. A, in corneal stroma collagen fibrils are self-assembled into lamellae. Fibrils are aligned in each layer and at right angle with respect to the fibrils in the adjacent layers (Komai and Ushiki 1991). B, in tendon, fibrils are organized into parallel bundles aligned in the direction of the load. The fibril bundles are defined by adjacent fibroblasts and/or cell processes (curved arrows). Straight arrows showing small cytoplasmic channels containing a single collagen fibrils

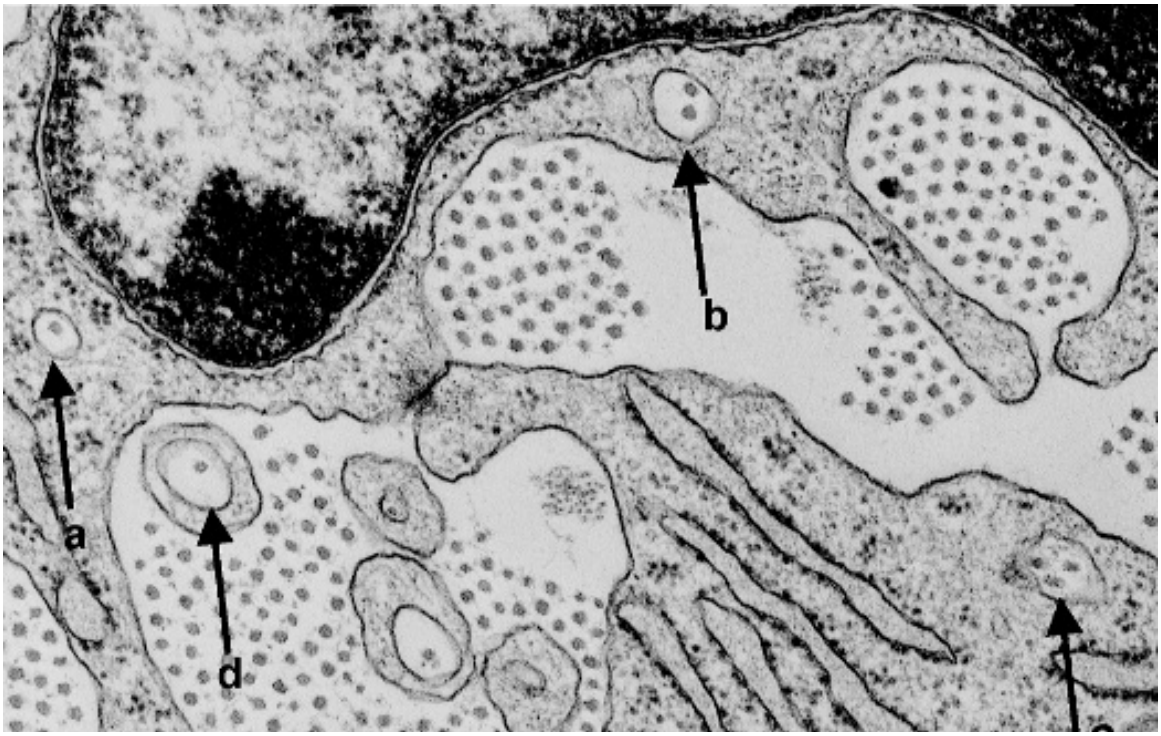

Figure 1-5: TEM micrograph of the fibripositors secretory pathway. One (a), two (b), or three (c) membrane-bound collagen fibrils are observed within cytoplasm. (d) represents a membrane bound collagen fibril in a plasma membrane extensions called fibripositors (Canty and Kadler 2005).

synthesis, posttranslational processing, packing, discharge, assembly into fibrils, assembly into bundles, and assembly into collagen macroaggregates are directly linked and regulated by the cells (Birk and Trelstad 1986) (Figure 1-6).

The second theory is based on the liquid crystalline properties of collagen molecules. Trelstad was the first to relate the lamellar organization of the collagenous matrix seen in corneal stroma to the cholesteric phase of liquid crystals (Trelstad 1982). As he noted, the lamellar rotation of collagen fibrils in corneal stroma does not follow bilateral symmetry which is in contrast to the rest of the body. Therefore, he reasoned that the driving force behind this phenomenon must be physical not biological. Bouligand reported for the first time the presence of twisted structures of self-assembled collagen

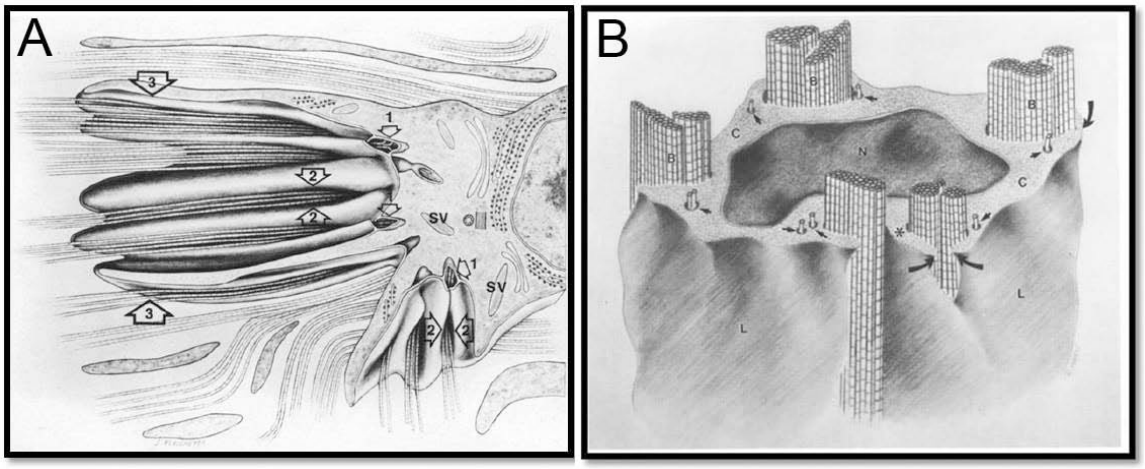

Figure 1-6: Artistic view of ECM compartmentization and discharging of organized collagen bundles into the ECM of A, cornea (Birk and Trelstad 1984) and B, tendon (Yang and Birk 1986). The synthesis, posttranslational modification, and packaging of procollagen occurs within a series of intracellular compartments. As illustrated for cornea (A), the secretory vacuoles (VS) release their contents by fusion with the cell surface which forms the first extracellular compartment. When vacuoles fuse in a compound manner, the small surface recess (1) within which the initial extracellular events in collagen fibril formation occur is formed. Larger recesses and surface folds (2) are formed by lateral fusion of the smaller recesses. Collagen fibrils are collected into fibril bundles (50-100 fibrils) within these compartments. Continuous breakdown and retraction of the cell's surface results in the fusion of the surface foldings which consequently forms large surface-associated compartments (3). Fibril bundles are joined within these compartments to form larger bundles and lamellae. As shown for tendon (B), a fractured cytoplasmic surface (C) containing a nuclear profile (N) and a free lateral surface (L) of a fibroblast are illustrated. One or more collagen fibrils, within cytoplasmic channels (arrows) and fibril bundles (B) located in the peripheral extracellular compartments.

fibrils *in vitro*, and suggested that it shows the same finger print patterns as that of cholesteric liquid crystals (Bouligand, Denefle et al. 1985). Since then the collagenous matrices in a few other tissues (e.g. cortical bone and tendon) have also been related to the phases of liquid crystals (Giraud-Guille 1988; Lepescheux 1988). In a series of papers Giraud-Guilles' group studied the organization of collagen molecules (and procollagen)

at high concentration. Using phase contrast microscopy this group showed that when concentrated to very high levels, this molecules shows the liquid crystalline properties

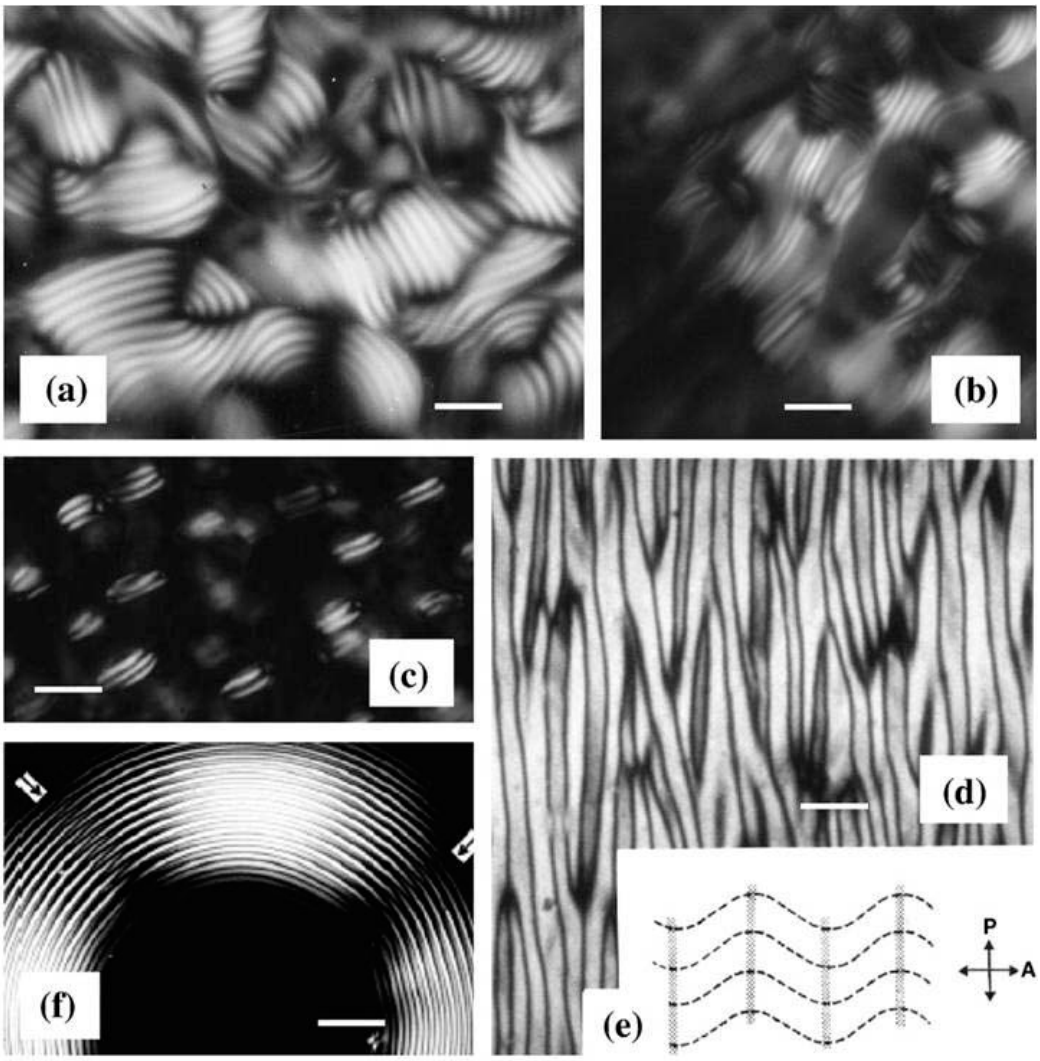

Figure 1-7: Self-organization patterns of collagen molecules at high concentrations observed using polarized light microscopy (Giraud-Guille, Mosser et al. 2008). a-c, finger print patterns typical of cholesteric liquid crystal phase observed in high concentration collagen solution. Cholesteric phases coexist with isotropic liquid phases. d, banded extinction patterns are observed after shear which are translated into undulating molecular direction (e). Evaporation of a collagen droplet results in the concentric rings of alternating molecular orientation and zigzag patterns (arrow) observed using polarized light microscopy technique. Bars in a-d are 10 µm and in f is 100 µm.

(Giraud-Guille 1988; Giraud-Guille 1989; Martin, Farjanel et al. 2000) (Figure 1-7). Upon increasing the temperature and pH the molecules self-assemble into fibrils and produce arc-shaped pattern very similar to the collagenous structures seen in bone (Figure 1-8).

Based on these observations, they proposed a model to explain the process in which high order organization of collagen fibrils is produced *in vivo.* According to this model, fibroblast cells-synthesize procollagen into the extracellular matrix at high concentration. Due to their liquid crystalline properties collagen molecules self-organize in the ECM. Enzymatic cleavage of the procollagen results in the self-assembly of the molecules into fibrils and consequently, translating the molecular organization into fibrillar organization.

Unfortunately, there is still not enough evidence to support either of the above theories. It is however possible that in different situations one of these processes is more prevalent. For example, during development which requires rapid formation of tissues, the liquid crystalline process may take place, but in wound healing (that requires the delivery of the ECM to a specific location), cells control the collagen deposition through their fibripositors. It should be noted that after healing the collagen organization in the wound area lacks the organization observed in the surrounding areas.

One of the main arguments against the liquid crystalline hypothesis is the *in vitro* investigations which showed that at the physiological conditions, procollagen molecules form spontaneously self-assembled aggregates at concentration above 1.5 mg/ml (Mould and Hulmes 1987). However, one should consider that *in vivo,* collagen molecules are interacting with variety of different molecules and macromolecules (e.g. proteoglycans

and fibronectin) and these interactions could prevent the molecules from premature self-assembly.

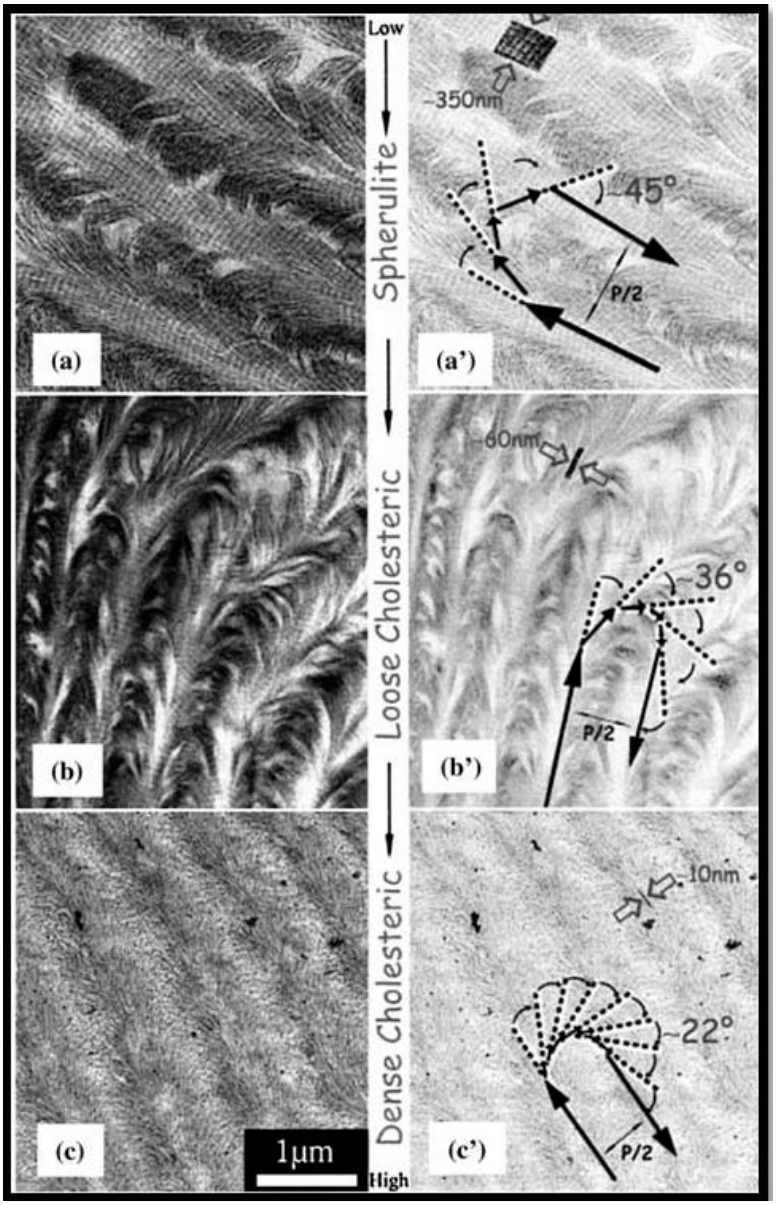

Figure 1-8: Formation of arc-shape pattern following the fibrillogenesis of collagen molecules at high concentrations. At higher concentrations the diameter of the fibrils as well as the rotation angle decrease (Giraud-Guille, Mosser et al. 2008)

1.2.2. Collagen Self-assembly in Vitro

In vitro, increasing the temperature of a neutralized solution of acid (telo-collagen) or pepsin extracted (atelo-collagen) type I collagen molecules results in the self-assembly of the monomers into an isotropic fibrillar network (Figure 1-9). The self-assembly spontaneously continues by end-to-end and lateral fusion of molecules (Birk, Nurminskaya et al. 1995; Graham, Holmes et al. 2000). In order for the fibril formation to continue, it is necessary that collagen molecules are arranged in such a fashion that their polarity is parallel. Consequently, self-assembly of the bipolar molecules will result in the formation of bipolar microfibrils.

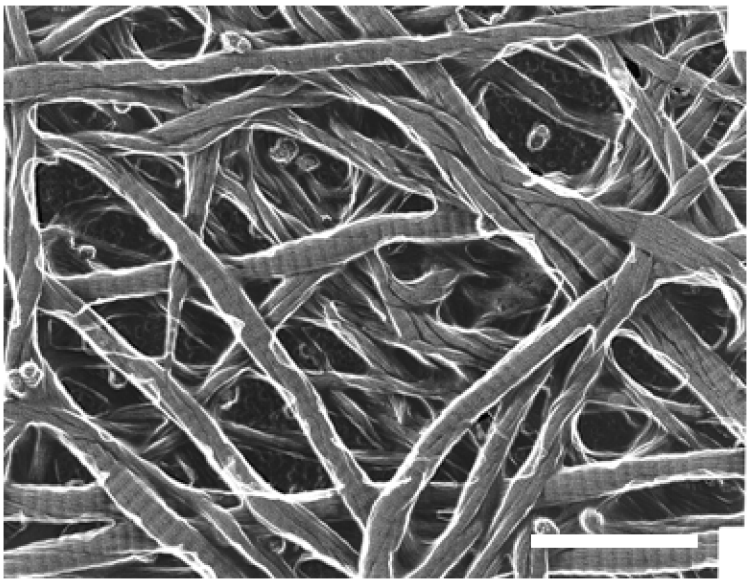

Figure 1-9: Self-assembly of the collagen molecules into a disorganized, polydispersed diameter fibrillar network. Bar is 100 nm.

The process of collagen self-assembly is an entropy driven process (Kadler, Hojima et al. 1987). Collagen fibril formation is an endothermic process. However, when fibril assembly occurs, collagen molecules are confined in a tight space which results in the decrease of the molecule's entropy (Miles and Ghelashvili 1999). Therefore, during

self-assembly collagen molecules gain Gibb's free energy by losing solvent molecules from their surface and form hydrophobic intermolecular bonds. To reach to the lowest energy state collagen molecules form fibrils with circular cross sections (and possibly D-banding). Depending on the stage of development and type of tissue, the diameter of the fibrils ranges from 12 to 500nm. A pentafibril, which is a 4 nm annulus composed of five collagen molecules, is the smallest unit of fibrils exhibiting the D-banding patterns (Scott 1990; Scott 1995). However, protofibrils (~10nm diameter) are the smallest fibrillar units frequently seen *in vivo* and aggregation of protofibrils results in the formation of larger fibrils. The chemical bond between collagen molecules inside a protofibril is in the form of a covalent bond, making them very stable structures (Scott 1990; Scott 1995). In contrast, the chemical bonds between protofibrils within a fibril are less stable and are reversible (e.g. hydrogen and electrostatic bonds). These properties make the protofibrils the recycling units of a collagen fibril: instead of breaking down to the molecular level as the result of fibrillar unfolding only the protofibrils will be released. Since forming fibrils from protofibrils is much easier and energy efficient (due to the formation of hydrogen bonds) than from molecular units (i.e. covalent bonds), it is possible that the existence of protofibril units make the folding and unfolding an energy efficient process (Scott 1995).

Lateral fusion of the small diameter fibrils is another mechanism to form thick fibrils. As mentioned before, small diameter fibrils are bipolar. The polarity of the fibrils plays an important role in the end to end and lateral fusion of the thin fibrils.

Similar to the case of fusion of molecules, in order for fibrillar *lateral* fusion to occur, the polarity of the fibrils must be parallel. *In vivo* studies have shown that in the developing chick cornea half of the collagen fibrils have a parallel polarities and in the other half it is

antiparallel (Kadler, Holmes et al. 1996) and therefore, the probability of lateral fusion would be less than 50%. Interestingly, studies on the developing chick cornea showed that from all the configurations available for the lateral fusion of the fibrils, only two have been seen: between two bipolar fibrils or between one bipolar and one N- unipolar fibril. In these cases the fusion occurs between a C- and an N- site (for review see (Kadler, Holmes et al. 1996), Figure 1-10). It has been suggested that formation of antiparallel fibrils is another mechanism to control the fibril diameter by preventing the lateral fusion.

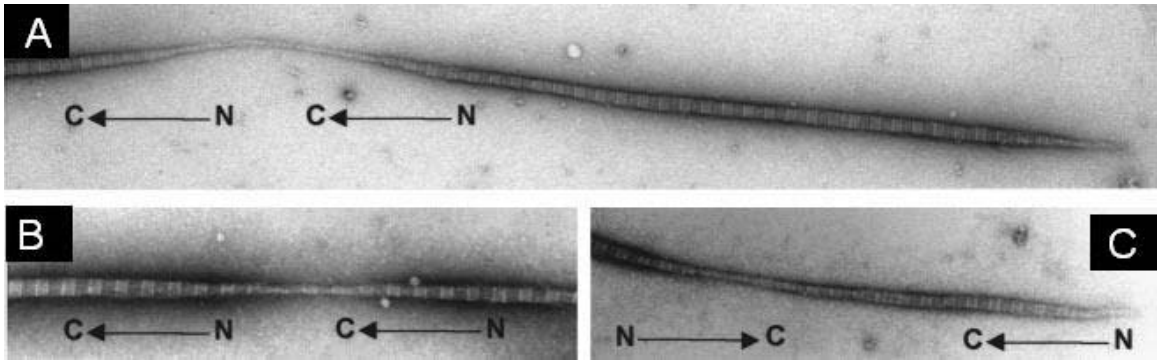

Figure 1-10: End-to-end fusion of the microfibrils and fibrils requires the presence of a C-tip. A and B shows the end-to-end fusion between two fibrils from a N- and a C-terminal resulting the formation of a unipolar fibril. C showing the fusion between two C-terminals which results in the formation of a bipolar fibril (Graham, Holmes et al. 2000)

1.2.3. Methods of Organizing Collagen in Vitro

As early as the 1950's, the ability of extracted collagen monomers to self-assemble into native-like fibrils was investigated extensively (Highberger, Gross et al. 1951; Gross, Highberger et al. 1954; Gross 1958; Gross 1958). These initial studies were both quantitatively and morphologically advanced and have provided the basis for

numerous investigations which have probed the assembly kinetics and resulting morphology of collagen assembled *ex vivo* (for review, (Prockop and Hulmes 1994)).

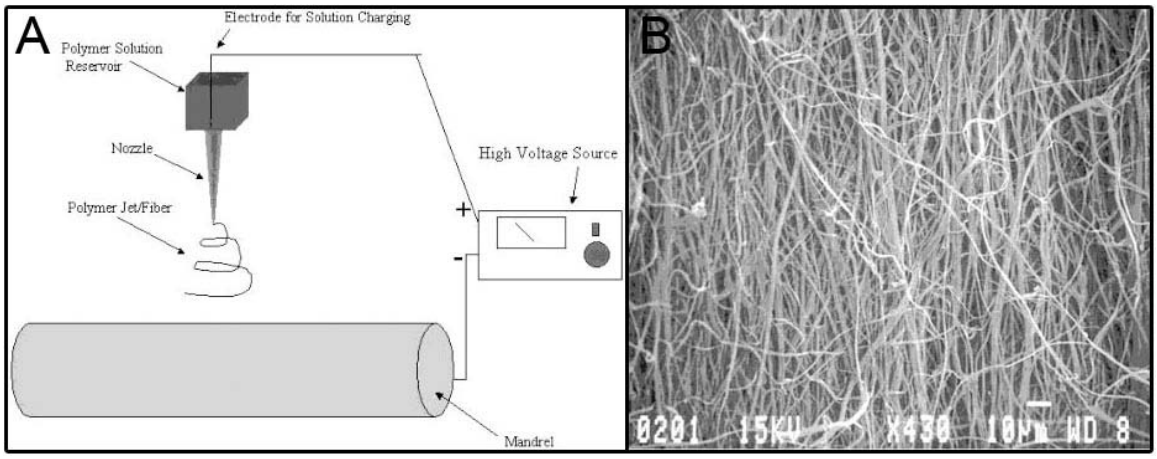

Figure 1-11: Collagen electro-spinning. Collagen solution is dispensed on a charged, rotating mandrel (A) results on the relatively aligned collagen bundles (B) [5]

The use of self-assembled, reconstituted fibrillar collagen as a scaffold for tissue engineering (used principally due to its natural biocompatibility *in vivo*) first began in the 1950's (Ehrmann and Gey 1956). A few years later Konigsberg realized that if the culture medium used had previously been exposed to a dense population of cells (for single embryonic muscle cells), it caused the single cell to produce a macroscopic colony of muscle cells (Konigsberg 1963). He concluded that one of the effects of pre-exposing the media might be synthesis of collagen fibrils by the dense population of the cells into media. To prove this hypothesis, he used collagen as a substrate for cell culturing and by doing so, he successfully eliminated the need to prior expose the media to the cells (Hauschka and Konigsberg 1966). Since then reconstituted type I collagen has been extensively used for cell culturing with the results of these studies indicating that collagen substrates enhance cell signaling, proliferation, and further collagen synthesis (Hauschka and Konigsberg 1966; Martin and Kleinman 1981; Kleinman, Luckenbill-

Edds et al. 1987). In tissue engineering, researchers typically seed the cells of interest into either 2D or 3D networks of randomly assembled collagen fibrils. Although promising results have been obtained for the engineering of structures which possess a low level of ECM organization (e.g. skin) (Naughton 2002), there has been only limited success when the target tissues comprise highly-organized ECMs (e.g. tendon, ligament, cornea and bone). This has lead to the realizaotion that a priori organizational cues (such as preorganized scaffold) may be critical to the engineering of load-bearing tissue (for review (Ruberti and Zieske 2008)).

Compared to the investigations on the random assembly of collagen, methods designed to "influence" organization of self-assembling collagen fibrils have received

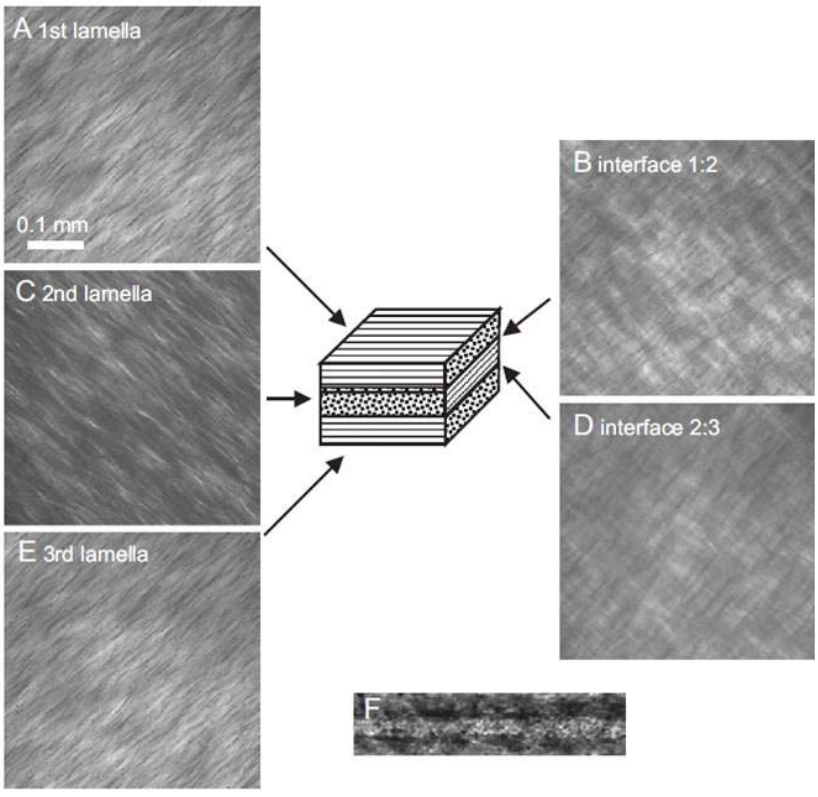

Figure 1-12: Using 7T horizontal magnetic fields and a series of gelation-rotation-gelation cycles Torbet et al were able organize collagen fibrils in and produce multi-layer constructs [58]

much less attention. One of the earliest such investigations attempted to align collagen fibrils in films by inclining a surface during polymerization (Elsdale and Bard 1972). In addition to this "drainage" method, several research groups have produced organized layer(s) of collagen fibrils, often with the intention of using them for guiding cell culture systems. Methods employed to influence collagen fibril organization during self-assembly include electro-spinning (Matthews, Wnek et al. 2002) (Figure 1-11), the use of strong magnetic fields (Dickinson, Guido et al. 1994; Dubey, Letourneau et al. 1999; Dubey, Letourneau et al. 2001) (Figure 1-12), flows through a microfluidic channel (Lee, Lin et al. 2006; Lanfer, Freudenberg et al. 2008), a combination of fluid flow and magnetic field (Guo and Kaufman 2007), dip-pen nanolithography (Wilson, Martin et al. 2001), cholesteric methods (Giraud-Guille, Besseau et al. 2003), and even freeze/thaw cycles (Faraj, van Kuppevelt et al. 2007). Furthermore, despite the great progress that has been made in controlling collagen organization, in general, the kinetics of collagen polymerization during "influenced" assembly has been neglected. The main contributing factor to this under-investigation is the size of collagen molecules. Since a collagen monomer is much smaller than the diffraction limit of visible light, fluorescence microscopy is the only possible method to observe collagen molecules. However, due to the short length of a collagen molecule, high ratio of fluorescence dye per molecule should be used. This will negatively influence the normal motion of the molecules, and is therefore not a suitable visualization method for a single molecule.

Studies have shown that when seeded on an organized collagen substrate, the cells adopt the alignment and organize themselves in the same direction as the substrate which they are on, resulting in the synthesis of organized ECM (Glass-Brudzinski, Perizzolo et

al. 2002) (Figure 1-13). Unfortunately, cells are only able to control the short range organization of the fibrils on the substrate. This has led to studies focusing on the production of 3D organized collagenous structures.

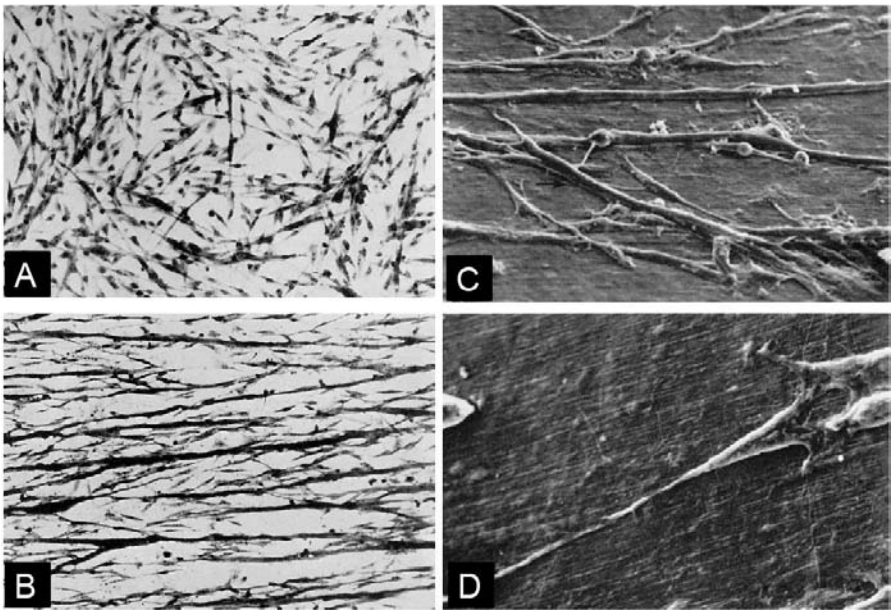

Figure 1-13: Bright field (A and B, magnification: x186) and SEM (C, x680, and D, x1640) micrographs of chick embryo breast myoblast cultured on disorganized (A) and aligned (B-D) collagen fibrils. When cultured on organized collagen template, cells adopt the direction of organization and spread out. Occasionally some cells deviate from the collagen organization and cross it (Yoshizato,

1.3. Collagen Ultra-structure

1.3.1. Control of Collagen Ultrastructure in Vivo

The morphology of the collagen fibrils *in vivo* is controlled via the interactions with several macromolecules present in the ECM. Proteoglycans (PGs), non fibril forming collagens (e.g. Fibril Associated Collagens with Interrupted Triple helices, FACITs, and network making fibrils, type IV collagen), fibronectin, laminin, and elastin are the main components of the ECM in addition to fibril forming collagens (Figure 1-

14). *In vivo,* collagen fibrils closely interact with proteoglycans and their associated glycosaminoglycans (GAGs) chains (Scott, Orford et al. 1981; Scott and Haigh 1985; Scott 1991; Scott and Thomlinson 1998). These interactions have been suggested to be the major factor controlling the ultrastructure of the collagen fibrils (Figure 1-15).

PGs are soluble macromolecules in the ECM and are composed of a globular protein core that covalently bonds to one or more GAG chains. GAGs are sulphated linear heterogeneous polysaccharides. Due to the existence of the sulphate and carboxyl groups, GAG chains are highly negatively charged resulting in repulsion force between the neighbouring molecules. There are generally five types of GAGs: dermatan sulfate, chondroitin sulfate, heparin and heparin sulfate, keratan sulfate, and hyaluronan (which is the only unsulfated GAG). Proteoglycans are usually categorized based on the nature of their GAG chains; keratan sulfate, dermatan sulfate, chondroitin sulfate, heparan sulfate, and heparin (for review refer to (Scott 1988; Scott 1995)). Five to ten GAG chains may bond to the core protein to form a large PG such as perlecan. The very large PGs have up to three globular regions that are attached together via a polypeptide chain and can have up to 100 GAG chains attached.

Small leucine rich proteoglycans (SLRPs) are the main group of PGs found in the loadbearing tissues (except in cartilage). Decorin and biglycan, (both chondroitin/dermatan sulfate PGs) and lumican, keratocan and fibromodulin (all keratan sulfate PGs) are all types of SLRPs, and are the PGs found in cornea (Tanihara, Inatani et al. 2002).

Studies on knock-out mice have shown that deficiency of these PGs (principally lumican) results in the opacity of the cornea which was the result of the polydisperse

diameter fibrils and irregular fibril spacing (Rada, Cornuet et al. 1993; Chakravarti, Magnuson et al. 1998; Chakravarti, Petroll et al. 2000; Chakravarti 2002; Song, Lee et al. 2003; Schonherr, Sunderkotter et al. 2004; Beecher, Chakravarti et al. 2006; Chakravarti, Zhang et al. 2006) (Figure 1-16).

These results strongly suggest that PGs play an important role in controlling the ultrastructure of the cornea. It is possible that when attached to a collagen fibril, PGs

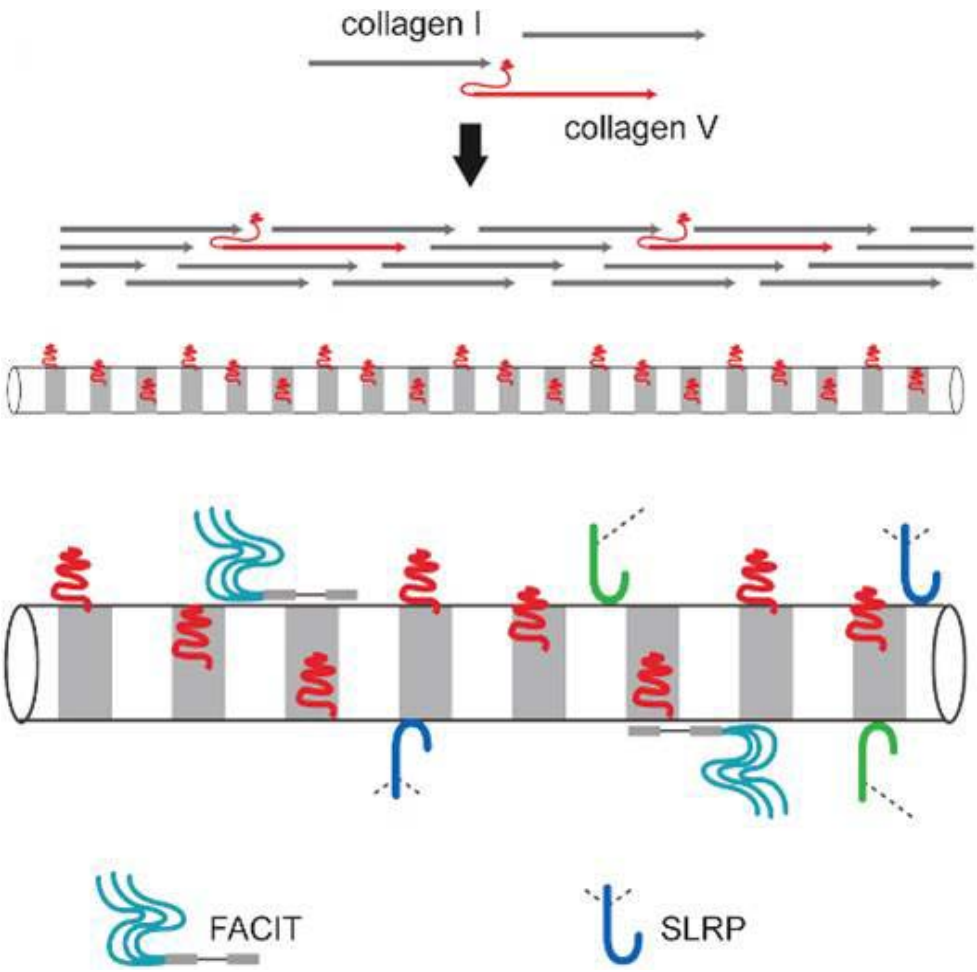

Figure 1-14: Collagen fibril complex in cornea. The heterotypic fibrils are composed of type I and V. Fibrils closely interact with proteoglycans (e.g. SLRPs) and other types of collagen (e.g. FACITs). These interactions have been suggested to control the fibrils' diameter and spacing (Birk and Bruckner 2005)

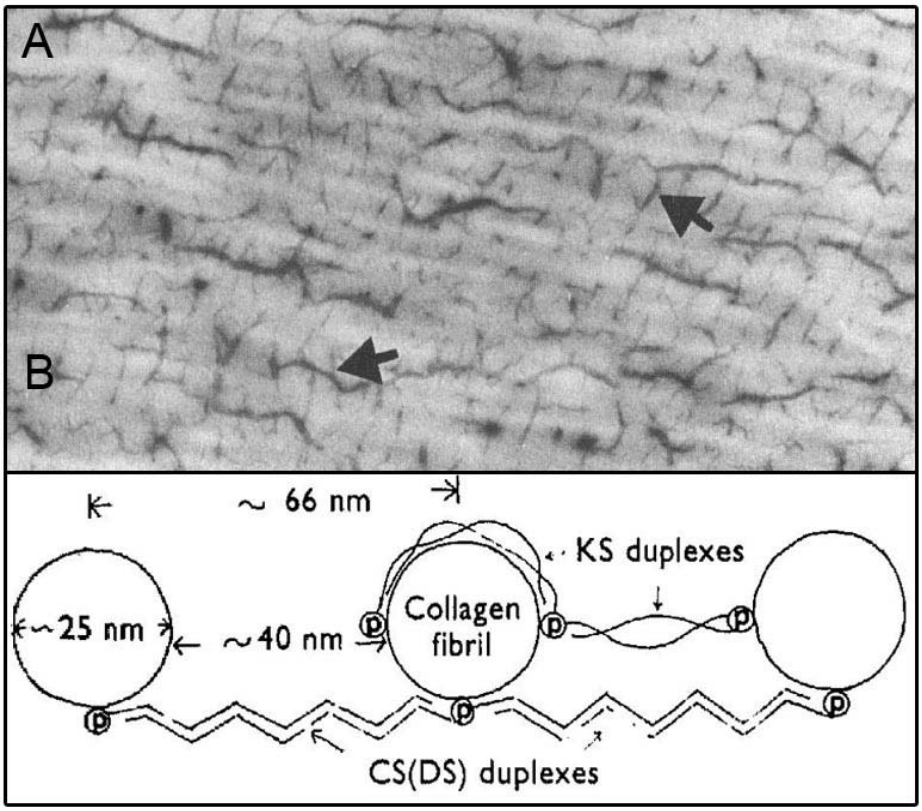

Figure 1-15: PG-collagen interaction. A, a TEM micrograph from a section of cornea stained with cuprilinic blue showing that PGs interact with collagen fibrils periodically along the length of the fibrils (Scott and Haigh 1988). B, proposed mechanism for the fibril diameter and spacing control by PG-fibrillar collagen interactions (Scott 1991)

control the fibrillar diameter and center-to-center spacing of the fibrils by prohibiting the lateral fusion of the fibrils through the repulsion force created between the neighboring GAG chains. The X-ray diffraction analysis (Meek, Scott et al. 1985) and molecular simulation of the decorin (Weber, Harrison et al. 1996) suggested that the core protein of this molecule (and other SLRPs) has an arch shape. Through its N- terminal, the molecule is capable of forming covalent bonds with the chondroitin sulfate GAG chains (Weber, Harrison et al. 1996; Vesentini, Redaelli et al. 2005). The inner diameter of the arch is about 2.5 nm which fits a collagen monomer with 1.5 nm diameter. Therefore, it is

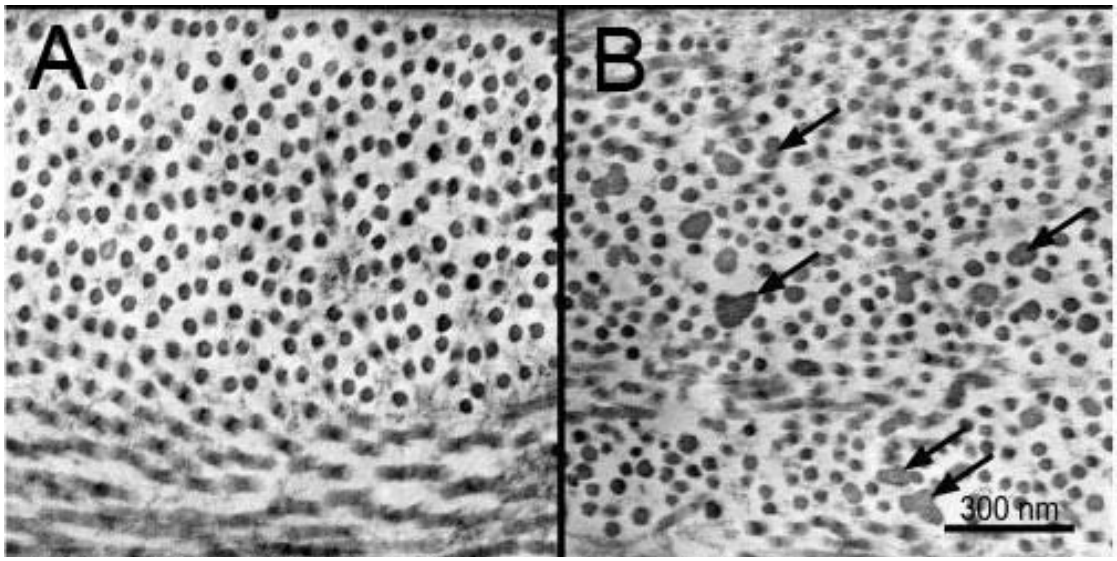

Figure 1-16: Comparison between the ultrastructure of the collagen fibrils in the wild type (A) and lumican knock-out (B) mice. In the wild type the fibrils are monodisperse, small diameter with regulated spacing. In the knock-out mice the fibrils are laterally fused which result in the irregular cross-sections (arrows) (Chakravarti, Zhang et al. 2006)

possible that decorin core attaches to a fibril by binding to one of the molecules on the surface of the fibril and controls the fibril's diameter and fibril-to-fibril spacing through its GAG chains (Figure 1-17). The histochemical studies of the collagen-PG interactions show that core proteins of the PGs periodically interact with the fibrils at the gap regions of D-bandings. GAG chains are organized along the fibrils or orthogonal to the long axis of the fibrils, with their length matching the distance between the two adjacent fibrils (Scott 1988). These observations support the hypothesis that GAG chains regulate the ultrastructure of the collagenous matrices (Scott 1991).

In addition to interactions with PGs and their GAG chains, fibril forming collagens interact with other types of fibril forming of non-fibril forming collagens. Heterotypic collagen fibrils in the cornea are example of interaction between two fibril forming collagens. Corneal fibrils are composed of type I and V collagen molecules

within each fibril (Linsenmayer, Fitch et al. 1983; Birk, Fitch et al. 1988; McLaughlin, Linsenmayer et al. 1989). Initially it was suggested that coexistence of type V with type I was a mechanism to control the fibrillar diameter (Birk, Fitch et al. 1988) (Figure 1-18). However, later studies showed that type V monomers are located in the core of the heterotypic collagen fibrils which suggests that they are primarily important in the

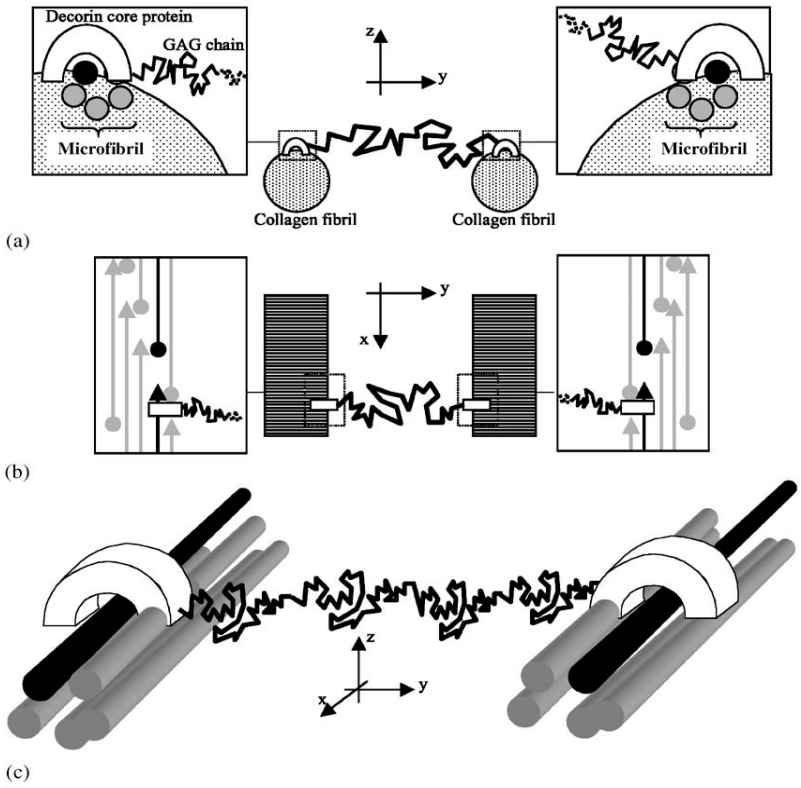

Figure 1-17: A proposed model of decorin-collagen fibrils interaction and control of fibrils spacing via the repulsion of their sulfated glycosaminoglycans (GAGs). The protein cores (horseshoe shaped structures are non-covalently bond to collagen monomers (black rod) in two adjacent fibrils and the GAG side chains (jagged black lines) are covalently bond to the core proteins. (a), schematic of the interaction. The illustration of the interactions in an equatorial plane (a) and in a longitudinal plane (b) where the connections are magnified. (c), a 3-D view of the proteoglycans complex-collagen monomer interaction (Vesentini, Redaelli et al. 2005).

initiation of fibrillogenesis by forming nucleation sites for type I monomers (Birk 2001; Wenstrup, Florer et al. 2004) (Figure 1-14).

Collagen fibrils also interact closely with non-fibril forming collagens (e.g. FACITs and network forming collagen, Figure 1-14). Collagen types XII and XIV are members of FACITs that have been shown to coexist with collagen fibrils in cornea (Gordon, Gerecke et al. 1987; Marion K. Gordon 1996). Although FACITs are generally assumed to be members of the collagen family, they have some similarities to proteoglycans. For example, post-transitional modification can occur for attachment to a GAG chain. They are short molecules with helical collagen domain separated with non-helical domains. They lie on the surface of collagen fibrils and form covalent bonds with the collagen molecules within the fibril (Vaughan, Mendler et al. 1988; Shaw and Olsen 1991). Their noncollagenous N-terminal domain protrudes from the surface of the fibrils and forms an interaction site with other ECM macromolecules (e.g. proteoglycans) (Holden, Meadows et al. 2001; Thur, Rosenberg et al. 2001).

1.3.2. Control of Collagen Ultrastructure in Vitro

Most of the research conducted on the morphology of self-assembled collagen fibrils *in vitro* has been focused on the effects of ECM macromolecules (e.g. decorin (Figure 1-19), lumican, or type V collagen) on collagen fibrillogenesis and its subsequent morphology, in contrast to efforts to control of ultrastructure for tissue engineering. Although the results of these studies confirm *in vivo* knock-out studies there are disagreements in the literature about the details. For example, although most of the studies show that both lumican and decorin result in the formation of collagen fibrils with

smaller diameter (Rada, Cornuet et al. 1993; Neame, Kay et al. 2000) Kuc and Scott showed that the fibrils formed in the presence of decorin have larger diameter (Kuc and Scott 1997). Both lumican and decorin have also been shown to affect the initial rate of fibril formation (lag time) however, lumican accelerates the fibril formation but decorin slows the initial fibrillogenesis (Kuc and Scott 1997; Sini, Denti et al. 1997; Neame, Kay et al. 2000). Interestingly, the studies reveal that the changes in the fibril diameter are only significant when the GAG chains of the PG are present (in contrast to only using the

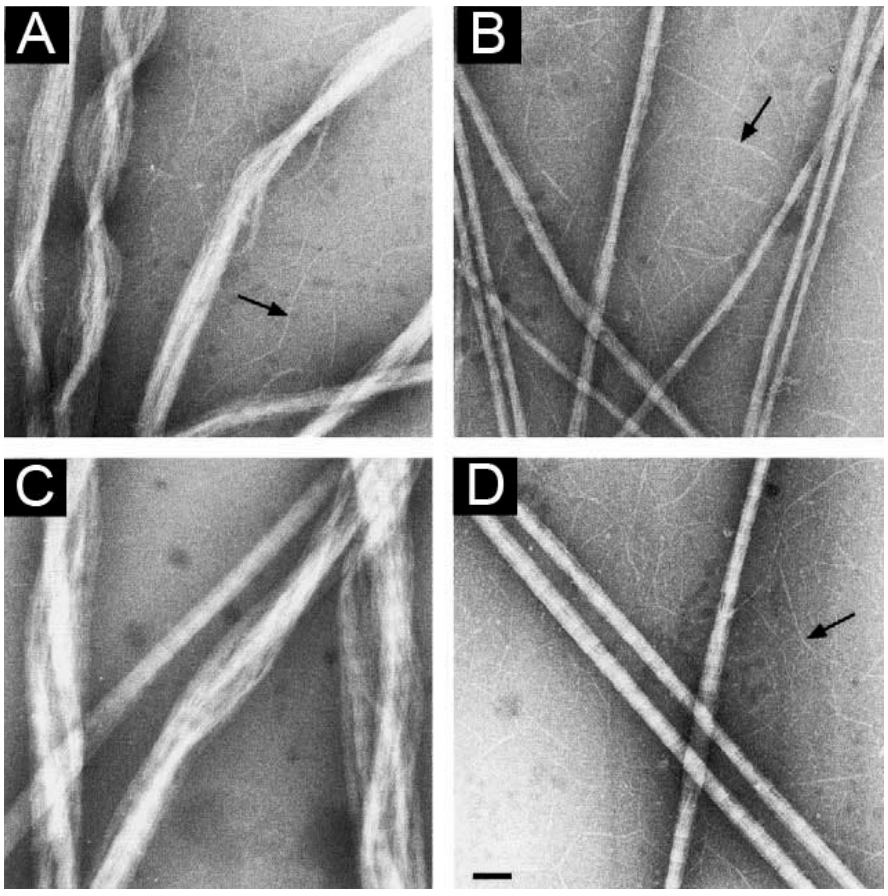

Figure 1-19: Collagen fibrillogenesis in the absence (A and C) and presence (B and D) of decorin 9 (A and B) and 30 (C and D) minutes after incubation. When fibrilized with decorin fibrils are uniform in diameter, no lateral fusion is seen and the D-banding is more distinct. Arrows indicate collagen filaments. (bar is 100 nm). (Brown, Lin et al. 2002)

core protein). However, the core protein alone is still effective on the acceleration or retardation of the initial fibril forming rate (Kuc and Scott 1997). The single study on the effects of PGs on the D-banding of the fibrils was conducted by Brown et. al. which showed that *in vitro* collagen fibrillogenesis in the presence of decorin influences the morphology of the fibrils and results in fibrils with more apparent D-banding (Brown, Lin et al. 2002).

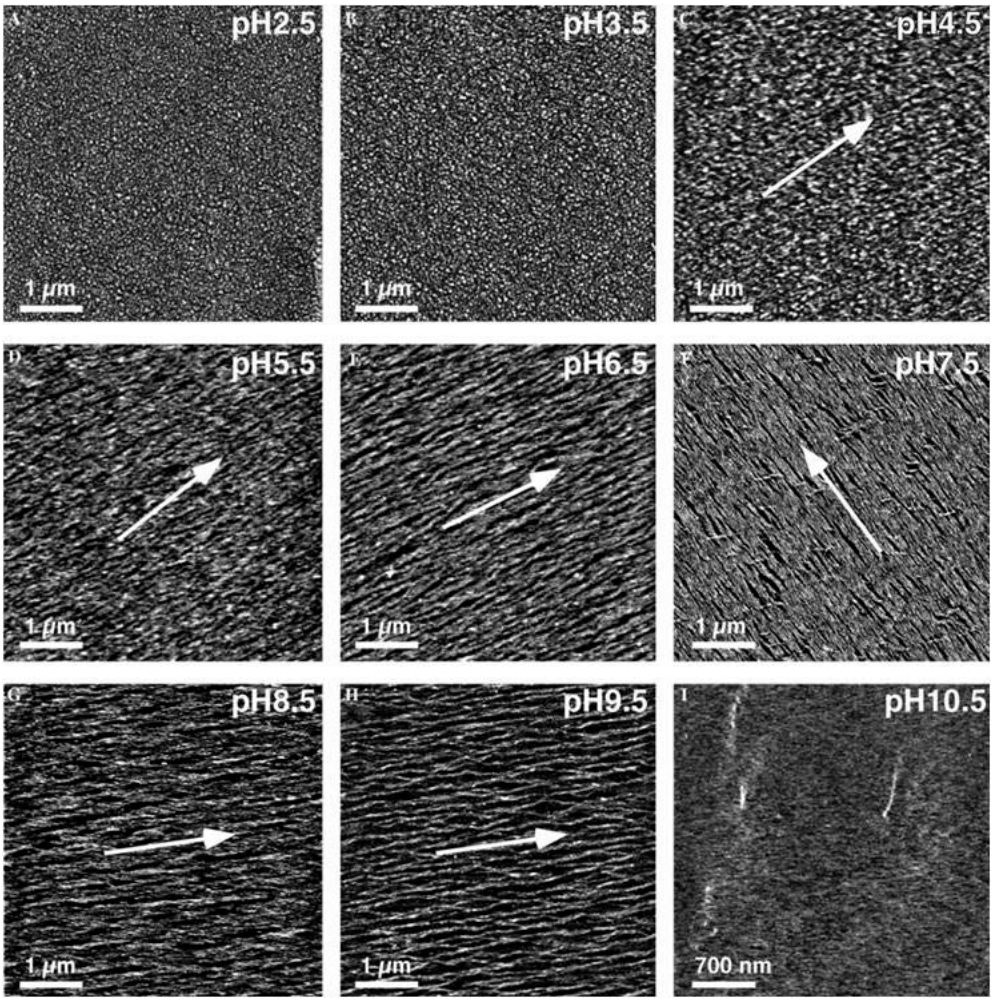

Figure 1-20: Collagen fibrils self-assembled on mica sheet at variou pH ranges. Jiang et al. showed that it is possible to control the fibrils' diameter, spacing and appearance (i.e. globular or fibrillar) by adjusting the pH and surface properties (Jiang, Horber et al. 2004)

Effects of pH and ionic strength on the organization of both cell synthesized (Bard, Hulmes et al. 1993; Huang and Meek 1999; Regini, Elliott et al. 2004) and self-assembled fibrils (Jiang, Horber et al. 2004; Harris and Reiber 2007; Koster, Leach et al. 2007) have also been studied. It has been shown that the diameter and morphology of the fibrils is highly dependent on these two factors. The narrow fibrils similar to the 20nm corneal stromal collagen fibrils only appear in the pH range of 6.9-7.4 (Bard, Hulmes et

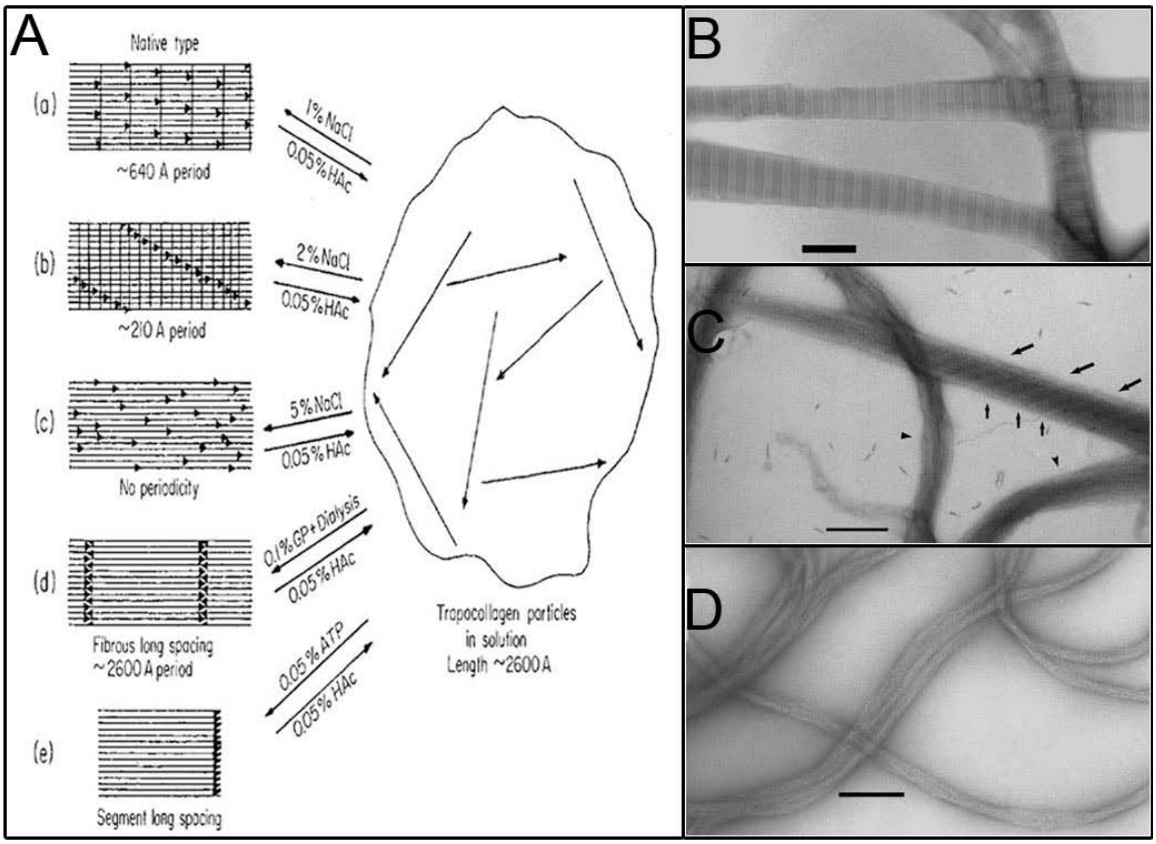

Figure 1-21: Effect of the ionic strength on the collagen morphology. A, schematic showing the dependence of the organization of the collagen molecules in a fibrils as a function of the ionic strength. 67nm D-banding, 21 nm banding, 260nm FLS, SLS, and no banding resulted by adjusting the ionic strength of the buffer solution (Wood 1964). B-D, sTEM micrographs showing 67nm D-banded fibrils (B, pH=7,150 mM NaCl), 21nm striated fibrils (C, pH=7, 50 mM Triz-HCl) and fibrils with no periodic banding patterns (D, pH=8, 50 mM Triz-HCl)

al. 1993). Jiang et. al. showed that it is possible to control the diameter and spacing of the collagen fibrils adsorbed to mica by adjusting the pH and ionic strength of the collagen solution (Jiang, Horber et al. 2004) (Figure 1-20).

The earlier research on collagen fibrillogenesis *in vitro* has been focused on the effects of pH and ionic strength on the arrangements of the molecules in a fibril. These investigations showed that in addition to the native quarter staggered fibrils (D-banded), collagen molecules could form striated fibrils with repeating patterns of 21nm, striated fibrils with a nonpolarized repeating patterns of 260nm (fibrous-long-spacing, FLS), 260 nm segmented fibrils with polarized patterns (segmented-long-spacing, SLS), and even fibrils with no periodicity (Wood 1964) (Figure 1-21).

References

Bard, J. B., D. J. Hulmes, et al. (1993). "Chick corneal development in vitro: diverse effects of pH on collagen assembly." J Cell Sci **105 (Pt 4)**(Pt 4): 1045-55.

Beecher, N., S. Chakravarti, et al. (2006). "Neonatal development of the corneal stroma in wild-type and lumican-null mice." Invest Ophthalmol Vis Sci **47**(1): 146-50.

Benjamin, H. B., E. Pawlowski, et al. (1964). "Collagen as Temporary Dressing and Blood Vessel Replacement." Arch Surg **88**: 725-7.

Birk, D. E. (2001). "Type V collagen: heterotypic type I/V collagen interactions in the regulation of fibril assembly." Micron **32**(3): 223-37.

Birk, D. E. and P. Bruckner (2005). Collagen Suprastructures. Collagen: Primer in Structure, Processing and Assembly**:** 185-205.

Birk, D. E., J. M. Fitch, et al. (1988). "Collagen type I and type V are present in the same fibril in the avian corneal stroma." J Cell Biol **106**(3): 999-1008.

Birk, D. E., M. V. Nurminskaya, et al. (1995). "Collagen fibrillogenesis in situ: fibril segments undergo post-depositional modifications resulting in linear and lateral growth during matrix development." Dev Dyn **202**(3): 229-43.

Birk, D. E. and R. L. Trelstad (1984). "Extracellular compartments in matrix morphogenesis: collagen fibril, bundle, and lamellar formation by corneal fibroblasts." J Cell Biol **99**(6): 2024-33.

Birk, D. E. and R. L. Trelstad (1986). "Extracellular compartments in tendon morphogenesis: collagen fibril, bundle, and macroaggregate formation." J Cell Biol **103**(1): 231-40.

Bouligand, Y., J. P. Denefle, et al. (1985). "Twisted architectures in cell-free assembled collagen gels: study of collagen substrates used for cultures." Biol Cell **54**(2): 143-62.

Brown, C. T., P. Lin, et al. (2002). "Extraction and purification of decorin from corneal stroma retain structure and biological activity." Protein Expr Purif **25**(3): 389-99.

Canty, E. G. and K. E. Kadler (2005). "Procollagen trafficking, processing and fibrillogenesis." J Cell Sci **118**(Pt 7): 1341-53.

Cassidy, J. J., A. Hiltner, et al. (1989). "Hierarchical structure of the intervertebral disc." Connect Tissue Res **23**(1): 75-88.

Chakravarti, S. (2002). "Functions of lumican and fibromodulin: lessons from knockout mice." Glycoconj J **19**(4-5): 287-93.

Chakravarti, S., T. Magnuson, et al. (1998). "Lumican regulates collagen fibril assembly: skin fragility and corneal opacity in the absence of lumican." J Cell Biol **141**(5): 1277-86.

Chakravarti, S., W. M. Petroll, et al. (2000). "Corneal opacity in lumican-null mice: defects in collagen fibril structure and packing in the posterior stroma." Invest Ophthalmol Vis Sci **41**(11): 3365-73.

Chakravarti, S., G. Zhang, et al. (2006). "Collagen fibril assembly during postnatal development and dysfunctional regulation in the lumican-deficient murine cornea." Dev Dyn **235**(9): 2493-506.

Dickinson, R. B., S. Guido, et al. (1994). "Biased cell migration of fibroblasts exhibiting contact guidance in oriented collagen gels." Ann Biomed Eng **22**(4): 342-56.

Dubey, N., P. C. Letourneau, et al. (1999). "Guided neurite elongation and schwann cell invasion into magnetically aligned collagen in simulated peripheral nerve regeneration." Exp Neurol **158**(2): 338-50.
Dubey, N., P. C. Letourneau, et al. (2001). "Neuronal contact guidance in magnetically aligned fibrin gels: effect of variation in gel mechano-structural properties." Biomaterials **22**(10): 1065-75.
Ehrmann, R. L. and G. O. Gey (1956). "The growth of cells on a transparent gel of reconstituted rat-tail collagen." J Natl Cancer Inst **16**(6): 1375-403.
Elsdale, T. and J. Bard (1972). "Collagen substrata for studies on cell behavior." J Cell Biol **54**(3): 626-37.
Engel, J. and H. P. Bächinger (2005). Structure, Stability and Folding of the Collagen Triple Helix. Collagen: Primer in Structure, Processing and Assembly**:** 7-33.
Exposito, J. Y., C. Cluzel, et al. (2002). "Evolution of collagens." Anat Rec **268**(3): 302-16.
Eyre, D. R., M. A. Paz, et al. (1984). "Cross-linking in collagen and elastin." Annu Rev Biochem **53**: 717-48.
Faraj, K. A., T. H. van Kuppevelt, et al. (2007). "Construction of collagen scaffolds that mimic the three-dimensional architecture of specific tissues." Tissue Eng **13**(10): 2387-94.
Fleischmajer, R., J. S. Perlish, et al. (1987). "Amino and carboxyl propeptides in bone collagen fibrils during embryogenesis." Cell Tissue Res **247**(1): 105-9.
Fleischmajer, R., R. Timpl, et al. (1981). "Ultrastructural identification of extension aminopropeptides of type I and III collagens in human skin." Proc Natl Acad Sci U S A **78**(12): 7360-4.
Giancotti, F. G. (1997). "Integrin signaling: specificity and control of cell survival and cell cycle progression." Current Opinion in Cell Biology **9**(5): 691-700.
Giraud-Guille, M. M. (1988). "Twisted plywood architecture of collagen fibrils in human compact bone osteons." Calcif Tissue Int **42**(3): 167-80.
Giraud-Guille, M. M. (1989). "Liquid crystalline phases of sonicated type I collagen." Biol Cell **67**(1): 97-101.
Giraud-Guille, M. M., L. Besseau, et al. (2003). "Liquid crystalline assemblies of collagen in bone and in vitro systems." J Biomech **36**(10): 1571-9.
Giraud-Guille, M. M., G. Mosser, et al. (2008). "Liquid crystallinity in collagen systems in vitro and in vivo." Current Opinion in Colloid & Interface Science **13**(4): 303-313.
Glass-Brudzinski, J., D. Perizzolo, et al. (2002). "Effects of substratum surface topography on the organization of cells and collagen fibers in collagen gel cultures." J Biomed Mater Res **61**(4): 608-18.
Gordon, M. K., D. R. Gerecke, et al. (1987). "Type XII collagen: distinct extracellular matrix component discovered by cDNA cloning." Proc Natl Acad Sci U S A **84**(17): 6040-4.
Graham, H. K., D. F. Holmes, et al. (2000). "Identification of collagen fibril fusion during vertebrate tendon morphogenesis. The process relies on unipolar fibrils and is regulated by collagen-proteoglycan interaction." J Mol Biol **295**(4): 891-902.

Gross, J. (1958). "Studies on the formation of collagen. I. Properties and fractionation of neutral salt extracts of normal guinea pig connective tissue." J Exp Med **107**(2): 247-63.
Gross, J. (1958). "Studies on the formation of collagen. II. The influence of growth rate on neutral salt extracts of guinea pig dermis." J Exp Med **107**(2): 265-77.
Gross, J., J. H. Highberger, et al. (1954). "Collagen Structures Considered as States of Aggregation of a Kinetic Unit. the Tropocollagen Particle." Proc Natl Acad Sci U S A **40**(8): 679-88.
Guo, C. and L. J. Kaufman (2007). "Flow and magnetic field induced collagen alignment." Biomaterials **28**(6): 1105-14.
Harris, J. R. and A. Reiber (2007). "Influence of saline and pH on collagen type I fibrillogenesis in vitro: fibril polymorphism and colloidal gold labelling." Micron **38**(5): 513-21.
Hauschka, S. D. and I. R. Konigsberg (1966). "The influence of collagen on the development of muscle clones." Proc Natl Acad Sci U S A **55**(1): 119-26.
Highberger, J. H., J. Gross, et al. (1951). "The interaction of mucoprotein with soluble collagen; an electron microscope study." Proc Natl Acad Sci U S A **37**(5): 286-91.
Holden, P., R. S. Meadows, et al. (2001). "Cartilage oligomeric matrix protein interacts with type IX collagen, and disruptions to these interactions identify a pathogenetic mechanism in a bone dysplasia family." J Biol Chem **276**(8): 6046-55.
Huang, Y. and K. M. Meek (1999). "Swelling studies on the cornea and sclera: the effects of pH and ionic strength." Biophys J **77**(3): 1655-65.
Hulmes, D. J., T. J. Wess, et al. (1995). "Radial packing, order, and disorder in collagen fibrils." Biophys J **68**(5): 1661-70.
Hulmes, D. J. S. (2008). Collagen Diversity, Synthesis and Assembly. Collagen**:** 15-47.
Jiang, F., H. Horber, et al. (2004). "Assembly of collagen into microribbons: effects of pH and electrolytes." J Struct Biol **148**(3): 268-78.
Kadler, K. (2004). "Matrix loading: assembly of extracellular matrix collagen fibrils during embryogenesis." Birth Defects Res C Embryo Today **72**(1): 1-11.
Kadler, K. E., C. Baldock, et al. (2007). "Collagens at a glance." J Cell Sci **120**(Pt 12): 1955-8.
Kadler, K. E., Y. Hojima, et al. (1987). "Assembly of collagen fibrils de novo by cleavage of the type I pC-collagen with procollagen C-proteinase. Assay of critical concentration demonstrates that collagen self-assembly is a classical example of an entropy-driven process." J Biol Chem **262**(32): 15696-701.
Kadler, K. E., D. F. Holmes, et al. (1996). "Collagen fibril formation." Biochem. J. **316**(1): 1-11.
Kleinman, H. K., L. Luckenbill-Edds, et al. (1987). "Use of extracellular matrix components for cell culture." Anal Biochem **166**(1): 1-13.
Klug, W. S., M. R. Cummings, et al. (1997). Concepts of genetics. Upper Saddle River, N.J., Prentice Hall.
Komai, Y. and T. Ushiki (1991). "The three-dimensional organization of collagen fibrils in the human cornea and sclera." Invest Ophthalmol Vis Sci **32**(8): 2244-58.
Konigsberg, I. R. (1963). "Clonal analysis of myogenesis." Science **140**: 1273-84.
Koster, S., J. B. Leach, et al. (2007). "Visualization of flow-aligned type I collagen self-assembly in tunable pH gradients." Langmuir **23**(2): 357-9.

Kuc, I. M. and P. G. Scott (1997). "Increased diameters of collagen fibrils precipitated in vitro in the presence of decorin from various connective tissues." Connect Tissue Res **36**(4): 287-96.
Kuznetsova, N. and S. Leikin (1999). "Does the triple helical domain of type I collagen encode molecular recognition and fiber assembly while telopeptides serve as catalytic domains? Effect of proteolytic cleavage on fibrillogenesis and on collagen-collagen interaction in fibers." J Biol Chem **274**(51): 36083-8.
Lanfer, B., U. Freudenberg, et al. (2008). "Aligned fibrillar collagen matrices obtained by shear flow deposition." Biomaterials **29**(28): 3888-95.
Lee, P., R. Lin, et al. (2006). "Microfluidic alignment of collagen fibers for in vitro cell culture." Biomed Microdevices **8**(1): 35-41.
Lepescheux, L. (1988). "Spatial organization of collagen in annelid cuticle: order and defects." Biol Cell **62**(1): 17-31.
Leung, M. K., L. I. Fessler, et al. (1979). "Separate amino and carboxyl procollagen peptidases in chick embryo tendon." J Biol Chem **254**(1): 224-32.
Linsenmayer, T. F., J. M. Fitch, et al. (1983). "Monoclonal antibodies against chicken type V collagen: production, specificity, and use for immunocytochemical localization in embryonic cornea and other organs." J Cell Biol **96**(1): 124-32.
Marion K. Gordon, J. W. F. T. F. L. J. M. F. (1996). "Temporal expression of types XII and XIV collagen mRNA and protein during avian corneal development." Developmental Dynamics **206**(1): 49-58.
Martin, G. R. and H. K. Kleinman (1981). "Extracellular matrix proteins give new life to cell culture." Hepatology **1**(3): 264-6.
Martin, R., J. Farjanel, et al. (2000). "Liquid crystalline ordering of procollagen as a determinant of three-dimensional extracellular matrix architecture." J Mol Biol **301**(1): 11-7.
Matthews, J. A., G. E. Wnek, et al. (2002). "Electrospinning of collagen nanofibers." Biomacromolecules **3**(2): 232-8.
McLaughlin, J. S., T. F. Linsenmayer, et al. (1989). "Type V collagen synthesis and deposition by chicken embryo corneal fibroblasts in vitro." J Cell Sci **94 (Pt 2)**(Pt 2): 371-9.
Meek, K. M., J. E. Scott, et al. (1985). "An X-ray diffraction analysis of rat tail tendons treated with Cupromeronic Blue." J Microsc **139**(Pt 2): 205-19.
Mellor, S. J., G. L. Atkins, et al. (1990). "A Kinetic Analysis of Type I Procollagen Processing in Developing Chick Embryo Cornea." Annals of the New York Academy of Sciences **580**(1): 484-488.
Miles, C. A. and M. Ghelashvili (1999). "Polymer-in-a-box mechanism for the thermal stabilization of collagen molecules in fibers." Biophys J **76**(6): 3243-52.
Mould, A. P. and D. J. Hulmes (1987). "Surface-induced aggregation of type I procollagen." J Mol Biol **195**(3): 543-53.
Naughton, G. K. (2002). "From lab bench to market: critical issues in tissue engineering." Ann N Y Acad Sci **961**: 372-85.
Neame, P. J., C. J. Kay, et al. (2000). "Independent modulation of collagen fibrillogenesis by decorin and lumican." Cell Mol Life Sci **57**(5): 859-63.
Ottani, V., D. Martini, et al. (2002). "Hierarchical structures in fibrillar collagens." Micron **33**(7-8): 587-96.

Prockop, D. and D. Hulmes (1994). Assembly of collagen fibrils de novo from soluble precursors: Polymerization and copolymerization of procollagen, pN-collagen, and mutated collagens. Extracellular Matrix Assembly and Structure. B. D. Yurchenco PD, Mecham RP. San Diego, Academic Press, Inc**:** 47-90.

Rada, J. A., P. K. Cornuet, et al. (1993). "Regulation of corneal collagen fibrillogenesis in vitro by corneal proteoglycan (lumican and decorin) core proteins." Exp Eye Res **56**(6): 635-48.

Ramachandran, G. N. (1956). "Structure of collagen." Nature **177**(4511): 710-1.

Ramachandran, G. N. and G. Kartha (1954). "Structure of collagen." Nature **174**(4423): 269-70.

Ramachandran, G. N. and G. Kartha (1955). "Structure of collagen." Nature **176**(4482): 593-5.

Ramachandran, G. N. and V. Sasisekharan (1961). "Structure of collagen." Nature **190**: 1004-5.

Regini, J. W., G. F. Elliott, et al. (2004). "The ordering of corneal collagen fibrils with increasing ionic strength." J Mol Biol **336**(1): 179-86.

Rosso, F., A. Giordano, et al. (2004). "From cell-ECM interactions to tissue engineering." J Cell Physiol **199**(2): 174-80.

Ruberti, J. W. and J. D. Zieske (2008). "Prelude to corneal tissue engineering - gaining control of collagen organization." Prog Retin Eye Res **27**(5): 549-77.

Schonherr, E., C. Sunderkotter, et al. (2004). "Decorin deficiency leads to impaired angiogenesis in injured mouse cornea." J Vasc Res **41**(6): 499-508.

Scott, J. E. (1988). "Proteoglycan-fibrillar collagen interactions." Biochem J **252**(2): 313-23.

Scott, J. E. (1990). "Proteoglycan:collagen interactions and subfibrillar structure in collagen fibrils. Implications in the development and ageing of connective tissues." J Anat **169**: 23-35.

Scott, J. E. (1991). "Proteoglycan: collagen interactions and corneal ultrastructure." Biochem Soc Trans **19**(4): 877-81.

Scott, J. E. (1995). "Extracellular matrix, supramolecular organisation and shape." J Anat **187 (Pt 2)**(Pt 2): 259-69.

Scott, J. E. and M. Haigh (1985). "'Small'-proteoglycan:collagen interactions: keratan sulphate proteoglycan associates with rabbit corneal collagen fibrils at the 'a' and 'c' bands." Biosci Rep **5**(9): 765-74.

Scott, J. E. and M. Haigh (1988). "Keratan sulphate and the ultrastructure of cornea and cartilage: a 'stand-in' for chondroitin sulphate in conditions of oxygen lack?" J Anat **158**: 95-108.

Scott, J. E., C. R. Orford, et al. (1981). "Proteoglycan-collagen arrangements in developing rat tail tendon. An electron microscopical and biochemical investigation." Biochem J **195**(3): 573-81.

Scott, J. E. and A. M. Thomlinson (1998). "The structure of interfibrillar proteoglycan bridges (shape modules') in extracellular matrix of fibrous connective tissues and their stability in various chemical environments." J Anat **192 (Pt 3)**: 391-405.

Shaw, L. M. and B. R. Olsen (1991). "FACIT collagens: diverse molecular bridges in extracellular matrices." Trends Biochem Sci **16**(5): 191-4.

Sini, P., A. Denti, et al. (1997). "Role of decorin on in vitro fibrillogenesis of type I collagen." Glycoconj J **14**(7): 871-4.
Song, J., Y. G. Lee, et al. (2003). "Neonatal corneal stromal development in the normal and lumican-deficient mouse." Invest Ophthalmol Vis Sci **44**(2): 548-57.
Tanihara, H., M. Inatani, et al. (2002). "Proteoglycans in the eye." Cornea **21**(7 Suppl): S62-9.
Thur, J., K. Rosenberg, et al. (2001). "Mutations in cartilage oligomeric matrix protein causing pseudoachondroplasia and multiple epiphyseal dysplasia affect binding of calcium and collagen I, II, and IX." J Biol Chem **276**(9): 6083-92.
Trelstad, R. L. (1982). "The bilaterally asymmetrical architecture of the submammalian corneal stroma resembles a cholesteric liquid crystal." Dev Biol **92**(1): 133-4.
Trelstad, R. L. and K. Hayashi (1979). "Tendon collagen fibrillogenesis: intracellular subassemblies and cell surface changes associated with fibril growth." Dev Biol **71**(2): 228-42.
van der Rest, M. and R. Garrone (1991). "Collagen family of proteins." Faseb J **5**(13): 2814-23.
Vaughan, L., M. Mendler, et al. (1988). "D-periodic distribution of collagen type IX along cartilage fibrils." J Cell Biol **106**(3): 991-7.
Vesentini, S., A. Redaelli, et al. (2005). "Estimation of the binding force of the collagen molecule-decorin core protein complex in collagen fibril." Journal of Biomechanics **38**(3): 433-443.
Wagner, D. R. and J. C. Lotz (2004). "Theoretical model and experimental results for the nonlinear elastic behavior of human annulus fibrosus." Journal of Orthopaedic Research **22**(4): 901-909.
Weber, I. T., R. W. Harrison, et al. (1996). "Model structure of decorin and implications for collagen fibrillogenesis." J Biol Chem **271**(50): 31767-70.
Wenstrup, R. J., J. B. Florer, et al. (2004). "Type V collagen controls the initiation of collagen fibril assembly." J Biol Chem **279**(51): 53331-7.
Wess, T. J. (2008). Collagen Fibrillar Structure and Hierarchies. Collagen**:** 49-80.
Wilson, D. L., R. Martin, et al. (2001). "Surface organization and nanopatterning of collagen by dip-pen nanolithography." Proc Natl Acad Sci U S A **98**(24): 13660-4.
Wood, G. C. (1964). "The precipitation of collagen fibers from solution." Int Rev Connect Tissue Res **2**: 1-31.
Yang, G. C. and D. E. Birk (1986). "Topographies of extracytoplasmic compartments in developing chick tendon fibroblasts." J Ultrastruct Mol Struct Res **97**(1-3): 238-48.
Yoshizato, K., T. Obinata, et al. (1981). "In Vitro Orientation of Fibroblasts and Myoblasts on Aligned Collagen Film." Development, Growth & Differentiation **23**(2): 175-184.

Chapter 2

Investigation of the Influence of Shear Stress on Self-Assembling Collagen Monomers and Production of Aligned Layers of Collagen Fibrils

Introduction

Collagen is the most abundant protein in vertebrates. It is the main tensile load-bearing molecule in the body and therefore, serves as the building block of the load-bearing tissues. Fibrillar collagens are the main component of the extracellular matrix (ECM). Along with other ECM macromolecules (e.g. fibronectin and proteoglycans) collagen fibrils provide a framework within which cells may attach and spread. Cell signaling, communication and motility may be achieved through cell-matrix adhesion and interaction (Giancotti 1997; Rosso, Giordano et al. 2004).

In animal tissues, load-bearing ECM typically comprises 3D arrangements of collagen fibrils in which the collagen organization reflects the tissue's mechanical function. Fibril forming collagens (i.e. I-III, V, XI) are the main load-bearing components of the ECM. These fibrils are characterized by their 67 nm periodic stritations (for review (Vuorio and de Crombrugghe 1990; Boot-Handford, Tuckwell et al. 2003)). The members of this group spontaneously assemble into fibers, fibrils, and bundles; bundles are eventually assembled into the higher order lamellae. It is notable that both the large scale and ultrastructure of the lamellae are well-adapted to match the functions of the

tissues. For example, to carry tensile load, collagen fibrils in tendon are organized into parallel bundles in the direction of the load. Corneal stroma demonstrates the highest level of ultrastructural organization in vertebrate animals. The collagenous matrix in cornea is composed of aligned fibrillar arrays of monodisperse diameter fibrils arranged in nematic stacks of alternating lamellae. The lamellae form a series of nested spherical shells which resist the biaxial tension produced by pressure within the ocular globe (15 mmHg). In humans, adjacent nested lamellae are typically oriented at right angles. To facilitate transparency, collagen fibrils in cornea have a monodisperse diameter (32.2±1 nm in human (Daxer, Misof et al. 1998)) and are uniformly distributed (61.9±4.5 nm center-to-center spacing in human (Gyi, Meek et al. 1988)). The natural selection of collagen as the molecule of choice for load-bearing tissues and minor changes in the collagen structure during evolution signifies the unique physiochemical properties of this molecule. Since collagen is widely distributed in vertebrates, using the methods developed to extract it from animal tissues (e.g. skin, cornea, and tendon), this molecule is readily available to the researchers. These unique characteristics distinguish collagen as an excellent candidate for tissue engineering. Therefore, gaining control over collagen organization and ultrastructure is of significant importance.

In this chapter, the influence of shear flow on the alignment and dynamics of the self-assembly of collagen molecules is presented. Two experimental setups have been designed and used to generate the shear flow. In the first method (section 2.1), using a microchannel, the effects of shear stress on the alignment and dynamics of self-assembled collagen molecules was studied. In the second method (section 2.2), using spin-coating method, the effects of the shear flow on the self-assembly of the confined

solution of molecules was investigated. At the end (section 2.3), using the optimal parameters developed for aligning collagen, a series of experiments were designed to organize collagen fibrils on polycarbonate membranes to be used as an organized template for cell culturing (as a tool for corneal tissue engineering).

2.1. Organization and Dynamics of Collagen Self-assembly Under the Influence of a Shearing Flow

The goal of this investigation was to produce aligned layers of collagen fibrils using shear flow. In addition, timelapse microscopy was used to investigate the dynamics of collagen self-assembly. An on-stage microchamber was employed to produce the shear flow. The dynamics of self-assembly at different shear rates were captured using Live Dynamic Differential Interference Contrast (LDDIC) microscopy. The morphology of the assembled fibrils was investigated by Quick-Freeze, Deep-Etch (QFDE) method, a high resolution electron microscopy technique.

2.1.1. *Materials and Methods*

2.1.1.1. Experimental Apparatus

Figure 2-1 represents the detailed experimental setup and apparatus for this experiment. Type I, pepsin extracted collagen solution (3mg/ml, Advanced BioMatrix, Inc., San Diego, CA) was injected into a temperature controlled (37°C) FCS2 perfusion chamber (Bioptechs Inc., Butler, PA) using a PHD-2000 syringe pump (Harvard Apparatus, Holliston, MA) at a rate of 36 ml/hr. Pepsin digestion is a widely used method to solubilize collagen molecules. This method however results in the removal of the telopeptides from the ends of the native collagen molecules (Bornstein and Sage 1980). The telopeptides are short (accounting for 2% of the molecules), nonhelical regions located at each end of the central helical region of collagen molecules (for review (Kadler, Holmes et al. 1996)). They have been shown to be the main sites of interfibrillar cross-linking, providing mechanical strength to the fibrils and tissues. In addition to the

mechanical strength, they have shown to be critical in fibril formation. Removal of one or both of the terminals has been linked to the formation of fibrils with nonuniform diameters, periodic striation patterns other than native 67 nm D-banding (Gelman, Poppke et al. 1979). As noted by Gelman et. al. (Gelman, Poppke et al. 1979), although pepsin digested collagen molecules result in the formation of the fibrils with abnormal

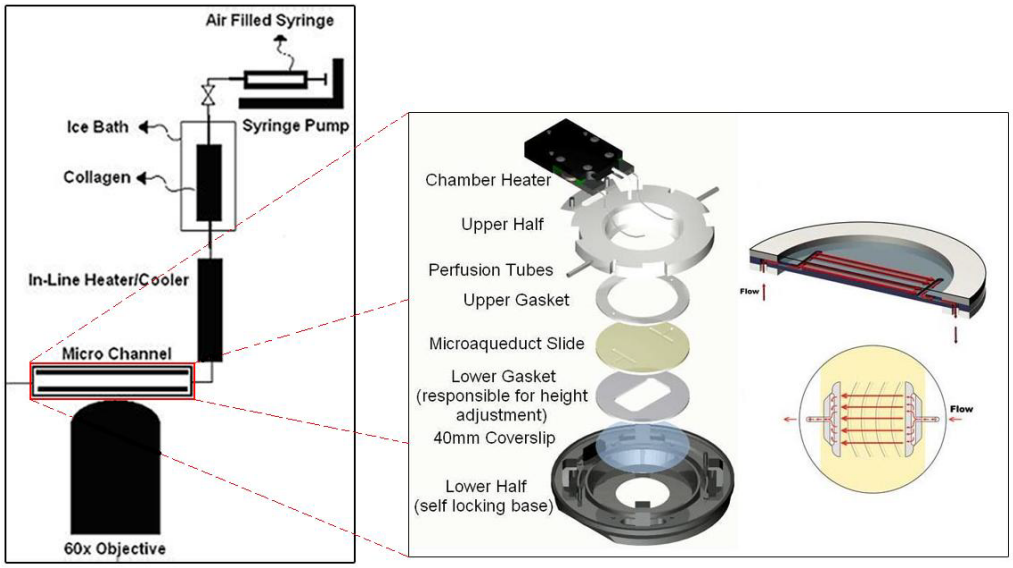

Figure 2-22: Schematic of the experimental setup and the microchamber. The magnified section shows the details of the microaqueduct slide, gasket, and perfusion tubes. The microchamber image is from http://www.bioptechs.com/

morphology, the formation of the fibrils from atelo-collagen molecules indicates that the required information for collagen self-assembly is inherent within the 300nm helical region of the molecules.

Considering these observation and accessibility of the pepsin extracted collagen (i.e. commercially available in large quantities), this form of collagen was chosen as the source of collagen molecules for these studies. The FCS2 chamber was composed of a top micro-aqueduct glass slide (Figure 2-1) with ports for inlet and outlet, a silicon rubber 12x24mm gasket, and a bottom coverslip. Since collagen self-assembly is a very

temperature sensitive process (Kadler, Hojima et al. 1988), it was necessary to keep the temperature history of the solution similar at all the shear rates. Therefore, instead of changing the flow rate to vary the shear rate, gaskets with different thickness were used to change the height of the microchamber. Also, a PID controlled SC-20 dual inline heater-cooler peltier (Harvard Apparatus, Holliston, MA) was used to preheat the solution to 37°C prior to the chamber entrance port (Fig. 1). To produce calculated shear rates of 500, 80, 20, and 9 s^{-1}, 100, 250, 500, and 750 μm height gaskets were used, respectively (Table 2-2).

2.1.1.2. Time-lapse Studies

Timelapse Differential Interference Contrast (DIC) (Guo, Hutcheon et al. 2007) microscopy (TE2000E; Nikon [Microvideo Instruments, Avon, MA]) was performed to observe and capture the dynamics of collagen self-assembly in the shear flow. DIC is a light microscopy method that relies on the enhancement of the differences in the index of refraction of the transparent specimen. Therefore, it is capable of detecting structures well-below the wavelength of light (Allen, Allen et al. 1981) and has excellent out-of-plane rejection.

Figure 2-2 is an illustration of a Nikon TE2000-E inverted microscope equipped with DIC module. From the top, the DIC column is composed of a light source, polarizer, Upper Nomarski modified Wollaston prism, condenser lens, objective lens, Lower Nomarski modified Wollaston prism, and analyzer (similar to the polarizer). The Wollaston prism separates the polarized light into two orthogonal rays. The two rays are in phase but spatially separated and vibrating at 90° apart. For a full illumination, the two rays are focused on the specimen using the condenser lens. Due to the differences in

index of refraction or the thickness of the samples, optical path difference is created in ray pairs and after being magnified by the objective lens the ray pair will be then combined into one plane by passing through the Nomarski prism. Due to the phase differences between the two rays, the regions of the specimen, where the optical paths increase along a reference direction appear brighter (or darker), while regions where the path differences decrease appears in reverse contrast. Therefore, as the difference in the optical path between the two rays increases, the image contrast is dramatically increased.

As mentioned before, DIC imaging has a very good out of plane rejection properties. The changes in the refractive indices of the sample in the planes other than the

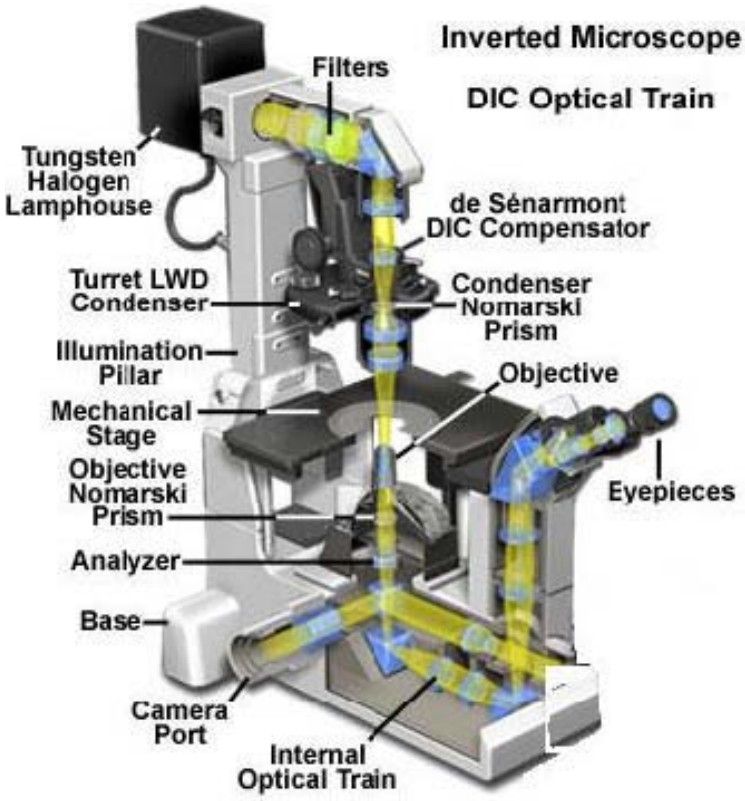

Figure 2-23: A schematic of Nikon TE2000 Inverted DIC microscope. Image from http://www.microscopyu.com/

plane of focus will be blurred and have a shallow spatial gradient in the focal plane and therefore their contribution to the final image will be minimal.

Since the goal of this investigation was to study the organization of the fibrils exactly on the coverlip, it was crucial to be able to lock the plane of focus. However, due to the small size of the fibril diameter, the DIC microscopy was performed using a 60x objective which has a very small depth of focus. Therefore, any temperature perturbation or vibration would result in the lost of the plane of focus. To solve this problem a Nikon perfect focus system (PFS®) was employed. This unit allowed us to lock the plane of focus to the glass coverslip with an advertised 50 nm resolution. The PFS system is designed to track the focus automatically such that the point of interest within a specimen is always kept in sharp focus no matter what mechanical or thermal changes take place. PFS uses an LED in the infrared range and an internal linear CCD detector, to detect the focal point, so it does not intrude on wavelengths used for observation. Thus it allows carrying out observation and maintaining focus at the same time, with negligible influence on captured images.

2.1.1.3. Quick-freeze, Deep-etch (QFDE) Microscopy

Several different methods have been developed to image biological samples (e.g. Transmission Electron Microscopy (TEM) and Scanning Electron Microscopy (SEM)). Due to the nature of these methods (i.e. interaction of electron with the specimen), they are predominantly performed on the dehydrated samples. The dehydration (or embedding process) could be potentially very destructive to the delicate structures of the biological samples. There have been a few techniques that have been developed to image samples in

their hydrated nature (e.g. Atomic Force Microscopy (AFM) and environmentally controlled SEM) but they all suffer from low resolution quality.

In an effort to image the hydrated samples, while preserving their native ultrastructures, QFDE method was developed by Heuser (Heuser, Reese et al. 1979). To preserve the hydrated structure of the samples, specimens are rapidly frozen to the liquid nitrogen temperature (-196ºC) (for review (Severs 2007). The rapid freezing prevents the formation of the ice crystals in the frozen surface of the samples which is destructive to the morphology of the samples. Depending on the method of freezing (i.e. plunge freezing, slam freezing, and high pressure freezing), the depth of the vitrified layer could range from 3 to 40 μm. Following the freezing, the excess water is sublaminated by increasing the temperature of the sample to -100ºC in a 10^{-7} torr vacuum chamber (i.e. etching step) which results in exposure of the fine structure of the tissue. The samples are usually etched for 12 minutes however this time could change depending on the nature of the sample. Platinum evaporation (at 12-45º and 2nm) and carbon evaporation (at 90º) is used to coat the exposed surface of the samples. Platinum coating is used to provide contrast and carbon coating is used to strengthen the replica.

The replica will be visualized using TEM, after the specimen is removed from the replica. This step is usually done by digesting the tissue in a liquid capable of dissolving the sample (in most cases bleach). Following a rinse in distilled (DI) water, the replicas are picked up using TEM grids which be directly transferred into a TEM, following air dehydration).

In this investigation, the coverslips were removed from the microchamber and rinsed with cold 1x Phosphate Buffered Saline (PBS) to stop the self-assembly and

remove the excess fluid from the coverslip. The coverslips were broken into smaller pieces (~2x2 mm) using razorblades and mounted onto a sample holder using a 10% Laponite solution (Rockwood Additives, Cheshire, UK). After mounting, the excess PBS was removed using filter paper and the sample was rapidly slam frozen onto a liquid nitrogen-cooled copper block using a Cryogun (DDK Inc., Wilmington, DE) and stored in liquid nitrogen. The frozen samples were transferred to a modified CFE-40 QFDE unit (Cressington scientific Instruments, Watford, UK) for replication. Samples were etched at -95°C for 30 minutes to remove vitrified ice. Samples were rotary coated at -125°C by evaporation of platinium/carbon at 20° angle for 12 seconds and pure carbon at 90° angle for 20 seconds (to strengthen the replica). Samples were transferred into household bleach to digest the collagen and rinsed with DI-water. Replicas were picked up on 600 mesh copper grids then viewed and digitally photographed with a JEOL transmission electron microscope (JEM 1010, Tokyo, Japan).

2.1.1.4. Fibrillar Growth Rate/Radius of Curvature Measurements

The NIH-Image J software was used to measure the growth rates and the radius of the curvature of collagen fibrils during polymerization. The growth of at least fifty randomly selected fibrils was tracked over a period of 5 minutes and the growth rates were reported as the mean ± SD.

2.1.1.5. Quantification of Fibrillar Alignment

Fibrillar orientation and alignment in LD-DIC images was assessed with a Fourier transform method described elsewhere (Chaudhuri, Nguyen et al. 1987; Sander and Barocas 2008). Briefly, images were imported into Matlab and a square region (1040 x

1040 pixels) from the center of the image was extracted. The 2-D discrete Fourier transform (DFT) of the image was obtained after the image gray scale intensity values were stretched across the full 8-bit range (0-255) and the image was filtered with a Welch window. Next, the power spectrum was band pass filtered with cutoff frequencies of 47 and 173, which correspond to fiber diameters of 11.1 and 3.0 pixels) to remove non-fibril related frequency content that arises from uneven background illumination, spurious signals from reflections, and high frequency noise. The remaining annular region was converted to polar coordinates and divided into 1° intervals to obtain number-averaged-line intensities, which were then rotated 90° degrees to give the fibril orientation distribution, $I(\theta)$, in the spatial domain. The mean angle of the distribution, μ, was calculated using circular statistics (Mardia and Jupp 2000) for centrally symmetric axial data according to the following equations:

$$a = \frac{\sum_{i=1}^{N} I(\theta_i)\cos(2\theta_i)}{\sum_{i=1}^{N} I(\theta_i)}, \quad b = \frac{\sum_{i=1}^{N} I(\theta_i)\sin(2\theta_i)}{\sum_{i=1}^{N} I(\theta_i)} \tag{1}$$

$$\mu = \begin{cases} \frac{1}{2}\tan^{-1}(b/a) & \text{if a } > 0 \\ \frac{1}{2}\left[\pi + \tan^{-1}(b/a)\right] & \text{if a } < 0 \end{cases} \tag{2}$$

To assess the strength of alignment in the images, $I(\theta)$, was converted to a second rank orientation tensor and the eigenvalues and eigenvectors were extracted to give the magnitudes and principal directions of orientation, respectively. The anisotropy index

provides a measure of the strength of alignment in the image and is defined as $\alpha = 1 - \lambda_1/\lambda_2$, where λ_1 and λ_2 are the minor and major eigenvalues, respectively. Under this convention, $\alpha = 1$ for a completely aligned network and $\alpha = 0$ for an isotropic network.

2.1.2. Results

2.1.2.1. LD-DIC

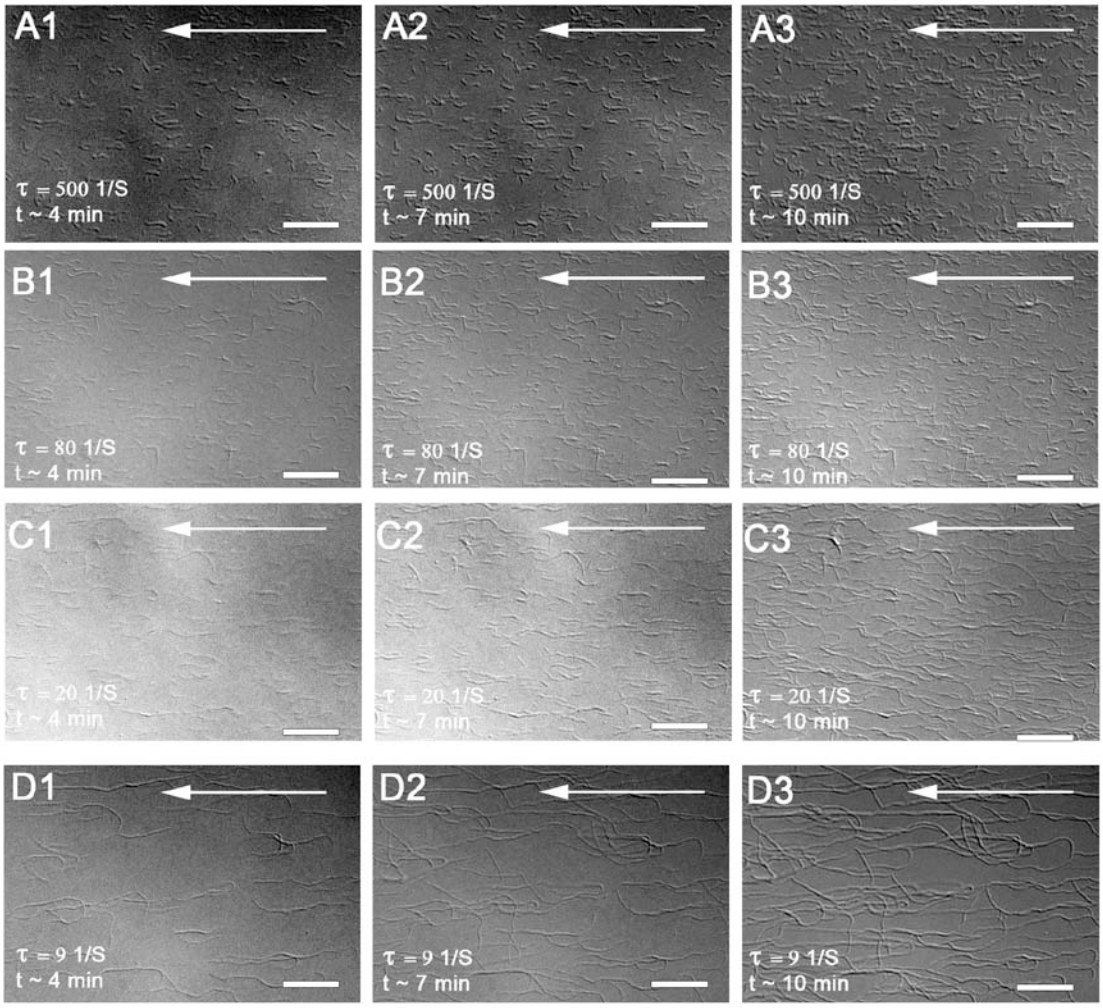

Figure 2-24: Serial DIC images of collagen fibrils self-assembly at 500, 80, 20 and 9 s-1 shear rates showing the fibrillar growth at the beginning (first columns, 1), middle (second columns, 2), and end of the experiments (third columns, 3). Flow is from right to left. Bars are 10 µm.

Collagen fibrils first appeared 180 ± 30 seconds after solution injection and fibrillar growth continued both in the longitudinal and lateral directions (Figure 2-3).

It should be mentioned that because of the resolution limit of the DIC (~25 nm), it is likely that the initial nucleation of fibrillar structures was not captured. The axial fibrillar growth rates were 0.05±0.01, 0.02±0.005 and 0.1±0.025 μm/s at 80, 20, and 9 s^{-1}

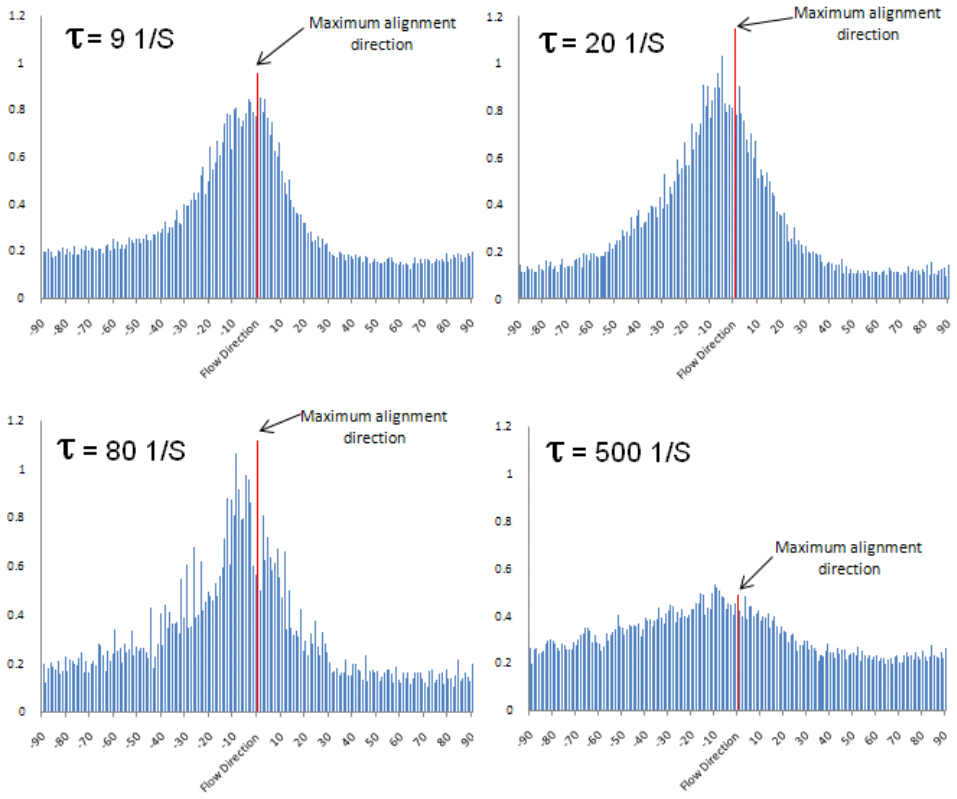

Figure 2-25: Showing the results of FTM on DIC images of self-assembled collagen fibrils at different shear rates of 500, 80, 20, and 9 S^{-1}

shear rates, respectively (Figure 2-6).

Due to the very short length of the fibrils, it was not possible to accurately measure the growth rate at 500 s^{-1}. At high shear rates collagen molecules were assembled into very short fibrils (2-3 μm at 500 s^{-1}, Figure 2-3A) and as the shear rate

decreased, the length of the fibrils increased. At 20 s^{-1} shear rate the fibrils were tens of μm in length. Greater fibril alignment was found for the 80 s^{-1} and 20 s^{-1} shear rates (Figure 2-4). At the highest shear rates (500 s^{-1}), collagen molecules formed very short and curly fibrils. Although the fibrils are generally aligned in the direction of the flow (Figure 2-6), the formation of "hooks" produced greater spread in the fibril orientation distribution and reduced the anisotropy index (Figure 2-4). At 9 s^{-1}, fibrils were tens of

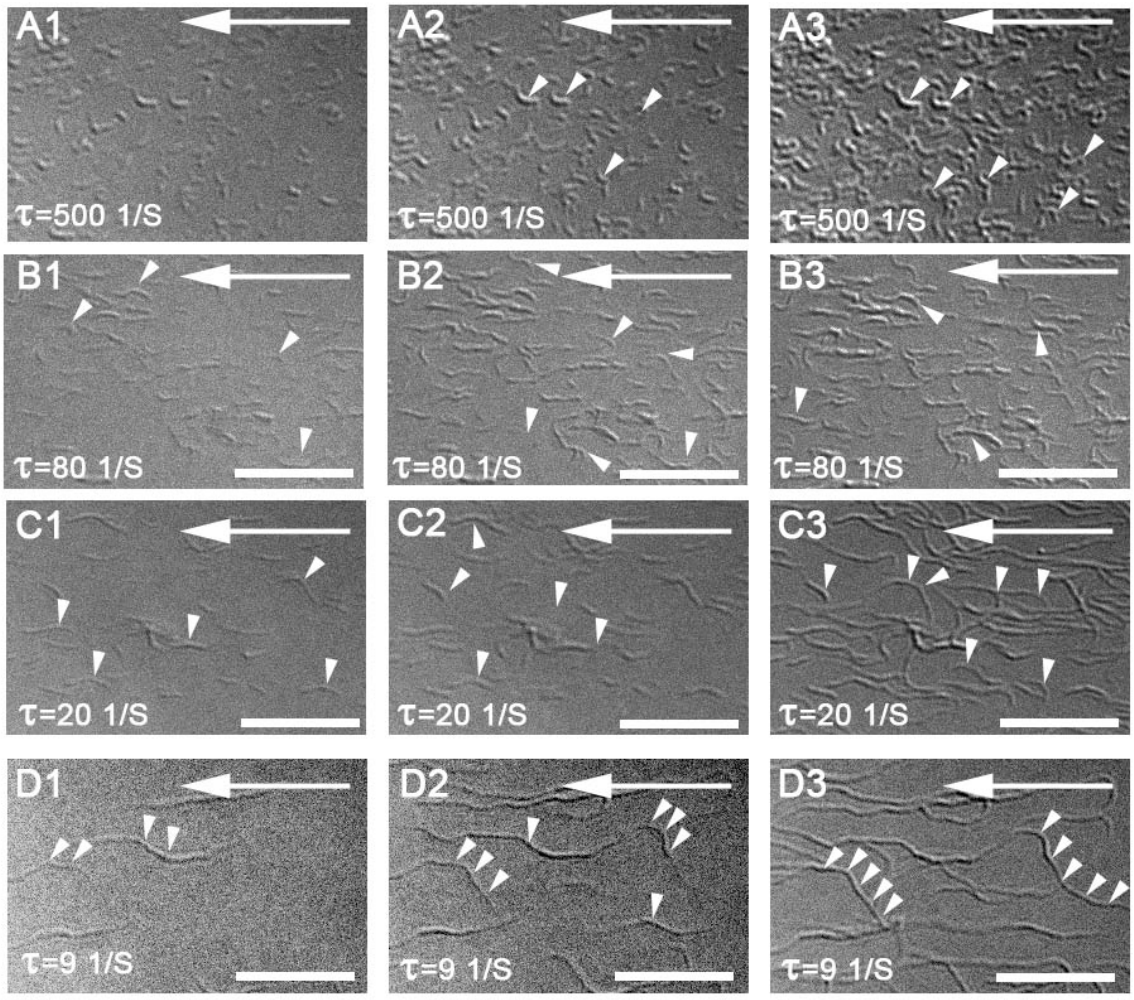

Figure 2-26: Higher magnification serial DIC images of collagen fibril self-assembly showing the different patterns of "hook" development at 500 (A1-3), 80 (B1-3), 20 (C1-3), and 9 (D1-3) S-1 shear rates. Bars are 10 μm.

μm in length but fibrils were loosely aligned in the flow direction (Figure 2-4).

DIC images also show some similarities between the patterns of collagen fibril

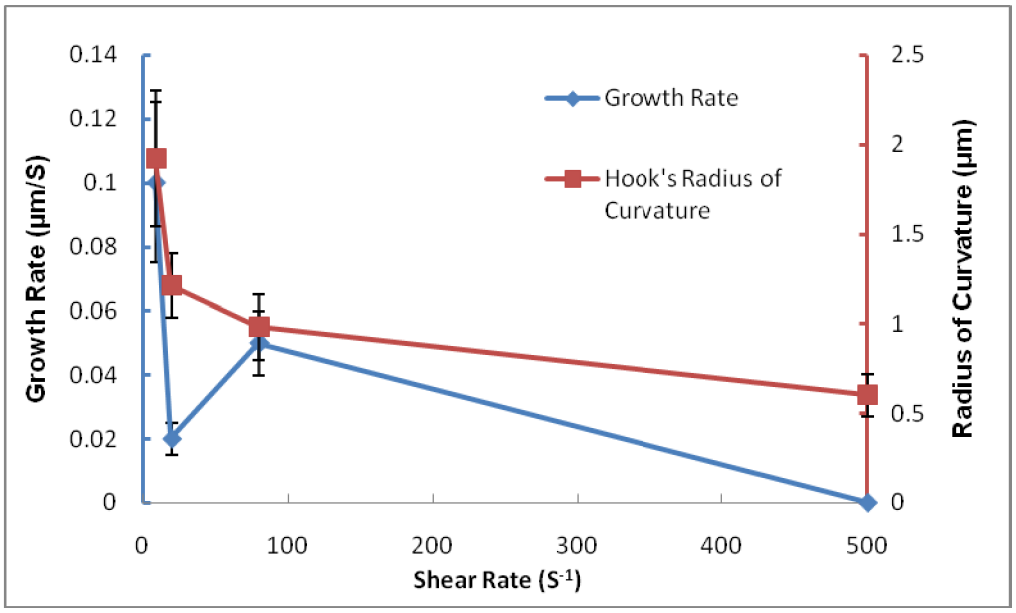

Figure 2-27: Plot of the growth rate and radius of the curvature of the "hooks" as a function of shear rate.

formation at different shear rates. At all shear rates, after growing in a roughly straight line along the flow direction, fibrils made an approximate 90° turn ("hooks", Figure 2-3 and Figure 2-5). At high shear rates the radius of the curvature of the hooks was small (0.6±0.12 μm) and fibrils made a complete 180° turn after which they continued growing in the opposite direction of the original fibril (i.e. downstream, Figure 2-5A1-A3). At lower shear rates, fibrils made larger loops and the radius of the curvature of the hooks increased to 0.98±0.18, 1.21±0.18, and 1.92±0.38 for 80, 20, and 9 s^{-1} shear rates, respectively (Figure 2-5).

The growth of the fibrils after the "hook", however, was different at various shear rates. At the high shear rates, fibrils often made a complete (180°) turn and continued

growing in the opposite direction. At lower shear rates, fibrils made an approximate 90° turn and growth continued either perpendicular to the flow (at the medium shear rate, Figure 2-5C) or even against the flow (low shear rates, Figure 2-5D).

Occasionally it was seen that the ends of growing fibrils were not tethered to the glass but instead were floating in the solution (data not shown). In these cases, the influence of the flow turned the free end of the fibril downstream. Eventually the fibril was tethered onto the glass and continued growing.

The number of fibrils formed (i.e. nucleation sites) was dependent also on shear rate (Table 2-1). At shear rates of 500 and 80 s^{-1}, the number of the fibrils formed after four minutes was two and three fold higher than for 20 and 9 s^{-1}, respectively.

Another interesting phenomenon seen with DIC and QFDE (Figure 2-7 and Figure 2-8D) was the merging and branching of the fibrils. Quite often it was seen that two short fibrils merged, or a single fibril branched into two or more separate fibrils.

Shear Rate	After 4 min	After 7 min	After 10 min
500	8.06±0.42	12.81±1.87	15.43±1.22
80	9.18±1.25	13.12±0.6	17.5±0.61
20	4.43±0.89	7.43±1.47	11.31±0.90
9	2.50±0.35	4.62±0.72	5.31±0.69

Table 2-1: Number of nucleation sites per 100 μm^2 for various shear rates at different time points

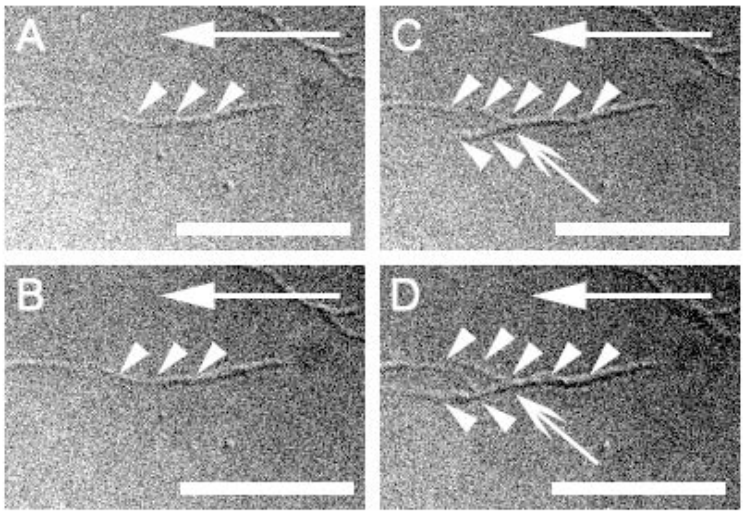

Figure 2-28: Composite DIC images showing the branching of the fibrils. Bars are 10 µm.

2.1.2.2. QFDE

QFDE images show that shear aligned collagen fibrils (and monomers) were tethered to the glass (Figure 2-8A, C, and D). The larger fibrils did not appear to have a circular cross section (possibly due to this strong surface interaction). Each fibril was comprised of 3-5 nm diameter microfibrils woven together (Figure 2-8A) to form "frayed", rope-like fibrillar aggregates. Microfibrils not associated with fibrils were also observed occasionally. These microfibrils formed unorganized "mats" on the glass surface between fibrils (Figure 2-8B).

The fibrillar alignment and behavior observed with DIC was confirmed with QFDE. Figure 2-8C shows hooks with a large radius of curvature characteristic of the low shear rate and hooks with a low radius of curvature characteristic of the high shear rate (Figure 2-8C inset). Figure 2-8D is a QFDE image showing the branching similar to that observed with DIC.

The fibrils assembled under the influence of shear stress did not exhibit the 67 nm D-banding pattern characteristic of native collagen fibrils (Figure 2-8A-D). The D-

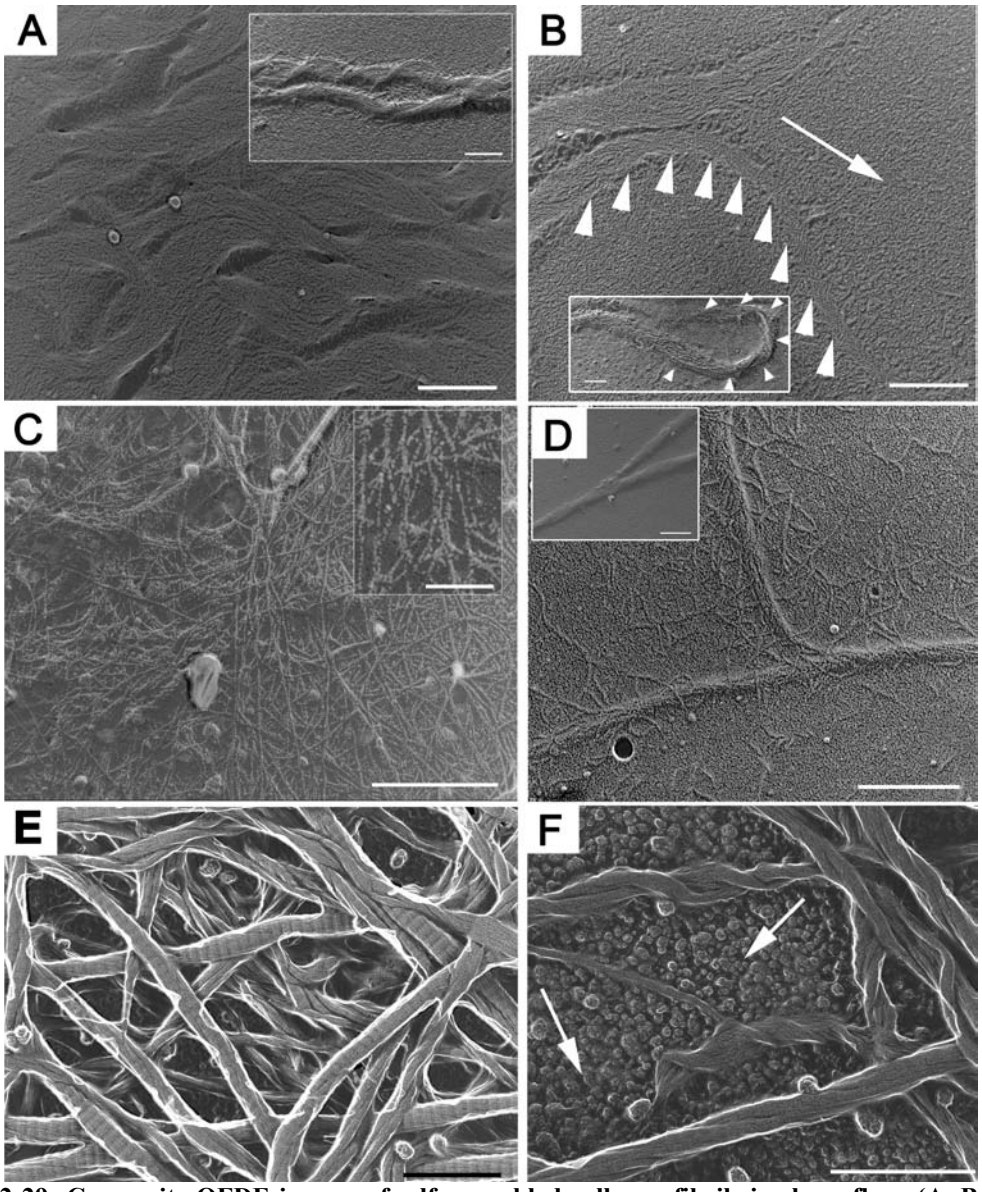

Figure 2-29: Composite QFDE images of self-assembled collagen fibrils in shear flow. (A, B and D) Rope-like fibrils were "frayed" in appearance. 2-5nm microfibrils can be clearly discerned. (B) Image shows "hooks" formed at a high shear rate. Microfibrils formed an unorganized mat (arrow) between fibrils. The inset shows a fibril which made a 180 turn and continued to grow in the opposite direction (arrow heads). (C) Regions of the sample with high density of the disorganized microfibrils. (D and the inset) Images show fibril branching. (E and F) The formation of D-banded fibrils when collagen molecules undergo self-assembly without flow. (F) Fibrils anchored to the coverslip. Arrows point to the glass surface. Bars in A-D are 100 nm (in 8B is 10 nm) and in E and F are 500nm.

banding is the result of the precise arrangement of molecules within each fibril (Meek,

Chapman et al. 1979). It is possible that applying shear stress to the monomers (and fibrils) may interfere with the normal fibril assembly. Also, it is possible that the interaction with the glass surface influences the molecular packing.

2.1.3. Discussion

Controlling the organization of collagen fibrils *in vitro* has been the topic of extensive research during the past few decades. More recently, and by development of micro-manufacturing methods, shearing flow of collagen molecules or fibrils has been used as a tool to align collagen fibrils (Lanfer, Freudenberg et al. 2008). Although this method has proven to be relatively successful, little is known about the dynamics of collagen self-assembly under such conditions. In this investigation we studied the dynamics and organization of collagen fibrils self-assembled under the influence of shear stress.

The process of shear-influenced self-assembly of collagen is extremely complex at the level of the monomer. There are three different physical processes simultaneously involved in this phenomenon: 1) Collagen accessibility to the surface (Taylor dispersion), 2) Hydrodynamic interactions between monomers and the solvent (alignment force), 3) Energetic interactions (between the glass surface/collagen and between collagen molecules and collagen aggregates - nucleation/adsorption:

1. Collagen accessibility to surface.

The diffusion of collagen monomers through the fluid and onto the coverslips provides a "source" of molecules necessary for surface coating and fibrillogenesis. The diffusion of the molecules is influenced by the convection velocity. Figure 2-9A is a schematic

representing the fluid dynamics inside the chamber. Since the width of the chamber is at least 10 times larger than the height of the chamber we can approximate the problem as 2-dimensional flow between two flat plates. Therefore, the flow field simplifies to a 2-D Poiseuille flow with the parabolic velocity profile of:

$$u = \frac{3Q}{4wh^3}\left(h^2 - y^2\right) \tag{3}$$

where

Q is the flow rate,

w is chamber width (12 mm),

and h is the chamber half height ($h = H/2$).

The values of the Reynolds (Re) number (Table 2-2) calculated from the eq. 4 show that Re << 1 and therefore the flow is of the form of a Stokes flow,

$$\mathrm{Re} = \frac{\rho \bar{U} D_h}{\mu} \tag{4}$$

where D_h is the hydraulic diameter (in this case H),

$\bar{U}$ is the average velocity ($\bar{U} = Q/wH$), and

μ is the dynamic viscosity of the solution (0.034 Pa.s, (Bueno and Ruberti 2008)).

A no-slip condition on the glass produces a shear stress and consequently shear rate on the glass (and in the flow) which are calculated according to the eq.5 and 6, respectively:

$$\tau = \mu \frac{\partial u}{\partial y} \tag{5}$$

$$\dot{\gamma} = 6\frac{\overline{U}}{H} = \frac{\tau}{\mu} \tag{6}$$

The maximum shear stress occurs on the coverslip and is calculated according to:

$$\tau_w = \frac{6\mu Q}{wH^2} \tag{7}$$

We start our analysis with the simple case of no flow (u = τ = 0). The movement of the molecules in solution (i.e. diffusion) is governed by a random walk (RW) process caused by the Brownian motion of the molecules. Based on the RW theory the average distance a molecule with diffusion coefficient D travels during time t would be:

$$d \sim \sqrt{D\,t} \tag{8}$$

Therefore the time required for a molecule to diffuse across the *H* of the channel would be:

$$t_{dif} \sim \frac{H^2}{D} \tag{9}$$

Given an average velocity of $\overline{U}$ in the channel we can calculate the time for a convected molecule to travel the length scale ℓ:

$$t_{conv} = \frac{wH\ell}{Q} \tag{10}$$

The ratio of these two time scales for a given length scale ℓ gives a measure of the ability of the diffusing molecule to reach the glass surface:

$$\frac{t_{dif}}{t_{conv}} = \frac{QH}{w\ell D} \tag{11}$$

This ratio is the dimensionless Peclet number (Pe). For Pe<<1, diffusion overcomes the convection and molecules can easily reach the surface. In contrast, for Pe>>1, convection dominates and collagen molecules pass through the chamber before they can diffuse onto the glass. In the latter case the process could become diffusion limited.

However, due to the velocity gradient in the transverse direction the effective dispersion of the molecules is enhanced in pressure-driven flows (Chatwin and Sullivan 1982) (Taylor dispersion (Taylor 1953)) according to :

$$D_{eff} = D + \frac{\overline{U}^2 H^2}{D} \mathrm{g}(shape, w/H) \tag{12}$$

where the dispersion coefficient *g,* is a function of the cross-sectional shape and aspect ratio of the molecule.

Ajdari et. al. showed that if the molecule residence time is larger than the time scale $\tau_D=w^2/D$, the dispersion in the longer dimension dominates (i.e. width of the channel) the dispersion in the shorter dimension (i.e. height) and therefore, in the effective diffusivity calculation (eq. 12), the height of the channel should be replaced with the width (Ajdari, Bontoux et al. 2006; Bontoux, Pepin et al. 2006). In these experiments, the average residence time of the collagen molecules in the microchannel for the slowest case is six orders of magnitudes smaller than the time-scale and therefore only the dispersion in the shorter length (i.e. height) is important. This reduces the problem to the dispersion of the molecules between two parallel plates for which *g* is

found to be 1/210. Using the Eq. 12 and the channel's dimensions, the new value of the diffusion coefficient was calculated to be 367 mm^2/s, as compared to 9E-6 mm^2/sec found for no flow conditions (Claire and Pecora 1997). It should be mentioned that using the same flow rate for different shear rates results in similar dispersivity at the different shear rates and therefore, monomers have the same accessibility to the surface at different shear rates. Therefore, for this series of experiments, the effective Peclet number was determined based on the effective dispersivity at each channel height.

Calculated values of Pe are given in Table 2-2. Because Pe was well below one (Pe = 2.27E-03 for all flow conditions), the flow was not diffusion limited, and a sufficient supply of monomer was available to the glass.

2a. Monomer/solvent interaction (in free solution)

The Weissenberg number (*Wi*) is a dimensionless number that has been extensively used as a measure of the flow strength over a polymer chain (Smith, Babcock et al. 1999):

$$Wi = \dot{\gamma}\varepsilon \tag{13}$$

where ε is the longest relaxation time of the polymer.

To compare the results of this investigation with the results of similar studies (e.g. on DNA), it was necessary to calculate the *Wi* number and hence, the relaxation of time of the collagen molecule. Since the equilibrium radius of a collagen molecule is smaller than the diffraction limit of the light, it was not possible to measure the relaxation time directly in this series of experiments. Therefore, to calculate *Wi* the equation for the longest relaxation time of a chain developed from the Rouse model (Larson, Hu et al. 1999; Joe, Eric et al. 2000) was used:

$$\varepsilon = \frac{\xi_{tot}\langle R^2\rangle_0}{6\pi^2 K_B T} \tag{14}$$

where ξ_{tot} is the drag coefficient, $\langle R\rangle_0$ is the molecule end-to-end distance, K_B is the Boltzmann constant, and T is the temperature.

The drag coefficient was calculated based on the Batchelor's theory of a slender body in Stokes flow (Li, Larson et al. 2000; Li, Hu et al. 2004; Batchelor 2006):

$$\xi_{tot} = \mu \frac{2\pi L}{\ln\left(\frac{L}{d}\right)} \tag{15}$$

where L and d are the molecule length and diameter, respectively.

The end-to-end distance was calculated according to:

$$\langle R^2\rangle_0 = b_K L \tag{16}$$

where b_K is the Kuhn Length of the chain. It is the length that satisfies the Brownian motion of the polymer. It has been found that the Kuhn length is twice the persistence length of the polymer ($b_K=2\ell_P$) (Kenji Kubota 1987). Therefore,

$$\langle R^2\rangle_0 = 2\ell_P L \tag{17}$$

Combining equations 14 to 17 with the parameters related to collagen (L = 300 nm (Sun, Luo et al. 2002), ℓ_p = 15 nm (Sun, Luo et al. 2002; Buehler and Wong 2007), d = 1.5nm, and T = 310 K), the longest relaxation time of collagen is 800 μs, which is much higher than the literature values of 117-160 μs (Yoshioka and O'Konski 1966; Ananthanarayanan and Veis 1972; J. C. Bernengo 1974; John C. Thomas 1979; Nestler, Hvidt et al. 1983). Since a flexible chain has a shorter relaxation time compared to a rigid rod, this difference could be due to the calculation of the drag coefficient, which is based on a rigid slender cylinder. These values are 250 times smaller than the relaxation time of λ-phage DNA (~2 S). Table 2-2 shows the calculated *Wi* number at different shear rates for a relaxation time of 800 μs. The *Wi* numbers are very small which indicates that the influence of the shearing flow is not strong enough for molecules the size of collagen.

H (mm)	Shear rate at the wall (1/s)	Pe	Re	Wi
0.1	500	2.27E-03	1.98E-04	3.91E-01
0.25	80	2.27E-03	4.96E-04	6.26E-02
0.5	20	2.27E-03	9.92E-04	1.56E-02
0.75	9	2.27E-03	1.49E-03	6.95E-03

Table 2-2: Values of average shear rates, shear rates at the wall, Peclet number (Pe), Reynolds number (Re), and Weissenberg number (Wi)

Collagen molecules are semi-flexible chains. The molecular flexibility parameter is measured by the ratio of the square of the contour length to the mean square of the end-to-end distance of molecule at equilibrium (Larson, Hu et al. 1999). Therefore, collagen

molecules are much less flexible than many other natural (e.g. 150 for DNA) and synthetic polymers. The results of both Brownian dynamic simulations and experimental studies of the semi-flexible polymers in a shear flow produced between two nonadsorbing surfaces show two depletion regions in the profile of polymer concentration across the channel height (Li, Hu et al. 2004; Saintillan, Shaqfeh et al. 2006). The first depletion region near the bounding surface is due to the hydrodynamic interactions which result in the migration of the molecules toward the center of the channel. Even under no flow ($Wi = 0$) this depletion zone exists. Increasing the Wi number increases the thickness of this layer. For $Wi < 100$ the nondimensionalized depletion thickness (ratio of the thickness to the radius of gyration) is a linear function of the Weissenberg number. The second depletion region located at the centerline is due to non-uniform stretching of the polymer in the inhomogeneous shear gradient. The maximum chain stretching occurs in an intermediate region between the centerline and the coverslip (Saintillan, Shaqfeh et al. 2006). The chain configuration in the flow will stochastically vary from a stretched state to coiled state, as predicted by De Gennes and which was shown experimentally for DNA (De Gennes 1974; Smith, Babcock et al. 1999). Although the fluctuations were initially attributed principally to the rotational component of the shear (De Gennes 1974) the stochastic nature of the fluctuations (as opposed to a periodic motion of the molecules) indicate that Brownian motion of the molecules is also involved (Smith, Babcock et al. 1999). Figure 2-9B is a schematic representation of the dynamics of the chain conformation in the flow based on the prediction of Smith et. al. (Smith, Babcock et al. 1999) for the DNA dynamic in the shear flow. The velocity gradient in y-direction produces a differential drag force across the chain, which causes the chain to stretch and

align in the flow direction in order to reduce drag (Figure 2-9B-c). Any perturbation in the chain due to the Brownian motion, the rotational component of the flow, and entropic forces will re-expose the chain to the velocity gradient (Figure 2-9B-d) resulting in stretching of the coil (Figure 2-9 and Figure 2-9B-c) or production of chain instability which will recoil the chain (Figure 2-9B-e). Thus, collagen molecules in the free solution shearing flow will undergo this stretch-recoiling-cycling and will avoid the surfaces and the centerline of the channel.

2b. Monomer/solvent interaction (tethered molecule)

Another contributing factor to the fibril formation observed in these studies involved the mechanism by which monomer and forming fibrils adsorbed to the glass. Here, we assume that one end of the collagen molecule attaches to the glass (Figure 2-9C), which allows us to reduce the problem to the case of a tethered semi-flexible molecule in shear flow. Similar to the polymer configuration in the bulk flow, the molecules undergo cyclic fluctuations (Ladoux and Doyle 2000; Rzehak, Kromen et al. 2000). After a collagen molecule becomes tethered to the glass (Figure 2-9C-a) the molecule will experience an increased drag force (due to the increased relative fluid velocity), which produces stretching and rotation towards the surface in the direction of the flow (Figure 2-9C-b and c). As the chain rotates toward the glass, the drag-related stretching force decreases (due to reduced solvent velocity) and the chain begins to recoil. At this point the molecule will either be repelled (due to exclusion effects) or adsorbed (due to the surface energy effects). If it does not adsorb, the chain will fluctuate and move further from the glass surface (Figure 2-9C-d and e). This will expose the chain to a higher fluid velocity induced stretch and it will cycle through b-e again. This cycle will continue until the

chain is adsorbed by a local surface (i.e. glass or a forming fibril). The experiments on the dynamics of DNA in the shear flow next to an absorbing surface demonstrate that the stretch of a molecule, <X>, is approximately 3 fold less than the stretch of the molecules in the bulk solution (<X>/L =0.15 compared to <X>/L = 0.4) (Li, Hu et al. 2004). In addition, the plot of the chain extension versus *Wi* reaches a plateau for small *Wi*, which indicates that very weak flows (~ *Wi* =10) are capable of stretching of the molecules. Dynamic simulations of a tethered DNA molecule in shear flow showed that depending on the *Wi* number, three regimes of chain conformation are possible. For *Wi*<1, the chain is slightly stretched with small fluctuations. For 1<*Wi*<20, both extension and fluctuations of the chain increase. For *Wi*>20, the extension is maximized but the fluctuation decreases. In this series of experiments the *Wi* (for single collagen molecules) was less than unity, which indicates that the collagen would only be slightly stretched by the shearing flow.

Scaling methods allow the prediction of the chain configuration of semi-flexible polymers (Gennes 1979). Ladoux and Doyle developed a model to explain the fluctuations of a tethered DNA chain next to the wall (Ladoux and Doyle 2000) based on this method. The chain extension in the flow is the balance the hydrodynamic force with the force, *f*, required to keep the ends at a separation distance of ℓ:

$$f \cong \xi \dot{\gamma} \delta y \tag{18}$$

where

δy is the chain's displacement in the y direction and

ξ is the drag coefficient.

Defining κ as the un-stretched fraction of the chain's length $\kappa = (1 - \ell / L)$, they reached the following asymptotic relation for *f*, δy, and κ for worm-like chain (WLC):

$$f \sim \kappa^{-2} \tag{19}$$

$$\delta y \sim \kappa \tag{20}$$

$$\kappa \sim \dot{\gamma}^{-1/3} \tag{21}$$

Therefore, increasing the shear rate causes larger extension of the chain in the flow, but the relationship is weak.

It should be mentioned that WLC is one of the ideal models (along with the freely-joined chain, FJC, and freely-rotating chain models) used to describe the configuration behavior of the polymer chains. This theory assumes that the chains are semi-flexible and composed of the monomers with persistent length ℓ_P. Therefore, for the lengths below the persistent length polymers act like rigid body which makes this model suited for less flexible polymers. In addition, in contrast to the FJC model, bending of the WLC polymer requires energy and the probabilities of the torsion angles are proportional to Boltzmann coefficient. Because of these properties, WLC provides a better approximation to the real chains (compared to the other ideal chain models). However similar to other ideal models WLC suffers from neglecting of the excluded volume effects (i.e. interactions between monomers within a chain).

Aggregation in free solution. At the experimental conditions, collagen molecules have the potential to undergo spontaneous self-assembly in the flow or while tethered to the glass (prior to adsorption). Although the residence time of molecules in the system prior to entrance to the imaging area was in the order of 45 seconds (which is much shorter than the time required to assemble - as measured by turbidity (Kadler, Hojima et al. 1988)), it is still possible that molecules self-assembled in the free fluid stream and formed very small fibrils (e.g. dimers, trimers, or penta-fibrils). This will dramatically change the dynamics of the chain configurations and hence the alignment of the fibrils. For example, a collagen dimer has a length of 570 nm (Bernengo, Ronziere et al. 1983) and diameter of ~2 nm and the longest relaxation time of 1.3 ms, which is one order of magnitude higher than the monomer's. The increase in the relaxation time increases *Wi* correspondingly. Therefore, the same flow rate and flow velocity has a much higher effect on the dimer and is much more effective at aligning the dimer in the flow direction. If substantial numbers of aggregates are adsorbing to the glass surface, then the alignment effect of the flow on resulting fibrils is likely to be far greater (Lanfer, Freudenberg et al. 2008).

3) Energetics

The process of shear-influenced polymerization on a surface is significantly more complicated than the simpler case of flexible molecule interaction with shear flow because there are two energetic phenomena which govern the process of collagen accumulation on the glass. The experimental conditions (pH=7, T=37°C) are designed to induce the collagen molecules to spontaneously self-assemble into higher order aggregates. Collagen self-assembly is an entropy-driven process during which monomer-

associated water molecules gain entropy following ejection during the formation of intermonomer associations (Kadler, Holmes et al. 1996). For type I collagen the Gibb's free energy associated with fibril assembly is -13 kCal/mol (Kadler, Hojima et al. 1987). The second important energetic interaction is provided by the rigid bounding surfaces (coverslips in the case of this study) which provide a high-energy interface that is adsorptive to collagen molecules (Usha, Maheshwari et al. 2006). The adsorption energy between our glass coverslips and the collagen monomers/aggregates is not known, however, it appears to exceed the assembly energy of the formation of D-banded collagen fibrils because it often prevents normal fibril formation (see Figure 2-8) which shows distorted collagen fibrils. The specific collagen-surface and collagen-collagen interactions likely influence the nucleation, direction and speed of collagen fibril assembly.

Nucleation of a collagen fibril or organized collagen aggregates appears to require the deposition of an initial mat of monomers on the glass, which in some way facilitates the continued aggregation of monomers in an organized manner (See Figure 2-8 for detailed images of collagen aggregates on collagen mat). Given that fibrils comprise arrays of aligned monomers, it is reasonable to assume that the initial alignment of the mat should strongly facilitate fibril nucleation and growth in a particular direction. Indeed, data from this investigation and others (Lanfer, Freudenberg et al. 2008) suggest that the formation of suitable nucleation sites is a strong function of the orientation of the initial surface coating of collagen. We have found that the number of nucleation sites for each shear rate generally increases with increasing shear rates indicating that alignment of the initial collagen mat is a potentially important parameter. The initial mat orientation

is likely to be produced during the very first wetting of the glass in the chamber. It is beyond the scope of this investigation to examine the contact line dynamics, which are likely to produce the initial mat orientation. However, we suggest that control of that process is likely to be critical to the subsequent organization and direction of growth of shear-aligned collagen structures grown on surfaces.

The direction of growth of a fibril or aggregate proceeds both upstream and downstream and is under the influence of the flow rate as indicated by the strength of alignment data and by the growth rate versus shear rate data. The relationships between growth rate, alignment and shear rate are complicated. With regard to direction of growth, fibrils grow generally in the direction of flow (but can sometimes be oblique to the flow direction). The orientation of the fibrillar aggregates is likely due to the combined effect of the initial collagen mat orientation and the shear rate. The orientation of the collagen mat is likely to influence the direction of growth by providing local sites of favorable adsorption in a particular direction (with aligned collagen). However, there appears to be a fundamental physical limitation which prevents the production of completely aligned fibrils on the glass using constant shearing flows. It is not clear how this limitation is produced, however, it is reflected by decreasing radius of curvature of the "hooks" we observe as a function of increasing shear rate. At the highest shear rates, the collagen fibrils can change direction by 180 degrees over the distance of about 2 monomer lengths on average (see inset in Figure 2-8C for a hook with a very small radius of curvature of ~100 nm). From our data, it is not possible to determine if this phenomenon is driven by the orientation of the collagen mat or by the dynamic shear effect on tethered molecules.

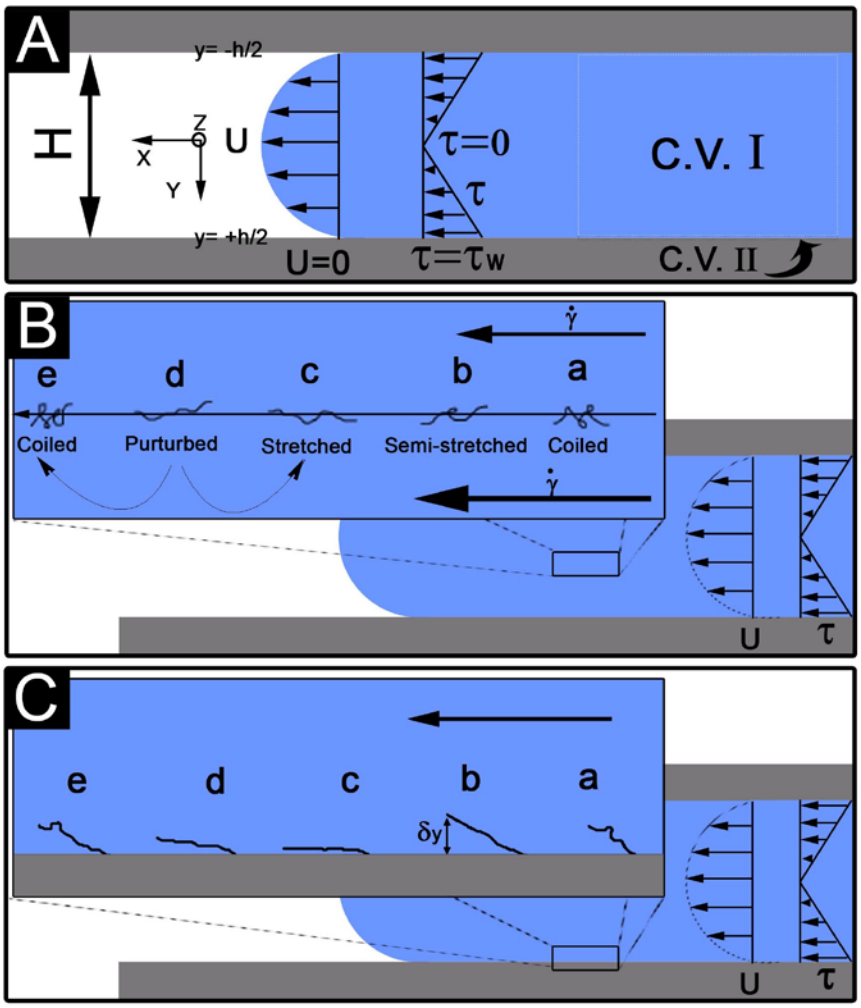

Figure 2-30: A schematic of the flow profile and different scenarios for molecular conformation in the flow and on the glass. (A), A representation of the pressure driven Poiseuille flow in a microchannel. The flow field is parabolic which results in a linear shear stress with Z. (B), A schematic of a non tethered chain in the flow field. The arrows are showing the shear stress vectors. Since the magnified boxed is from a region below the centerline the shear stress above the chain has a smaller magnitude than the shear stress below the chain. (C) An illustration of the fluctuations of a tethered molecule. After binding to the glass (a), the chain will stretch further (b) which produces a torque which brings the chain close to the surface (c). Due to the energy of the surface it is possible that chain binds to the glass at this stage. If not, due to the Brownian motion the chain will fluctuate and move further from the glass surface (d and e). This will expose the chain to stronger flow which causes the chain to stretch and enters the cycle b-e again. This cycle will continue until each part of the chain is absorbed onto the surface

If we consider the upstream side of a fibril/aggregate, the shear rate will influence the directional probability of a tethered monomer adsorbing to the collagen mat. If the mat is strongly aligned, the tethered monomer will have an increased probability of adsorbing in the direction of the alignment (either upstream or downstream). If the shear rate strongly influences the probability distribution of the tethered molecule orientation in the direction of flow, the likelihood of adsorption upstream will decrease and predispose the molecule to adsorption in the downstream direction. The combination of a highly-aligned mat with increased shear rate favors downstream adsorption because there exists a locally oriented mat (receptive to adsorption) within reach of the tethered molecule even when it is oriented downstream. The small radius of the change in direction of the adsorbed aggregates at shear rates reflects this shift in adsorption probability.

2.2. Production of Aligned Arrays of Collagen Fibrils From Confined, Shear-induce Solution of Collagen Molecules

As was discussed in the section 2.1., the free end of a tethered molecule in the free solution would constantly sample the volume of a hemisphere with a center of the pinning point and of a radius equal to the length of a collagen molecule above the coverslip (due to Brownian motion). In fact due to the interaction between the collagen molecule and glass surface the probability of the free end sampling the volume further from the solid surface is higher. In the presence of the flow, the motions of the molecules are influenced and are biased in the direction of the flow which results in the extension and alignment of the molecules. Increasing the shear rate as a method to increase the strength of the flow (to overcome the Brownian motion) results in the formation of the very short fibrils with more pronounced hook formations which result in the significant decrease in the strength of the alignment.

Another method of influencing the Brownian motion of the molecules in the flow is confining the monomers in a thin film adjacent to the solid surface. In fact, Binder showed that decreasing the film thickness results in the chain conformation transitions to 2D (Binder 1992). Confinement of the molecules between a solid surface and free surface restricts the motion of the molecules in the flow direction. Therefore, using confinement it would be possible to attain stronger flow at lower shear rates (hence, reducing the hooks). Therefore, confining the molecules in a tight space close to the coverlips would reduce the volume available to monomers to diffuse and therefore, increase the chance of the molecules to align in the direction of the flow. Bakajin et. al. showed that (Bakajin,

Duke et al. 1998) confinement results in the enhanced alignment of the DNA molecules in the hydrodynamic flow.

Spin coating is method that has been widely used in the semiconductor industry to coat the substrates with thin films of polymers. This method which relies on the continuous or transient flow of the solution on a rotating disc is capable of producing thin film of solution while applying shear flow in the radial direction (due to the centrifugal force). In this condition the only velocity components are rotational and radial and the fluid behavior is therefore controlled by the balance between the centripetal and viscous

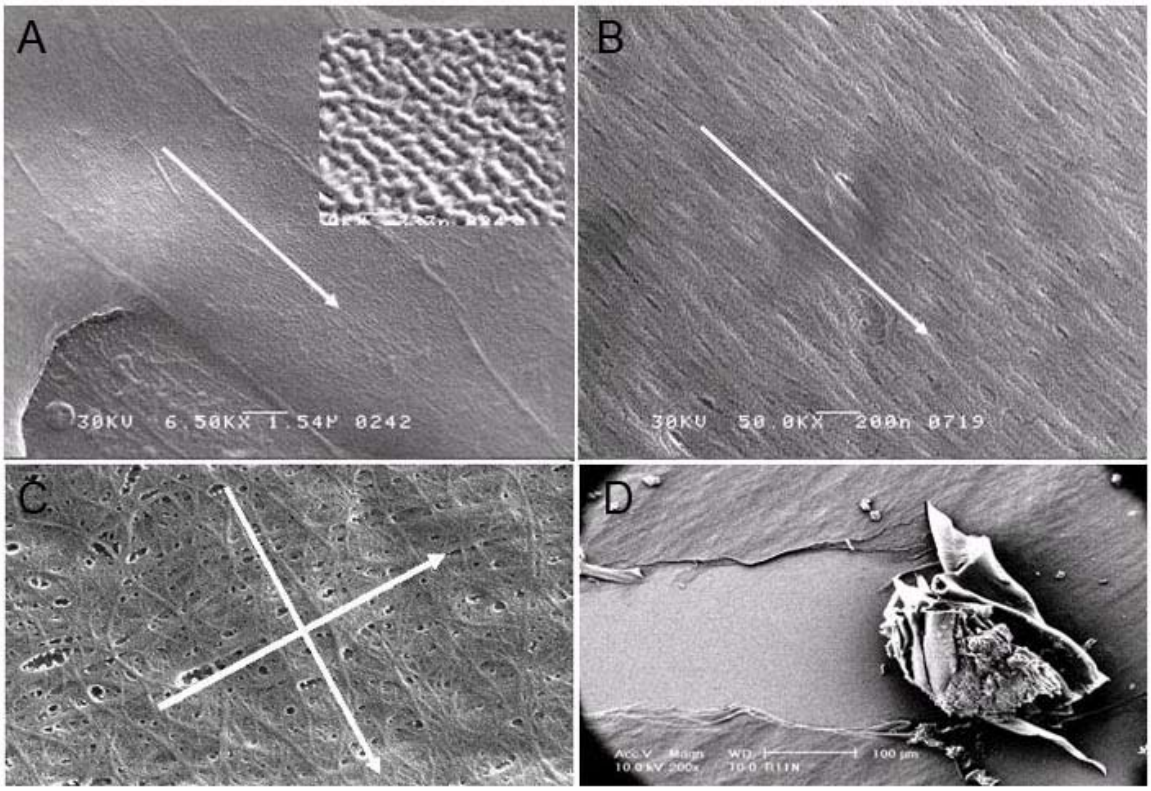

Figure 2-31: SEM images showing the feasibility of aligning collagen fibrils using spin coating. A and B, showing the collagen fibrils aligned in the radial direction. C, production of orthogonal layers of collagen fibrils using an offset disc. D, showing the multi-lamellae structure of the fibrils self-assembled on a coverslip (Ruberti, Melotti et al. 2003; Braithwaite and Ruberti 2006)

forces (Rauscher, Kelly et al. 1973).

Using spin coating, Ruberti et al. (Ruberti, Melotti et al. 2003; Braithwaite and Ruberti 2006) produced organized layers of collagen fibrils *in vitro* (Figure 2-10). The goal of this study is to investigate the organization of the self-assembled collagen molecules in a confined, shearing flow produced using spin coating.

2.2.1. Materials and Methods

2.2.1.1. Experimental Apparatus

Figure 2-11 represents the experimental setup for this investigation. Experiments were carried out in an environmentally controlled (37°C and 100% RH) spin-coater (VVS-400A-6NPP/LITE, Laurell Technologies).

The spin coater chamber was equipped with an in-house designed heat exchanger (Figure 2-12). Briefly, the heat exchanger is composed of zigzag shaped air channels designed inside an aluminum block (Figure 2-12, inset). Five 120W cartridge heaters and

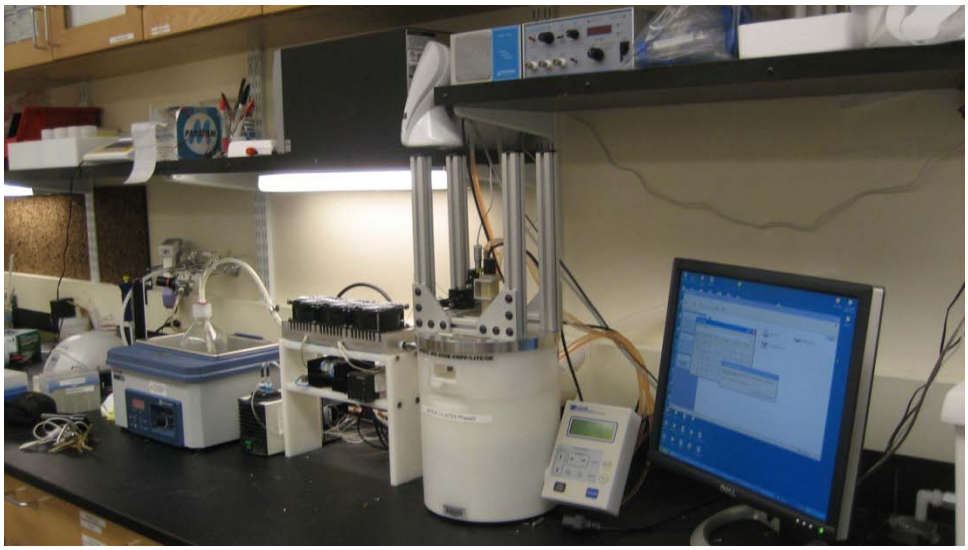

Figure 2-32: Experimental setup for the spin-coating

a CNi32200 temperature controller (OMEGA Engineering, INC, Stamford, Connecticut) are used to control the temperature. A series of fins and three fans were placed on the top of the heat exchanger to increase the rate of heat convection. Prior to entering the heat exchanger, pressurized air was injected into a sealed water container kept at 37°C. Constant flow of air will force humid air formed in the container into the heat exchanger providing 98-100% RH in the spin coating chamber. A thermocouple placed within 1 centimeter of the tip of the in-line cooler was used as a feedback signal for the temperature controller.

A cold, neutralized pepsin extracted solution of collagen type I (Pepsin extracted from calf dermis, Advanced BioMatrix, Inc., San Diego, CA) was dispensed on the center of the 37ºC rotating disc. An in-line temperature controlled heater/cooler (SC-20, Warner Instruments, Hamden, CT) was used to keep the solution cold prior to dispensing on the

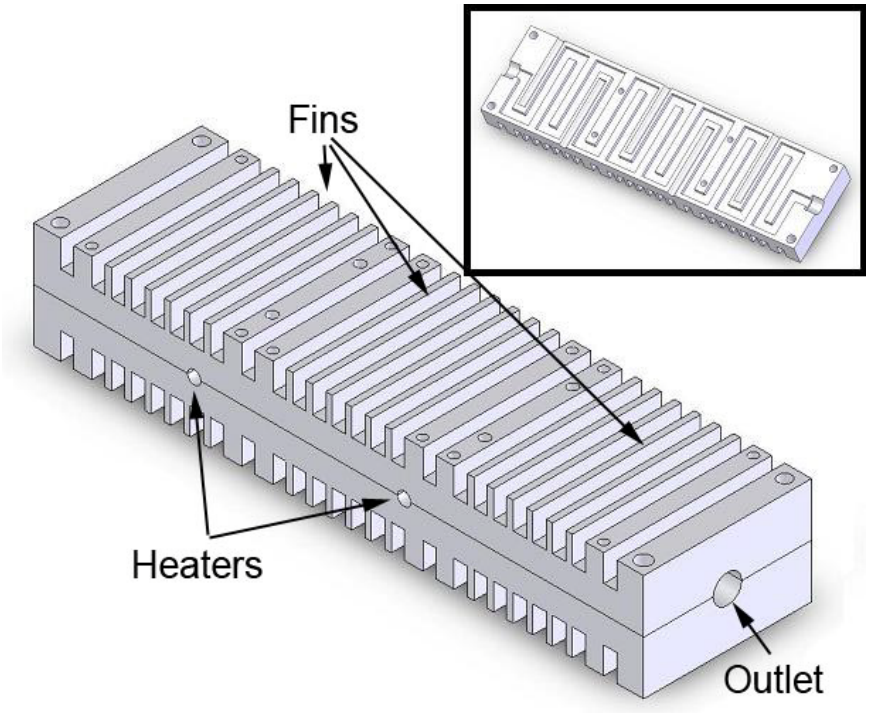

Figure 2-33: Schematic of the heat-exchanger design and apparatus

glass. Following contact with the glass surface collagen molecules will begin to self-assemble into fibrils. While the thin flow profile keeps the molecules in close proximity to the surface, the shear stress will extend the molecules in the flow direction, resulting in the alignment molecules (and the resulting fibrils) (Sec. 2.1). Flow rate, spin rate, and dispensing time were the experimental parameters chosen for this study. DIC microscopy (using a 60x-1.4NA objective) was used to investigate the macro-scale organization. Scanning electron microscopy (SEM) was used to investigate the ultra-structure of the fibrils.

2.2.1.2. Flow Generation

While kept at 4ºC using an ice bath, collagen solution was injected into in-line cooler using a syringe pump (PHD-2000, Harvard Apparatus, Holliston, MA). The collagen

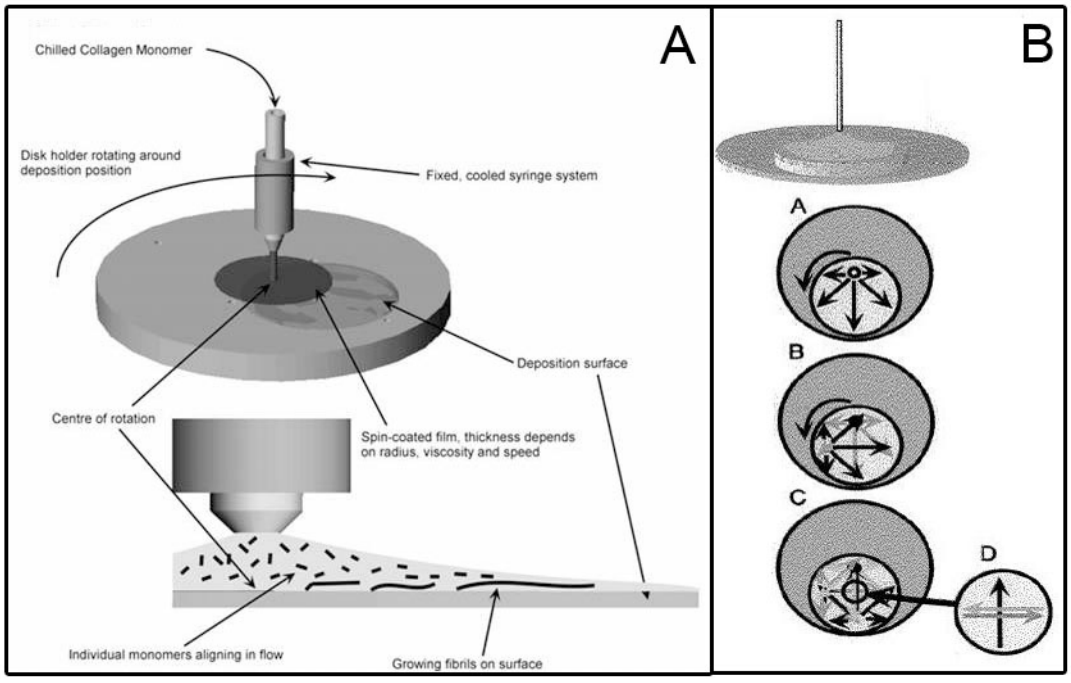

Figure 2-34: Schematic of the spin-coating experiments (A) and the offset disc method to produce orthogonal layer

flow rate was adjusted using the pump and the spinning velocity was controlled using the software provided with the spin coater. For formation of the single layer of radially aligned fibrils, the collagen was injected into the center of the rotating disc (Figure 2-13A). For the formation of orthogonal sheets of fibrils, coverslips were placed off-center from the center of rotation. After coating of a single layer, the coverslip was rotated 90 degrees and another layer of collagen was coated (Figure 2-13B).

2.2.1.3. Experimental conditions

For the situation where there is a steady flow rate of fluid onto a spinning disk the solution requires an analysis of the full Navier-Stokes equation. Leneweit et al. (Leneweit, Roesner et al. 1999) outline work by Rauscher et al. (Rauscher, Kelly et al. 1973) that generates a deceptively simple solution to the steady flow problem. To first order, this solution is:

$$h = \left(\frac{3}{2\pi} \frac{Q\nu}{\omega^2 r^2} \right)^{1/3} \tag{22}$$

$$u = \frac{r\omega^2 h^2}{\nu} \left(\frac{z}{h} - \frac{1}{2} \left[\frac{z}{h} \right]^2 \right) \tag{23}$$

Where, u is the radial velocity as a function of z away from the disk at a position r radially, h is the thickness of the film, ω is the rotation rate of the disk, ν is the kinematic viscosity of the solution and Q is the volume flow rate.

The above solutions therefore allow the layer profile and velocity gradient to be calculated for relevant flow conditions. Figure 2-14 presents representative data for flow conditions for various spin velocity and flow rates. For both flow conditions depicted,

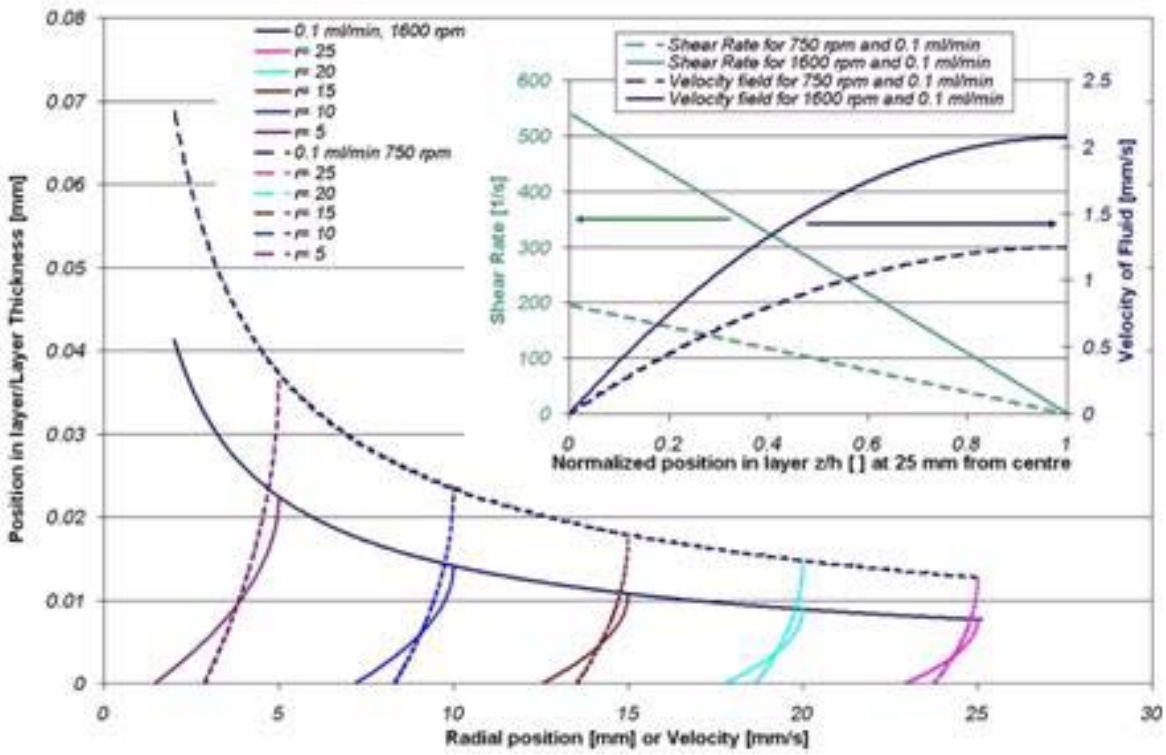

Figure 2-35: Estimated film thickness and velocity profile for the parameters chosen

the fluid layers are of the order of 10 μm at 25 mm from the point of deposition. In addition, from 10 mm to 25 mm neither layer thickness varies by more than 10 μm.

Thus, with very simple procedure a thin, virtually flat layer can be generated that will confine the growing collagen film and provide shear rates in excess of 100 s^{-1} near the substrate surface. Table 2-3 represents the parameter space matrix for flow rate (Q) and spin rate (ω). Based on the eqs. 22 and 23 the proposed values for Q and ω correspond to the shear rates in the range of 200 to 1000 1/s at 20mm from the center of the deposition.

2.2.1.4. Assessments

Collagen fibril alignment was investigated by DIC microscopy. In order to explore and compare the organization of the fibrils across the coverslip, images from 9 regions (center and every 90º at 15mm and 25mm distance from the center) of the

converslip were taken for further analysis. Scanning electron microscopy (SEM) was used to investigate the morphology and diameter of the collagen fibrils.

Spin rate (ω, rpm) / Flow rate(Q, ml/min)	750	1000	2000	3000
0.3	✓	✓	✓	✓
0.5	✓	✓	✓	✓
1	✓	✓	✓	✓

Table 2-3: The experimental parameters chosen for collagen self-assembly using spin coating

2.2.2. Results

2.2.2.1. DIC Imaging

Figure 2-15 and Figure 2-16 are composite DIC images of the collagen fibrils self-assembled at different spinning rates and flow rates. As the images show, this method is capable of producing *locally* aligned collagen fibrils at these conditions. As expected, the density of the fibrils increases as the flow rate increases. The organization of the fibrils appeared to be influenced strongly by the shear rate.

The collagen fibrils were best organized at of 1000 rpm rotational speed. At 750 rpm, although there was a local organization discernable at high magnifications, fibrils did not show any general organization across the image (Figure 2-15A and B). In addition, clumps of collagen fibrils were frequently observed on the surface. High rotation speeds (e.g. 3000 rpm) resulted in the self-assembly of the collagen molecules into globular aggregates (Figure 2-15D). In some areas of the sample high shear rate resulted in a dense coating of the coverslip with aggregates which did not show any fibrillar structures or orientation (Figure 2-15C).

The DIC imaging across the coverslip revealed that the collagen self-assembly

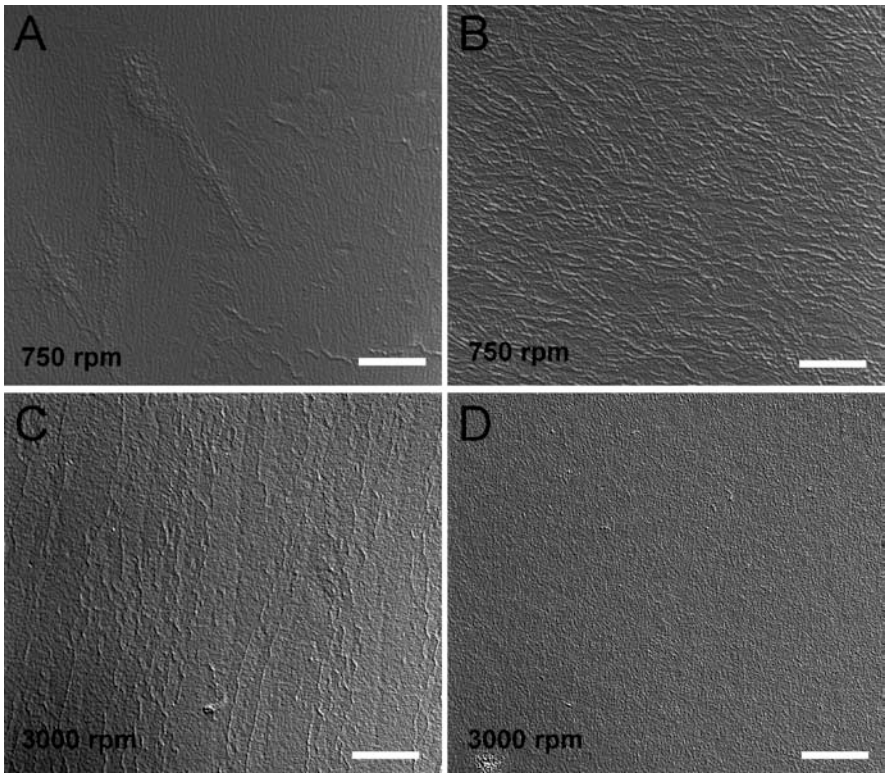

Figure 2-36: DIC images of self-assembled collagen fibrils at 750 (A and B) and 3000 (C and D) rpm. Please note the asymmetric self-assembly patterns across the coverslip at each shear rate. Bars 20 µm.

was not symmetric across the coverslips (Figure 2-16 and Figure **2-17**). While in some areas of the coverslips fibrils were completely aligned in the radial direction (Figure 2-16 A1, B1, and C1), fibrils in other regions were barely organized (Figure 2-16A2, B2, and C2). Figure 2-17 clearly shows the boundary between the areas of organized collagen fibrils and the areas with negligible coating of disorganized collagen fibrils.

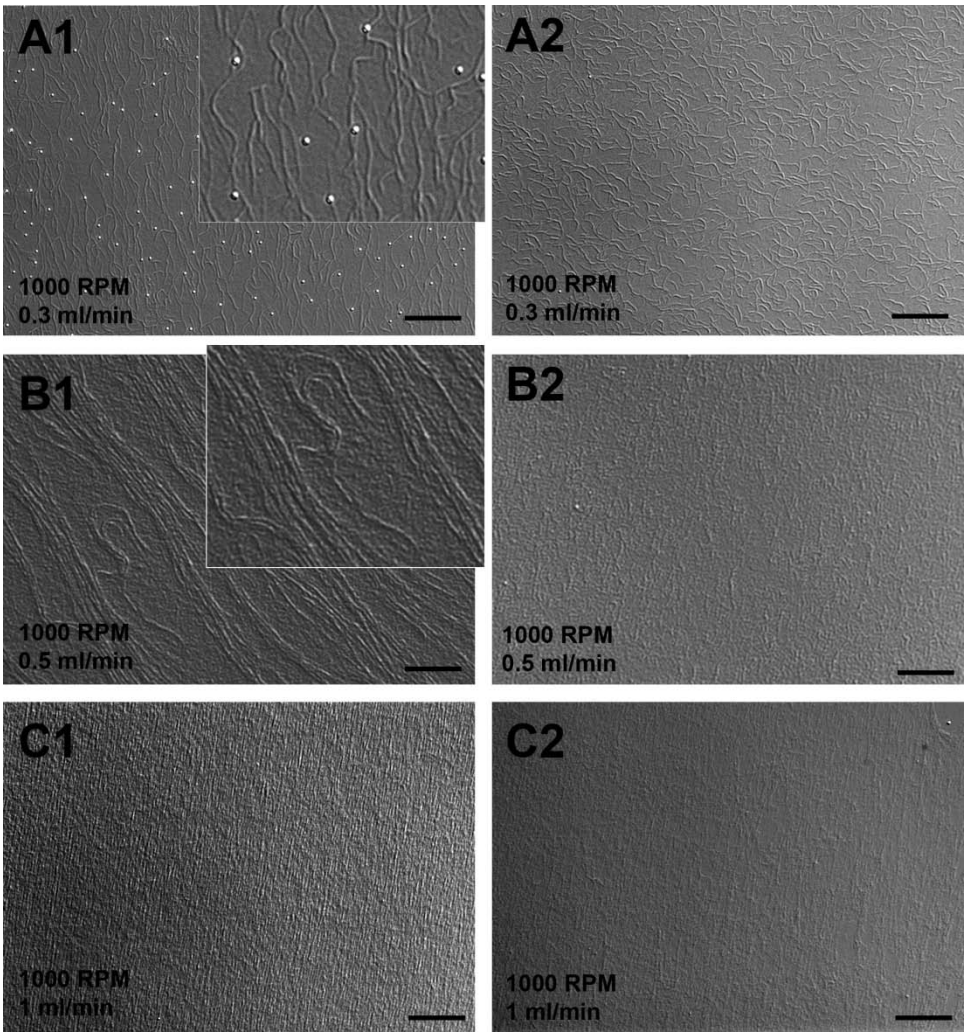

Figure 2-37: Collagen fibrils aligned using spin coating at 1000 rpm and different flow rates. Images were captured 1.5 cm from the center of the coverslip. Although the method resulted in the well aligned collagen fibrils (A1, B1, and C1), the organization was not symmetric across the disc (A2, B2, and C2). Bars are 10 µm.

When the flow profile was investigated using high speed imaging technique, it appeared that the profile was not uniform across the spinning disc which could be due to the instability of the rotating disc.

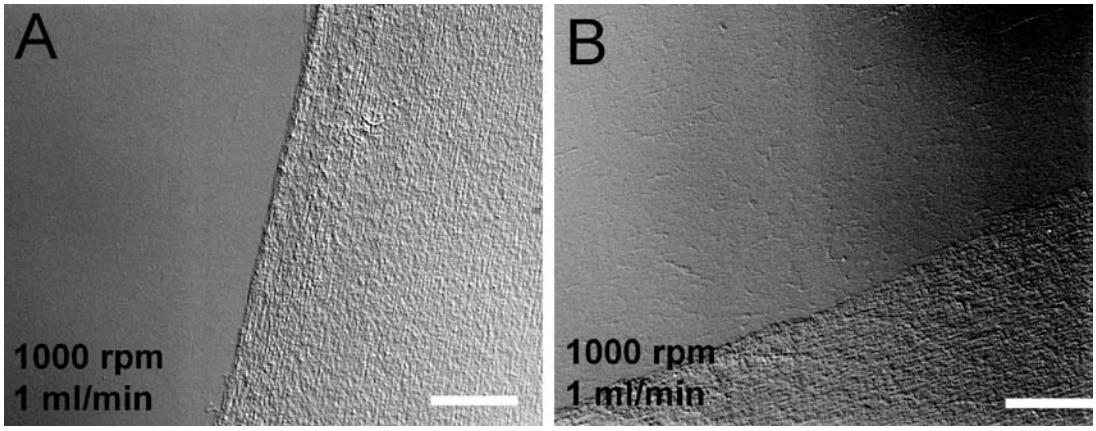

Figure 2-38: Representative DIC images of asymmetric collagen self-assembly patterns on the coverslips. The experimental conditions for these images are 1000 rpm and 1 ml/min (the images are from two different runs).

2.2.2.2. SEM Imaging

The SEM images of the collagen fibrils confirmed the DIC observations. While in some regions collagen fibrils formed an organized layer (Figure 2-18A). In a different region of the surface collagen molecules self-assembled into organized arrays but disorganized in other regions (Figure 2-18B, C and D). In addition, SEM imaging revealed that similar to the fibrils self-assembled in microchamber (Sec. 2.1), fibrils formed using spin coating did not exhibit the 67nm periodic D-banding patterns.

2.2.3. Discussion

The goal of this investigation was to produce organized layer(s) of collagen fibrils by applying directional shear stress to the collagen molecules while confining them into

close apposition to the solid surfaces. Confinement of the molecules should restrict the Brownian motion of the free end of the tethered molecules in the direction of the flow. Therefore, using confinement, smaller shear rates would be required to stretch collagen molecules and produce organized arrays of collagen fibrils. This effect is advantageous because, as shown in the Sec. 2.1, high shear rates results in the formation of the hooks

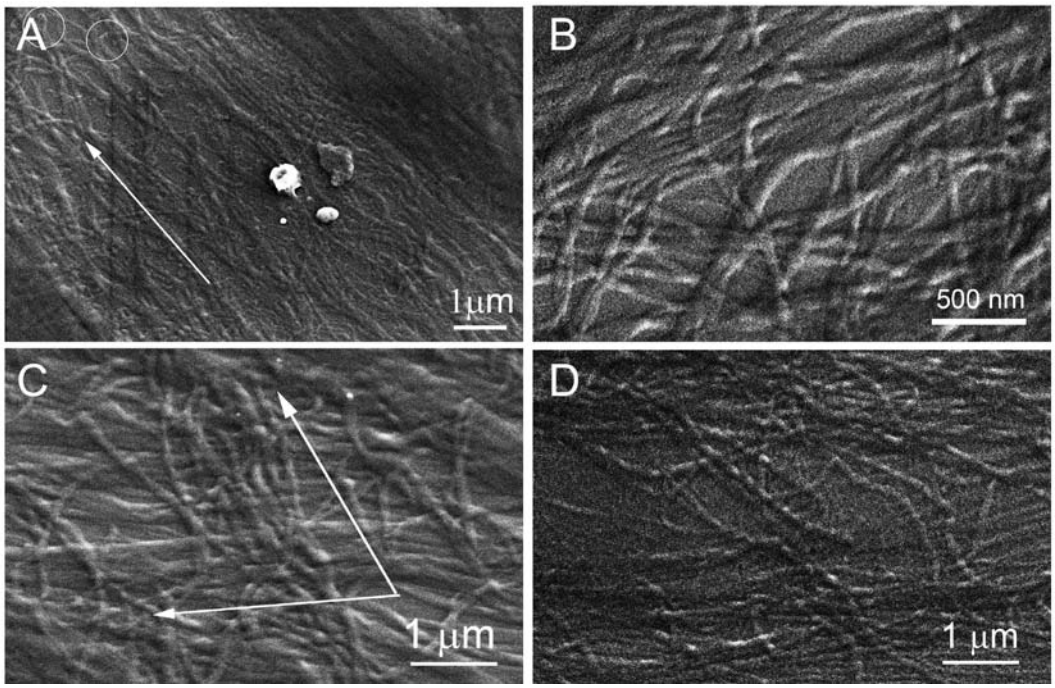

Figure 2-39: SEM images of spin-coated collagen fibrils at 1000 RPM

which results in a significant decrease of the alignment of the collagen fibrils. In this investigation, spin coating method is used to apply hydrodynamic shear stress on the molecules while confining them in a thin film adjacent to the spinning disc. The results of collagen self-assembly using spin coating revealed that using this method, it is possible to produce organized arrays of collagen fibrils, with the best organizations at 1000 rpm. The organization (and patterns of collagen self-assembly) however were not symmetric across the coverslips. Despite a high degree of collagen organization in some areas,

fibrils were disorganized in other regions of the coverslips. While at low spinning rates collagen fibrils were loosely organized and formed a clump of fibrils on the glass, collagen fibrils formed at high shear rates self-assembled into globular aggregates. These collagen self-assembly patterns could be due to the insufficiency or excess shear rate. While the shear rate at 750 rpm (~200 1/S) is not sufficient to completely organize collagen molecules (and resulting fibrils), the shear rate at 3000 rpm is too strong and does not allow the molecules to self-assemble on the glass.

It should be mentioned that, the calculated film thickness (which is greater than a few microns) is still at least one order of magnitude bigger than the length of a collagen molecule. Previous investigations showed that in order for the confinement to be effective on the conformation of the molecules, the thickness of the thin film should be in the order of 2Rg, where Rg is the radius of gyration of a collagen molecule. From a scaling theory for the flexible polymers, the Rg for a semi flexible chain is scaled as (Kraus, Muller-Buschbaum et al. 2000):

$$R_g \cong aN^{\nu} \tag{24}$$

where, a is the monomer size (diameter), N is the polymerization index (i.e. number of monomers in a polymer) and ν is the Flory's coefficient which is 3/5 for a good solvent. In the case of a collagen molecule, a is the persistent length of a monomer (ℓ_P) and N is the ratio of the contour length to the persistent length (i.e. flexibility index). Inserting these numbers (ℓ_P =15 nm and N=20) in the Eq. 24, the calculated radius of gyration for a collagen molecule is 90nm which is in good agreement with the Rg determined from the dynamic light scattering of a lathyritic collagen (74.5±2.0 nm (Kenji Kubota 1987)). Therefore, Rg of collagen molecules is significantly smaller than the film thicknesses

produced with spin coating, which indicates that confinement will have negligible effect on the organization of the collagen fibrils. As discussed in the Sec. 2.1, since these experiments are performed at physiological conditions, collagen molecules have a tendency to undergo a spontaneous self-assembly. Self-assembly of the molecules into the larger aggregates (e.g. dimmers, trimers, and etc.) would result in the increase of the length and diameter of the chains, which consequently increases the effect of the confinement significantly. In addition, as was discussed in the Sec. 2.1, increase in the length of the polymer chains enhances the flow strength to influence the orientation of the molecule (i.e. by increasing the *Wi* number). Therefore, spontaneous self-assembly of the monomers plays a significant role in organizing the collagen molecules in the spin coating process and generation of aligned collagen fibrils.

The DIC images also showed that similar to the collagen fibrils self-assembled in the simple shear flow, spin-coated collagen fibrils exhibit the transverse fibrillar growth or "hooks". The formation of the hook structures in the spin-coated collagen fibrils indicate that hooks are purely due to the nature of the shear-influenced collagen self-assembly (as discussed in depth in the Sec. 2.1) and even application of the thin film confinement does not prevent the formation of the hooks.

Asymmetric self-assembly of the collagen molecules across the coverslips was the biggest downside with the spin coating method. As was discussed before, collagen molecules are confined in a 2-10 μm thick fluid film adjacent to the spinning disc. Therefore, film stability plays a critical role in the uniform coating of the coverslips and global organization of the self-assembled collagen fibrils. Video imaging of the spinning disc showed that the disc is unstable, especially at low speeds.

The SEM imaging also revealed that the collagen fibrils formed using spin-coating do not show the D-banding patterns of native collagen fibrils. Collagen self-assembly is an energy driven process. The banding is the result of precise longitudinal and lateral arrangement of the molecules within a fibril. The influence of the shear stress and glass-molecules interactions could interfere with the normal interaction of the molecules (which result in D-banding) and prevent the formation of the D-banded fibrils (Sec. 2.1)

2.3. Production of Aligned Layer of Collagen Fibrils on Polycarbonate Membrane

It is well known that cells seeded on organized substrates align themselves in the same direction and produce organized ECM. This phenomenon has been shown for both biological (e.g. collagen (Yoshizato, Obinata et al. 1981) and fibrin (Dubey, Letourneau et al. 2001)) and nonbiological (e.g. polyurethane (Lee, Shin et al. 2005)) substrates. When cultured on collagen substrates, cells deposited more collagen and cell signaling and proliferation was enhanced (Hauschka and Konigsberg 1966; Martin and Kleinman 1981; Kleinman, Luckenbill-Edds et al. 1987).

Corneal stroma is composed of the aligned layers of uniform diameter (e.g. 32nm in human) collagen fibrils. While fibrils in each layer are aligned in the same direction, they are often at right angles to the adjacent layer. The purpose of this section is to produce and deposit organized arrays of collagen fibrils on polycarbonate membranes (PM) to be used as a template for cell culturing as an attempt for corneal tissue engineering. Considering the results of the previous sections (i.e. microfluidic chambers and spin coating), shear deposition of collagen solution was chosen for this study.

2.3.1. Materials and Methods

2.3.1.1. Experimental Apparatus

Figure 2-19 shows the experimental setup for this study. Cold, neutralized solution of collagen monomers (2.4 mg/ml, Advanced BioMatrix, Inc., San Diego, CA) was injected into the flow chamber using a syringe pump (PHD-2000, Harvard Apparatus, Holliston, MA). To produce uniform flow, the flow was devided into four lines prior to entering the

chamber. An in-house microfluid chamber (75 cm in length, 200 cm in width, and 0.05 cm in height) was designed and built as the microfluidic chamber. The chamber was

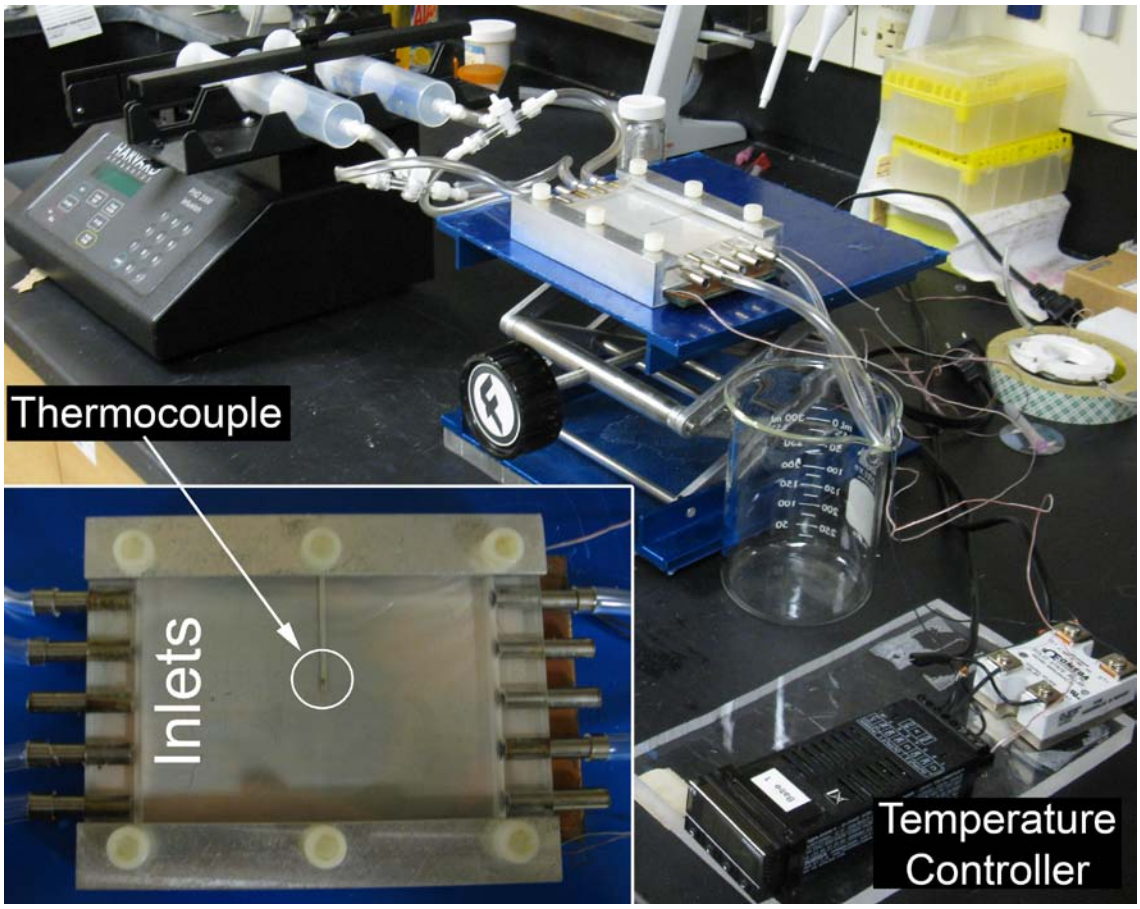

Figure 2-40: Experimental setup for aligning collagen on polycarbonate membrane

equipped with a heater (bottom plate) which was controlled via a PID controlled temperature controller and a thermocouple placed at the center of the chamber as the feedback signal. To produce different shear rates, the height of the channel was varied using gaskets with different heights. Flow rates in the ranges of 2 to 15 ml/min were investigated.

2.3.1.2. Assessments

Scanning electron microscopy (SEM) was used to investigate the morphology and diameter of the collagen fibrils.

2.3.2. Results and Discussion

Figure 2-20 is a SEM micrograph of the collagen fibrils self-assembled on the polycarbonate membrane. Collagen fibrils self-assembled using this method were only partially and locally aligned. Increasing or decreasing the shear stress did not seem to affect the strength of the alignment significantly.

In the investigations of the Sec. 2.1. and 2.2. collagen fibrils were assembled on a coverlips: a smooth, impenetrable surface. In contrast, polycarbonate membrane used as the surface in this section are not smooth. Although extreme attention was paid to have the membranes as flat as possible, due to their delicate structure it is possible that they weren't completely flat. In addition, the membranes are permeable (with 80 nm holes) which indicate their surface is not smooth. These two factors could potentially affect the

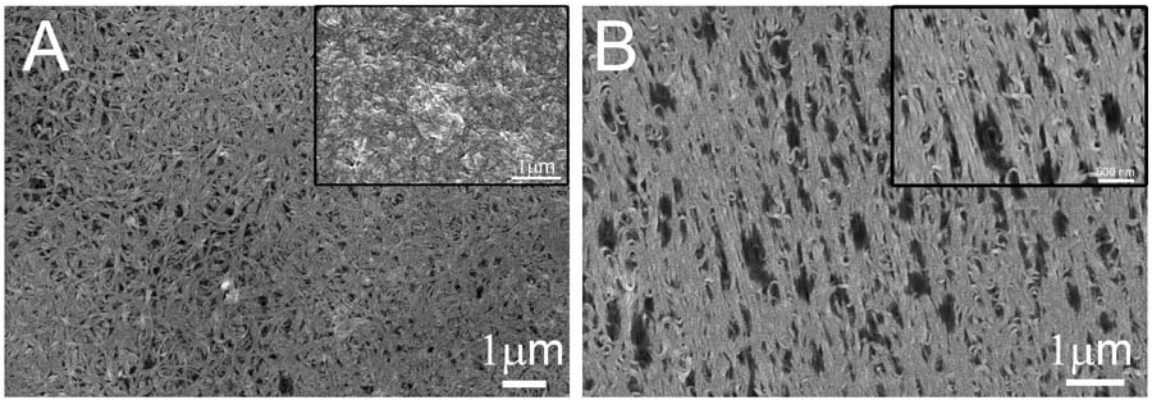

Figure 2-41: SEM micrographs of collagen fibrils self-assembled under the influence of shear stress on a polycarbonate membrane

flow field close to the surface and disturb the streamlines. This could be the main reason that collagen fibrils did not show a long range alignment similar to what was seen on the coverslip surface.

In addition, similar to fibrils self-assembled using spin coating, these fibrils did not show D-banding patterns.

Conclusion

In this study we examined the dynamics of shear-influenced collagen assembly on a glass surface using live differential interference contrast imaging. We also investigated the detailed morphology of the collagen fibrillar aggregates using high resolution Quick Freeze Deep Etch electron microscopy. The experiments demonstrate that collagen self-assembly in a shear flow is a complex physical event which includes the effect of shear rate, self-assembly energetics and surface energy. In spite of the modest theoretical influence of shear rate on the statistical alignment of single, tethered collagen monomers, there is an observable influence of flow on the direction of assembly of collagen on the glass surface. Even at very low shear rate ($9s^{-1}$) the fibrils demonstrate clear alignment in the direction of flow. The best fibril alignment was observed at 80 and 20 s^{-1}. However, it does not appear to be possible to produce completely aligned collagen using the shear-influenced assembly approach. At all shear rates, fibrils would often change direction producing what we term “hooks”. Hook formation was most pronounced at high shear rates where fibrils would change direction 180 degrees (upstream to downstream within a few molecular lengths.) The presence of the hooks was confirmed by QFDE imaging. At lower shear-rates, the hooks could result in fibril growth perpendicular to the flow or even against it. These directional changes are possibly due to the combination of the

influence of the organization of the collagen mat (which was produced on first wetting of the glass) and the influence of the shear rate at the glass surface. In addition to the directional growth behavior of the fibrils, both branching and merging of collagen was observed dynamically during fibril assembly. QFDE images show that the collagen fibrils often comprise smaller possibly molecular units which are wound together to form rope like aggregates. However, the anticipated D-banding characteristic of native collagen fibrils was not seen in the shear-assembled collagen fibrils/aggregates. We propose that the surface energy of the glass is adequate to "distort" the fibrillar structure enough to prevent proper nucleation of banded fibrils. Ultimately, the data from these studies has shown that applying shear flow to the collagen molecules causes them to self-assemble into reasonably aligned collagen fibrils/aggregates. However, there appears to be a physical limitation to producing alignment due to growth instabilities which manifest in the form of what we term "hooks". Further, the influence of the surface, which must be energetic enough to adsorb the collagen, appears to also distort the fibrils, preventing normal D-banding. The key to shear-alignment of collagen may reside in producing a highly oriented initial layer of collagen (perhaps via a high shear rate or surface energy patterning) followed by a more modest shearing flow of available monomers).

References

Ajdari, A., N. Bontoux, et al. (2006). "Hydrodynamic Dispersion in Shallow Microchannels: the Effect of Cross-Sectional Shape." Analytical Chemistry **78**(2): 387-392.

Allen, R. D., N. S. Allen, et al. (1981). "Video-enhanced contrast, differential interference contrast (AVEC-DIC) microscopy: a new method capable of analyzing microtubule-related motility in the reticulopodial network of Allogromia laticollaris." Cell Motil **1**(3): 291-302.

Ananthanarayanan, S. and A. Veis (1972). "The molecular parameters of monomeric and acid-soluble collagens. Low shear gradient viscosity and electric birefringence." Biopolymers **11**(7): 1365-77.

Bakajin, O. B., T. A. J. Duke, et al. (1998). "Electrohydrodynamic Stretching of DNA in Confined Environments." Physical Review Letters **80**(12): 2737.

Bard, J. B., D. J. Hulmes, et al. (1993). "Chick corneal development in vitro: diverse effects of pH on collagen assembly." J Cell Sci **105 (Pt 4)**(Pt 4): 1045-55.

Batchelor, G. K. (2006). "Slender-body theory for particles of arbitrary cross-section in Stokes flow." Journal of Fluid Mechanics Digital Archive **44**(03): 419-440.

Beecher, N., S. Chakravarti, et al. (2006). "Neonatal development of the corneal stroma in wild-type and lumican-null mice." Invest Ophthalmol Vis Sci **47**(1): 146-50.

Benjamin, H. B., E. Pawlowski, et al. (1964). "Collagen as Temporary Dressing and Blood Vessel Replacement." Arch Surg **88**: 725-7.

Bernengo, J. C., M. C. Ronziere, et al. (1983). "A hydrodynamic study of collagen fibrillogenesis by electric birefringence and quasielastic light scattering." J Biol Chem **258**(2): 1001-6.

Besseau, L. and M. M. Giraud-Guille (1995). "Stabilization of fluid cholesteric phases of collagen to ordered gelated matrices." J Mol Biol **251**(2): 197-202.

Binder, K. (1992). "Phase Transitions in Reduced Geometry." Annual Review of Physical Chemistry **43**(1): 33-59.

Birk, D. E. (2001). "Type V collagen: heterotypic type I/V collagen interactions in the regulation of fibril assembly." Micron **32**(3): 223-37.

Birk, D. E. and P. Bruckner (2005). Collagen Suprastructures. Collagen: Primer in Structure, Processing and Assembly**:** 185-205.

Birk, D. E., J. M. Fitch, et al. (1988). "Collagen type I and type V are present in the same fibril in the avian corneal stroma." J Cell Biol **106**(3): 999-1008.

Birk, D. E., M. V. Nurminskaya, et al. (1995). "Collagen fibrillogenesis in situ: fibril segments undergo post-depositional modifications resulting in linear and lateral growth during matrix development." Dev Dyn **202**(3): 229-43.

Birk, D. E. and R. L. Trelstad (1984). "Extracellular compartments in matrix morphogenesis: collagen fibril, bundle, and lamellar formation by corneal fibroblasts." J Cell Biol **99**(6): 2024-33.

Birk, D. E. and R. L. Trelstad (1985). "Fibroblasts create compartments in the extracellular space where collagen polymerizes into fibrils and fibrils associate into bundles." Ann N Y Acad Sci **460**: 258-66.

Birk, D. E. and R. L. Trelstad (1986). "Extracellular compartments in tendon morphogenesis: collagen fibril, bundle, and macroaggregate formation." J Cell Biol **103**(1): 231-40.
Bontoux, N., A. Pepin, et al. (2006). "Experimental characterization of hydrodynamic dispersion in shallow microchannels." Lab Chip **6**(7): 930-5.
Boot-Handford, R. P., D. S. Tuckwell, et al. (2003). "A novel and highly conserved collagen (pro(alpha)1(XXVII)) with a unique expression pattern and unusual molecular characteristics establishes a new clade within the vertebrate fibrillar collagen family." J Biol Chem **278**(33): 31067-77.
Boote, C., S. Dennis, et al. (2005). "Lamellar orientation in human cornea in relation to mechanical properties." J Struct Biol **149**(1): 1-6.
Bornstein, P. and H. Sage (1980). "Structurally Distinct Collagen Types." Annual Review of Biochemistry **49**(1): 957-1003.
Bouligand, Y., J. P. Denefle, et al. (1985). "Twisted architectures in cell-free assembled collagen gels: study of collagen substrates used for cultures." Biol Cell **54**(2): 143-62.
Braithwaite, G. J. C. and J. W. Ruberti (2006). Layered aligned polymer structures and methods of making same. United States.
Brown, C. T., P. Lin, et al. (2002). "Extraction and purification of decorin from corneal stroma retain structure and biological activity." Protein Expr Purif **25**(3): 389-99.
Buehler, M. J. and S. Y. Wong (2007). "Entropic elasticity controls nanomechanics of single tropocollagen molecules." Biophys J **93**(1): 37-43.
Bueno, E. M. and J. W. Ruberti (2008). "Optimizing collagen transport through track-etched nanopores." Journal of Membrane Science **321**(2): 250-263.
Canty, E. G. and K. E. Kadler (2005). "Procollagen trafficking, processing and fibrillogenesis." J Cell Sci **118**(Pt 7): 1341-53.
Canty, E. G., Y. Lu, et al. (2004). "Coalignment of plasma membrane channels and protrusions (fibripositors) specifies the parallelism of tendon." J Cell Biol **165**(4): 553-63.
Cassidy, J. J., A. Hiltner, et al. (1989). "Hierarchical structure of the intervertebral disc." Connect Tissue Res **23**(1): 75-88.
Chakravarti, S. (2002). "Functions of lumican and fibromodulin: lessons from knockout mice." Glycoconj J **19**(4-5): 287-93.
Chakravarti, S., T. Magnuson, et al. (1998). "Lumican regulates collagen fibril assembly: skin fragility and corneal opacity in the absence of lumican." J Cell Biol **141**(5): 1277-86.
Chakravarti, S., W. M. Petroll, et al. (2000). "Corneal opacity in lumican-null mice: defects in collagen fibril structure and packing in the posterior stroma." Invest Ophthalmol Vis Sci **41**(11): 3365-73.
Chakravarti, S., G. Zhang, et al. (2006). "Collagen fibril assembly during postnatal development and dysfunctional regulation in the lumican-deficient murine cornea." Dev Dyn **235**(9): 2493-506.
Chapman, D. (1966). "Liquid crystals and cell membranes." Ann N Y Acad Sci **137**(2): 745-54.

Chatwin, P. C. and P. J. Sullivan (1982). "The effect of aspect ratio on longitudinal diffusivity in rectangular channels." Journal of Fluid Mechanics Digital Archive **120**(-1): 347-358.
Chaudhuri, S., H. Nguyen, et al. (1987). "A Fourier Domain Directional Filterng Method for Analysis of Collagen Alignment in Ligaments." Biomedical Engineering, IEEE Transactions on **BME-34**(7): 509-518.
Cintron, C., H. Covington, et al. (1983). "Morphogenesis of rabbit corneal stroma." Invest Ophthalmol Vis Sci **24**(5): 543-56.
Cintron, C., B. S. Hong, et al. (1981). "Quantitative analysis of collagen from normal developing corneas and corneal scars." Curr Eye Res **1**(1): 1-8.
Claire, K. and R. Pecora (1997). "Translational and Rotational Dynamics of Collagen in Dilute Solution." J. Phys. Chem. B **101**(5): 746-753.
Comper, W. D. and T. C. Laurent (1978). "Physiological function of connective tissue polysaccharides." Physiol Rev **58**(1): 255-315.
Coulombre, A. (1965). "Problems in corneal morphogenesis." Advances in Morphogenesis **4**: 81.
Danielson, K. G., H. Baribault, et al. (1997). "Targeted disruption of decorin leads to abnormal collagen fibril morphology and skin fragility." J Cell Biol **136**(3): 729-43.
Daxer, A., K. Misof, et al. (1998). "Collagen fibrils in the human corneal stroma: structure and aging." Invest Ophthalmol Vis Sci **39**(3): 644-8.
De Gennes, P. G. (1974). "Coil-stretch transition of dilute flexible polymers under ultrahigh velocity gradients." The Journal of Chemical Physics **60**(12): 5030-5042.
Denis, F. A., A. Pallandre, et al. (2005). "Alignment and assembly of adsorbed collagen molecules induced by anisotropic chemical nanopatterns." Small **1**(10): 984-91.
Dickinson, R. B., S. Guido, et al. (1994). "Biased cell migration of fibroblasts exhibiting contact guidance in oriented collagen gels." Ann Biomed Eng **22**(4): 342-56.
Doane, K. J., J. P. Babiarz, et al. (1992). "Collagen fibril assembly by corneal fibroblasts in three-dimensional collagen gel cultures: small-diameter heterotypic fibrils are deposited in the absence of keratan sulfate proteoglycan." Exp Cell Res **202**(1): 113-24.
Donald, A. M. and A. H. Windle (1992). Liquid Crystalline Polymers, Cambridge University Press.
Du, Y., E. C. Carlson, et al. (2008). "Rescue of the Stromal Phenotype in Lumican Null Mice by Human Corneal Stem Cell Transplantation." Invest. Ophthalmol. Vis. Sci. **49**(5): 4522-.
Dubey, N., P. C. Letourneau, et al. (1999). "Guided neurite elongation and schwann cell invasion into magnetically aligned collagen in simulated peripheral nerve regeneration." Exp Neurol **158**(2): 338-50.
Dubey, N., P. C. Letourneau, et al. (2001). "Neuronal contact guidance in magnetically aligned fibrin gels: effect of variation in gel mechano-structural properties." Biomaterials **22**(10): 1065-75.
Ehrmann, R. L. and G. O. Gey (1956). "The growth of cells on a transparent gel of reconstituted rat-tail collagen." J Natl Cancer Inst **16**(6): 1375-403.

Ellis, E. A. (2006). "Solutions to the Problem of Substitution of ERL 4221 for Vinyl Cyclohexene Dioxide in Spurr Low Viscosity Embedding Formulations." Microscopy Today **14**(4): 32.
Elsdale, T. and J. Bard (1972). "Collagen substrata for studies on cell behavior." J Cell Biol **54**(3): 626-37.
Engel, J. and H. P. Bächinger (2005). Structure, Stability and Folding of the Collagen Triple Helix. Collagen: Primer in Structure, Processing and Assembly**:** 7-33.
Exposito, J. Y., C. Cluzel, et al. (2002). "Evolution of collagens." Anat Rec **268**(3): 302-16.
Eyre, D. R., M. A. Paz, et al. (1984). "Cross-linking in collagen and elastin." Annu Rev Biochem **53**: 717-48.
Faraj, K. A., T. H. van Kuppevelt, et al. (2007). "Construction of collagen scaffolds that mimic the three-dimensional architecture of specific tissues." Tissue Eng **13**(10): 2387-94.
Fini, M. E. and B. M. Stramer (2005). "How the cornea heals: cornea-specific repair mechanisms affecting surgical outcomes." Cornea **24**(8 Suppl): S2-S11.
Fleischmajer, R., J. S. Perlish, et al. (1987). "Amino and carboxyl propeptides in bone collagen fibrils during embryogenesis." Cell Tissue Res **247**(1): 105-9.
Fleischmajer, R., R. Timpl, et al. (1981). "Ultrastructural identification of extension aminopropeptides of type I and III collagens in human skin." Proc Natl Acad Sci U S A **78**(12): 7360-4.
Frank, C. B. (2004). "Ligament structure, physiology and function." J Musculoskelet Neuronal Interact **4**(2): 199-201.
Fratzl, P., K. Misof, et al. (1998). "Fibrillar structure and mechanical properties of collagen." J Struct Biol **122**(1-2): 119-22.
Friedel, G. (1922). "Les e´tats me´somorphes de la matie`re." Ann. de Phys. **18**: 273-474.
Gelman, R. A., D. C. Poppke, et al. (1979). "Collagen fibril formation in vitro. The role of the nonhelical terminal regions." J Biol Chem **254**(22): 11741-5.
Gennes, P.-G. d. (1979). Scaling concepts in polymer physics. Ithaca, N.Y., Cornell University Press.
Giancotti, F. G. (1997). "Integrin signaling: specificity and control of cell survival and cell cycle progression." Current Opinion in Cell Biology **9**(5): 691-700.
Giraud-Guille, M. M. (1988). "Twisted plywood architecture of collagen fibrils in human compact bone osteons." Calcif Tissue Int **42**(3): 167-80.
Giraud-Guille, M. M. (1989). "Liquid crystalline phases of sonicated type I collagen." Biol Cell **67**(1): 97-101.
Giraud-Guille, M. M. (1992). "Liquid crystallinity in condensed type I collagen solutions. A clue to the packing of collagen in extracellular matrices." J Mol Biol **224**(3): 861-73.
Giraud-Guille, M. M. (1996). "Twisted liquid crystalline supramolecular arrangements in morphogenesis." Int Rev Cytol **166**: 59-101.
Giraud-Guille, M. M., L. Besseau, et al. (2000). "Structural aspects of fish skin collagen which forms ordered arrays via liquid crystalline states." Biomaterials **21**(9): 899-906.
Giraud-Guille, M. M., L. Besseau, et al. (2003). "Liquid crystalline assemblies of collagen in bone and in vitro systems." J Biomech **36**(10): 1571-9.

Giraud-Guille, M. M., G. Mosser, et al. (2008). "Liquid crystallinity in collagen systems in vitro and in vivo." Current Opinion in Colloid & Interface Science **13**(4): 303-313.

Glass-Brudzinski, J., D. Perizzolo, et al. (2002). "Effects of substratum surface topography on the organization of cells and collagen fibers in collagen gel cultures." J Biomed Mater Res **61**(4): 608-18.

Gobeaux, F., G. Mosser, et al. (2008). "Fibrillogenesis in dense collagen solutions: a physicochemical study." J Mol Biol **376**(5): 1509-22.

Gong, H., T. F. Freddo, et al. (1992). "Age-related changes of sulfated proteoglycans in the normal human trabecular meshwork." Experimental Eye Research **55**(5): 691-709.

Gordon, M. K., D. R. Gerecke, et al. (1987). "Type XII collagen: distinct extracellular matrix component discovered by cDNA cloning." Proc Natl Acad Sci U S A **84**(17): 6040-4.

Graham, H. K., D. F. Holmes, et al. (2000). "Identification of collagen fibril fusion during vertebrate tendon morphogenesis. The process relies on unipolar fibrils and is regulated by collagen-proteoglycan interaction." J Mol Biol **295**(4): 891-902.

Gross, J. (1958). "Studies on the formation of collagen. I. Properties and fractionation of neutral salt extracts of normal guinea pig connective tissue." J Exp Med **107**(2): 247-63.

Gross, J. (1958). "Studies on the formation of collagen. II. The influence of growth rate on neutral salt extracts of guinea pig dermis." J Exp Med **107**(2): 265-77.

Gross, J., J. H. Highberger, et al. (1954). "Collagen Structures Considered as States of Aggregation of a Kinetic Unit. the Tropocollagen Particle." Proc Natl Acad Sci U S A **40**(8): 679-88.

Gross, J. and D. Kirk (1958). "The heat precipitation of collagen from neutral salt solutions: some rate-regulating factors." J Biol Chem **233**(2): 355-60.

Guo, C. and L. J. Kaufman (2007). "Flow and magnetic field induced collagen alignment." Biomaterials **28**(6): 1105-14.

Guo, X., A. E. Hutcheon, et al. (2007). "Morphologic characterization of organized extracellular matrix deposition by ascorbic acid-stimulated human corneal fibroblasts." Invest Ophthalmol Vis Sci **48**(9): 4050-60.

Gyi, T. J., K. M. Meek, et al. (1988). "Collagen interfibrillar distances in corneal stroma using synchrotron X-ray diffraction: a species study." International Journal of Biological Macromolecules **10**(5): 265-269.

Harris, J. R. and A. Reiber (2007). "Influence of saline and pH on collagen type I fibrillogenesis in vitro: fibril polymorphism and colloidal gold labelling." Micron **38**(5): 513-21.

Hauschka, S. D. and I. R. Konigsberg (1966). "The influence of collagen on the development of muscle clones." Proc Natl Acad Sci U S A **55**(1): 119-26.

Hay, E. D. and J. P. Revel (1969). "Fine structure of the developing avian cornea." Monogr Dev Biol **1**: 1-144.

Heuser, J. E., T. S. Reese, et al. (1979). "Synaptic vesicle exocytosis captured by quick freezing and correlated with quantal transmitter release." J Cell Biol **81**(2): 275-300.

Highberger, J. H., J. Gross, et al. (1951). "The interaction of mucoprotein with soluble collagen; an electron microscope study." Proc Natl Acad Sci U S A **37**(5): 286-91.
Hitt, A. L., A. R. Cross, et al. (1990). "Microtubule solutions display nematic liquid crystalline structure." J Biol Chem **265**(3): 1639-47.
Holden, P., R. S. Meadows, et al. (2001). "Cartilage oligomeric matrix protein interacts with type IX collagen, and disruptions to these interactions identify a pathogenetic mechanism in a bone dysplasia family." J Biol Chem **276**(8): 6046-55.
Huang, Y. and K. M. Meek (1999). "Swelling studies on the cornea and sclera: the effects of pH and ionic strength." Biophys J **77**(3): 1655-65.
Hulmes, D. J. (2002). "Building collagen molecules, fibrils, and suprafibrillar structures." J Struct Biol **137**(1-2): 2-10.
Hulmes, D. J., T. J. Wess, et al. (1995). "Radial packing, order, and disorder in collagen fibrils." Biophys J **68**(5): 1661-70.
Hulmes, D. J. S. (2008). Collagen Diversity, Synthesis and Assembly. Collagen**:** 15-47.
J. C. Bernengo, B. R. D. H. (1974). "Electrical birefringence study of monodisperse collagen solutions." Biopolymers **13**(3): 641-647.
Jester, J. V., W. M. Petroll, et al. (1999). "Corneal stromal wound healing in refractive surgery: the role of myofibroblasts." Prog Retin Eye Res **18**(3): 311-56.
Jiang, F., H. Horber, et al. (2004). "Assembly of collagen into microribbons: effects of pH and electrolytes." J Struct Biol **148**(3): 268-78.
Joe, S. H., S. G. S. Eric, et al. (2000). "Brownian dynamics simulations of single DNA molecules in shear flow." Journal of Rheology **44**(4): 713-742.
John C. Thomas, G. C. F. (1979). "Dynamic light scattering from collagen solutions. II. Photon correlation study of the depolarized light." Biopolymers **18**(6): 1333-1352.
Kadler, K. (2004). "Matrix loading: assembly of extracellular matrix collagen fibrils during embryogenesis." Birth Defects Res C Embryo Today **72**(1): 1-11.
Kadler, K. E., C. Baldock, et al. (2007). "Collagens at a glance." J Cell Sci **120**(Pt 12): 1955-8.
Kadler, K. E., Y. Hojima, et al. (1987). "Assembly of collagen fibrils de novo by cleavage of the type I pC-collagen with procollagen C-proteinase. Assay of critical concentration demonstrates that collagen self-assembly is a classical example of an entropy-driven process." J Biol Chem **262**(32): 15696-701.
Kadler, K. E., Y. Hojima, et al. (1988). "Assembly of type I collagen fibrils de novo. Between 37 and 41 degrees C the process is limited by micro-unfolding of monomers." J Biol Chem **263**(21): 10517-23.
Kadler, K. E., D. F. Holmes, et al. (1996). "Collagen fibril formation." Biochem. J. **316**(1): 1-11.
Kenji Kubota, Y. T. S. F. (1987). "Dynamic light-scattering study of semiflexible polymers: Collagen." Biopolymers **26**(10): 1717-1729.
Kleinman, H. K., L. Luckenbill-Edds, et al. (1987). "Use of extracellular matrix components for cell culture." Anal Biochem **166**(1): 1-13.
Klug, W. S., M. R. Cummings, et al. (1997). Concepts of genetics. Upper Saddle River, N.J., Prentice Hall.
Komai, Y. and T. Ushiki (1991). "The three-dimensional organization of collagen fibrils in the human cornea and sclera." Invest Ophthalmol Vis Sci **32**(8): 2244-58.
Konigsberg, I. R. (1963). "Clonal analysis of myogenesis." Science **140**: 1273-84.

Koster, S., J. B. Leach, et al. (2007). "Visualization of flow-aligned type I collagen self-assembly in tunable pH gradients." Langmuir **23**(2): 357-9.
Kraus, J., P. Muller-Buschbaum, et al. (2000). "Confinement effects on the chain conformation in thin polymer films." EPL (Europhysics Letters)(2): 210.
Kuc, I. M. and P. G. Scott (1997). "Increased diameters of collagen fibrils precipitated in vitro in the presence of decorin from various connective tissues." Connect Tissue Res **36**(4): 287-96.
Kuznetsova, N. and S. Leikin (1999). "Does the triple helical domain of type I collagen encode molecular recognition and fiber assembly while telopeptides serve as catalytic domains? Effect of proteolytic cleavage on fibrillogenesis and on collagen-collagen interaction in fibers." J Biol Chem **274**(51): 36083-8.
Ladoux, B. and P. S. Doyle (2000). "Stretching tethered DNA chains in shear flow." EPL (Europhysics Letters)(5): 511.
Lanfer, B., U. Freudenberg, et al. (2008). "Aligned fibrillar collagen matrices obtained by shear flow deposition." Biomaterials **29**(28): 3888-95.
Larson, R. G., H. Hu, et al. (1999). "Brownian dynamics simulations of a DNA molecule in an extensional flow field." Journal of Rheology **43**(2): 267-304.
Lee, C. H., H. J. Shin, et al. (2005). "Nanofiber alignment and direction of mechanical strain affect the ECM production of human ACL fibroblast." Biomaterials **26**(11): 1261-70.
Lee, P., R. Lin, et al. (2006). "Microfluidic alignment of collagen fibers for in vitro cell culture." Biomed Microdevices **8**(1): 35-41.
Leikin, S., D. C. Rau, et al. (1995). "Temperature-favoured assembly of collagen is driven by hydrophilic not hydrophobic interactions." Nat Struct Biol **2**(3): 205-10.
Leneweit, G., K. G. Roesner, et al. (1999). "Surface instabilities of thin liquid film flow on a rotating disk." Experiments in Fluids **26**: 75-85.
Lepescheux, L. (1988). "Spatial organization of collagen in annelid cuticle: order and defects." Biol Cell **62**(1): 17-31.
Leung, M. K., L. I. Fessler, et al. (1979). "Separate amino and carboxyl procollagen peptidases in chick embryo tendon." J Biol Chem **254**(1): 224-32.
Li, L., H. Hu, et al. (2004). "DNA molecular configurations in flows near adsorbing and nonadsorbing surfaces." Rheologica Acta **44**(1): 38-46.
Li, L., R. G. Larson, et al. (2000). "Brownian dynamics simulations of dilute polystyrene solutions." Journal of Rheology **44**(2): 291-322.
Linsenmayer, T. F., J. M. Fitch, et al. (1983). "Monoclonal antibodies against chicken type V collagen: production, specificity, and use for immunocytochemical localization in embryonic cornea and other organs." J Cell Biol **96**(1): 124-32.
Lotz, J. C. and A. J. Kim (2005). "Disc regeneration: why, when, and how." Neurosurg Clin N Am **16**(4): 657-63, vii.
Maier, W. and A. Saupe (1960). "A simple molecular-statistics theory of the nematic nematic liquid-crystalline phase." Zeitschrift für Naturforschung **15a**: 15.
Marchini, M., R. Strocchi, et al. (1979). "Ultrastructural observations on collagen and proteoglycans in the annulus fibrosus of the intervertebral disc." Basic Appl Histochem **23**(2): 137-48.
Mardia, K. V. and P. E. Jupp (2000). Directional statistics. Chichester ; New York, J. Wiley.

Marion K. Gordon, J. W. F. T. F. L. J. M. F. (1996). "Temporal expression of types XII and XIV collagen mRNA and protein during avian corneal development." Developmental Dynamics **206**(1): 49-58.
Martin, G. R. and H. K. Kleinman (1981). "Extracellular matrix proteins give new life to cell culture." Hepatology **1**(3): 264-6.
Martin, R., J. Farjanel, et al. (2000). "Liquid crystalline ordering of procollagen as a determinant of three-dimensional extracellular matrix architecture." J Mol Biol **301**(1): 11-7.
Matthews, J. A., G. E. Wnek, et al. (2002). "Electrospinning of collagen nanofibers." Biomacromolecules **3**(2): 232-8.
McLaughlin, J. S., T. F. Linsenmayer, et al. (1989). "Type V collagen synthesis and deposition by chicken embryo corneal fibroblasts in vitro." J Cell Sci **94 (Pt 2)**(Pt 2): 371-9.
Meek, K. M. and C. Boote (2004). "The organization of collagen in the corneal stroma." Exp Eye Res **78**(3): 503-12.
Meek, K. M., J. A. Chapman, et al. (1979). "The staining pattern of collagen fibrils. Improved correlation with sequence data." J Biol Chem **254**(21): 10710-4.
Meek, K. M., J. E. Scott, et al. (1985). "An X-ray diffraction analysis of rat tail tendons treated with Cupromeronic Blue." J Microsc **139**(Pt 2): 205-19.
Meij, J. T., E. C. Carlson, et al. (2007). "Targeted expression of a lumican transgene rescues corneal deficiencies in lumican-null mice." Mol Vis **13**: 2012-8.
Mellor, S. J., G. L. Atkins, et al. (1990). "A Kinetic Analysis of Type I Procollagen Processing in Developing Chick Embryo Cornea." Annals of the New York Academy of Sciences **580**(1): 484-488.
Miles, C. A. and M. Ghelashvili (1999). "Polymer-in-a-box mechanism for the thermal stabilization of collagen molecules in fibers." Biophys J **76**(6): 3243-52.
Mosser, G., A. Anglo, et al. (2006). "Dense tissue-like collagen matrices formed in cell-free conditions." Matrix Biol **25**(1): 3-13.
Mould, A. P. and D. J. Hulmes (1987). "Surface-induced aggregation of type I procollagen." J Mol Biol **195**(3): 543-53.
Naughton, G. K. (2002). "From lab bench to market: critical issues in tissue engineering." Ann N Y Acad Sci **961**: 372-85.
Neame, P. J., C. J. Kay, et al. (2000). "Independent modulation of collagen fibrillogenesis by decorin and lumican." Cell Mol Life Sci **57**(5): 859-63.
Nestler, F. H., S. Hvidt, et al. (1983). "Flexibility of collagen determined from dilute solution viscoelastic measurements." Biopolymers **22**(7): 1747-58.
Nikon. (www.microscopyu.com). "Polarized light microscopy diagram." from http://www.microscopyu.com/.
Ottani, V., D. Martini, et al. (2002). "Hierarchical structures in fibrillar collagens." Micron **33**(7-8): 587-96.
Parry, D. A. (1988). "The molecular and fibrillar structure of collagen and its relationship to the mechanical properties of connective tissue." Biophys Chem **29**(1-2): 195-209.
Ploetz, C., E. I. Zycband, et al. (1991). "Collagen fibril assembly and deposition in the developing dermis: segmental deposition in extracellular compartments." J Struct Biol **106**(1): 73-81.

Prockop, D. and D. Hulmes (1994). Assembly of collagen fibrils de novo from soluble precursors: Polymerization and copolymerization of procollagen, pN-collagen, and mutated collagens. Extracellular Matrix Assembly and Structure. B. D. Yurchenco PD, Mecham RP. San Diego, Academic Press, Inc**:** 47-90.

Provenzano, P. P. and R. Vanderby, Jr. (2006). "Collagen fibril morphology and organization: implications for force transmission in ligament and tendon." Matrix Biol **25**(2): 71-84.

Rada, J. A., P. K. Cornuet, et al. (1993). "Regulation of corneal collagen fibrillogenesis in vitro by corneal proteoglycan (lumican and decorin) core proteins." Exp Eye Res **56**(6): 635-48.

Ramachandran, G. N. (1956). "Structure of collagen." Nature **177**(4511): 710-1.

Ramachandran, G. N. and G. Kartha (1954). "Structure of collagen." Nature **174**(4423): 269-70.

Ramachandran, G. N. and G. Kartha (1955). "Structure of collagen." Nature **176**(4482): 593-5.

Ramachandran, G. N. and V. Sasisekharan (1961). "Structure of collagen." Nature **190**: 1004-5.

Rauscher, J. W., R. E. Kelly, et al. (1973). "An Asymptotic Solution for the Laminar Flow of a Thin Film on a Rotating Disk." J. Appl. Mech **40**: 43-47.

Rauscher, J. W., R. E. Kelly, et al. (1973). "An asymptotic solution for the laminar flow of thin films on a rotating disk." Journal of Applied Mechanics **40**: 43-47.

Regini, J. W., G. F. Elliott, et al. (2004). "The ordering of corneal collagen fibrils with increasing ionic strength." J Mol Biol **336**(1): 179-86.

Reinitzer, F. (1888). "Beiträge zur Kenntniss des Cholesterins." Monatshefte für Chemie / Chemical Monthly **9**(1): 421-441.

Ren, R., A. Hutcheon, et al. (2008). "Human primary corneal fibroblasts synthesize and deposit proteoglycans in long-term 3-D cultures." Dev Dyn **In Press**.

Ren, R., A. E. Hutcheon, et al. (2008). "Human primary corneal fibroblasts synthesize and deposit proteoglycans in long-term 3-D cultures." Dev Dyn **237**(10): 2705-15.

Rosso, F., A. Giordano, et al. (2004). "From cell-ECM interactions to tissue engineering." J Cell Physiol **199**(2): 174-80.

Ruberti, J. W., S. A. Melotti, et al. (2003). "Nanoscale Engineering of Type I Collagen Fibrils to Mimic the Multiple Layers of Aligned Lamellae in Cornea." Invest. Ophthalmol. Vis. Sci. **44**(5): 4218-.

Ruberti, J. W. and J. D. Zieske (2008). "Prelude to corneal tissue engineering - gaining control of collagen organization." Prog Retin Eye Res **27**(5): 549-77.

Rzehak, R., W. Kromen, et al. (2000). "Deformation of a tethered polymer in uniform flow." The European Physical Journal E - Soft Matter **2**(1): 3-30.

Saintillan, D., E. S. G. Shaqfeh, et al. (2006). "Effect of flexibility on the shear-induced migration of short-chain polymers in parabolic channel flow." Journal of Fluid Mechanics **557**(-1): 297-306.

Sander, E. A. and V. H. Barocas (2008). "Comparison of 2D fiber network orientation measurement methods." J Biomed Mater Res A **19**: 19.

Schonherr, E., C. Sunderkotter, et al. (2004). "Decorin deficiency leads to impaired angiogenesis in injured mouse cornea." J Vasc Res **41**(6): 499-508.

Scott, J. E. (1988). "Proteoglycan-fibrillar collagen interactions." Biochem J **252**(2): 313-23.
Scott, J. E. (1990). "Proteoglycan:collagen interactions and subfibrillar structure in collagen fibrils. Implications in the development and ageing of connective tissues." J Anat **169**: 23-35.
Scott, J. E. (1991). "Proteoglycan: collagen interactions and corneal ultrastructure." Biochem Soc Trans **19**(4): 877-81.
Scott, J. E. (1995). "Extracellular matrix, supramolecular organisation and shape." J Anat **187 (Pt 2)**(Pt 2): 259-69.
Scott, J. E. and M. Haigh (1985). "'Small'-proteoglycan:collagen interactions: keratan sulphate proteoglycan associates with rabbit corneal collagen fibrils at the 'a' and 'c' bands." Biosci Rep **5**(9): 765-74.
Scott, J. E. and M. Haigh (1988). "Keratan sulphate and the ultrastructure of cornea and cartilage: a 'stand-in' for chondroitin sulphate in conditions of oxygen lack?" J Anat **158**: 95-108.
Scott, J. E., C. R. Orford, et al. (1981). "Proteoglycan-collagen arrangements in developing rat tail tendon. An electron microscopical and biochemical investigation." Biochem J **195**(3): 573-81.
Scott, J. E. and A. M. Thomlinson (1998). "The structure of interfibrillar proteoglycan bridges (shape modules') in extracellular matrix of fibrous connective tissues and their stability in various chemical environments." J Anat **192 (Pt 3)**: 391-405.
Severs, N. J. (2007). "Freeze-fracture electron microscopy." Nat. Protocols **2**(3): 547-576.
Shaw, L. M. and B. R. Olsen (1991). "FACIT collagens: diverse molecular bridges in extracellular matrices." Trends Biochem Sci **16**(5): 191-4.
Sini, P., A. Denti, et al. (1997). "Role of decorin on in vitro fibrillogenesis of type I collagen." Glycoconj J **14**(7): 871-4.
Smith, D. E., H. P. Babcock, et al. (1999). "Single-polymer dynamics in steady shear flow." Science **283**(5408): 1724-7.
Song, J., Y. G. Lee, et al. (2003). "Neonatal corneal stromal development in the normal and lumican-deficient mouse." Invest Ophthalmol Vis Sci **44**(2): 548-57.
Stewart, G. T. (2003). Liquid crystals in biology I. Historical, biological and medical aspects. Liquid Crystals, Taylor & Francis Ltd. **30:** 541.
Stewart, G. T. (2004). Liquid crystals in biology II. Origins and processes of life. Liquid Crystals, Taylor & Francis Ltd. **31:** 443-471.
Sun, Y. L., Z. P. Luo, et al. (2002). "Direct quantification of the flexibility of type I collagen monomer." Biochem Biophys Res Commun **295**(2): 382-6.
Tanihara, H., M. Inatani, et al. (2002). "Proteoglycans in the eye." Cornea **21**(7 Suppl): S62-9.
Taylor, G. (1953). "Dispersion of Soluble Matter in Solvent Flowing Slowly through a Tube." Proceedings of the Royal Society of London. Series A, Mathematical and Physical Sciences **219**(1137): 186-203.
Thur, J., K. Rosenberg, et al. (2001). "Mutations in cartilage oligomeric matrix protein causing pseudoachondroplasia and multiple epiphyseal dysplasia affect binding of calcium and collagen I, II, and IX." J Biol Chem **276**(9): 6083-92.

Torbet, J., M. Malbouyres, et al. (2007). "Orthogonal scaffold of magnetically aligned collagen lamellae for corneal stroma reconstruction." Biomaterials **28**(29): 4268-76.
Torbet, J. and M. C. Ronziere (1984). "Magnetic alignment of collagen during self-assembly." Biochem J **219**(3): 1057-9.
Trelstad, R. L. (1971). "Vacuoles in the embryonic chick corneal epithelium, an epithelium which produces collagen." J Cell Biol **48**(3): 689-94.
Trelstad, R. L. (1982). "The bilaterally asymmetrical architecture of the submammalian corneal stroma resembles a cholesteric liquid crystal." Dev Biol **92**(1): 133-4.
Trelstad, R. L. and A. J. Coulombre (1971). "Morphogenesis of the collagenous stroma in the chick cornea." J Cell Biol **50**(3): 840-58.
Trelstad, R. L. and K. Hayashi (1979). "Tendon collagen fibrillogenesis: intracellular subassemblies and cell surface changes associated with fibril growth." Dev Biol **71**(2): 228-42.
Usha, R., R. Maheshwari, et al. (2006). "Structural influence of mono and polyhydric alcohols on the stabilization of collagen." Colloids and Surfaces B: Biointerfaces **48**(2): 101-105.
van der Rest, M. and R. Garrone (1991). "Collagen family of proteins." Faseb J **5**(13): 2814-23.
Vaughan, L., M. Mendler, et al. (1988). "D-periodic distribution of collagen type IX along cartilage fibrils." J Cell Biol **106**(3): 991-7.
Vesentini, S., A. Redaelli, et al. (2005). "Estimation of the binding force of the collagen molecule-decorin core protein complex in collagen fibril." Journal of Biomechanics **38**(3): 433-443.
Vuorio, E. and B. de Crombrugghe (1990). "The family of collagen genes." Annu Rev Biochem **59**: 837-72.
Wagner, D. R. and J. C. Lotz (2004). "Theoretical model and experimental results for the nonlinear elastic behavior of human annulus fibrosus." Journal of Orthopaedic Research **22**(4): 901-909.
Weber, I. T., R. W. Harrison, et al. (1996). "Model structure of decorin and implications for collagen fibrillogenesis." J Biol Chem **271**(50): 31767-70.
Wenstrup, R. J., J. B. Florer, et al. (2004). "Type V collagen controls the initiation of collagen fibril assembly." J Biol Chem **279**(51): 53331-7.
Wess, T. J. (2008). Collagen Fibrillar Structure and Hierarchies. Collagen**:** 49-80.
Wilson, D. L., R. Martin, et al. (2001). "Surface organization and nanopatterning of collagen by dip-pen nanolithography." Proc Natl Acad Sci U S A **98**(24): 13660-4.
Woltman, S. J., G. P. Crawford, et al. (2007). Liquid crystals : frontiers in biomedical applications. Hackensack, NJ, World Scientific.
Wood, G. C. (1964). "The precipitation of collagen fibers from solution." Int Rev Connect Tissue Res **2**: 1-31.
Yang, G. C. and D. E. Birk (1986). "Topographies of extracytoplasmic compartments in developing chick tendon fibroblasts." J Ultrastruct Mol Struct Res **97**(1-3): 238-48.

Yevdokimov Yu, M., V. I. Salyanov, et al. (1983). "A mesophase (liquid crystal) state of DNA complexes with anthracycline antibiotics." Biomed Biochim Acta **42**(7-8): 855-66.

Yoshioka, K. and C. T. O'Konski (1966). "Electric properties of macromolecules. IX. Dipole moment, polarizability, and optical anisotropy factor of collagen in solution from electric birefringence." Biopolymers **4**(5): 499-507.

Yoshizato, K., T. Obinata, et al. (1981). "In Vitro Orientation of Fibroblasts and Myoblasts on Aligned Collagen Film." Development, Growth & Differentiation **23**(2): 175-184.

Zhao, X. C., R. W. Yee, et al. (2006). "The zebrafish cornea: structure and development." Invest Ophthalmol Vis Sci **47**(10): 4341-8.

Chapter 3

Production of Organized Lamellae of Collagen Fibrils Precipitated From a High Concentration Solution of Monomers

Introduction

Collagen is thought to have evolved over 700 MYA and is present in all animal phyla from the simplest (and oldest) metazoans to the most advanced extant mammals (Exposito, Cluzel et al. 2002). Fibrillar collagens (types I, II, III, V and XI) are the principal structural component in load-bearing extracellular matrix (ECM) which provides a network for cells to interact and form three dimensional, multi-cellular organisms. Metazoans likely owe a good deal of their phenomenal evolutionary success to the utility of collagen as a structural material. Collagen in the load-bearing tissues is often arranged into bundles of parallel fibrils capable of supporting *in vivo* mechanical loads (Parry 1988; Fratzl, Misof et al. 1998). The predominant theory of collagen fibril deposition during the development of highly-anisotropic tissues such as ligament and tendon suggests that collagen is deposited directly by mesenchymal fibroblasts via cell surface features termed "fibripositors" (Birk and Trelstad 1984; Birk and Trelstad 1985; Birk and Trelstad 1986; Ploetz, Zycband et al. 1991; Canty, Lu et al. 2004). For tissues

such as the cornea and anulus fibrosus, which possess a complex fibrillar 2D+ arrangement, comprising alternating arrays of aligned fibrils, it is more difficult to imagine how individual cells can produce the matrix organization. Directly depositing alternating lamellae requires tight control over cell motion and a mechanism which promotes efficient fibril fusion (as it has been suggested that cells fibriposit in two directions at once (Birk and Trelstad 1984)). However, there is evidence in the literature which suggests that collagen fibrillogenesis occurs at a distance from immobilized cells and in a tightly confined space. In corneal tissue, cells must maximize control of collagen fibril morphology and organization to generate a transparent collagenous matrix. There are thus numerous detailed investigations of the development of the organized lamellar matrix found in the corneal stroma. These investigations have demonstrated that during corneal development in both the chick and the zebrafish, orthogonal arrays of collagen are deposited by confluent immobilized sheets of epithelium through a basement membrane (Trelstad 1971; Zhao, Yee et al. 2006). Thus, there is likely little influence of the cell (via motion or direct placement of molecules) on the orientation of the fibrils. In the corneas of all submammalian classes, pairs of orthogonal fibrillar arrays are shifted relative to adjacent pairs of fibrillar arrays such that there is an overall clockwise rotation from the outer to inner cornea. This rotation does not exhibit bilateral symmetry, instead the stromal lamellar orientation in both eyes rotate in the same direction, suggesting physical (liquid crystal) rather than cell-directed control of the fibrillar orientation (Coulombre 1965; Trelstad 1982). In the zebrafish, the primary stromal lamellae (each only one fibril thick) gain fibrils during secondary stromal synthesis through a mechanism of accretion which is unlikely to be controlled by an immediately adjacent

cell (Zhao, Yee et al. 2006). This is because the lamellae are extremely thin relative to keratocyte cell thickness. Finally, in developing corneas, the stroma is produced in a confined space suggesting that confinement is a potential mediator of organization.

We subscribe to the view that collagen is not a passively manipulated element, but rather the principal component in a cooperative engineering material system; a system which significantly enhances the ability of fibroblastic cells to produce and optimize load-bearing tissues. Such tissue is often characterized by its highly anisotropic and ordered collagen fibrillar organization (cornea (Hay and Revel 1969), ligament and tendon (Provenzano and Vanderby 2006), and anulus fibrosus (Marchini, Strocchi et al. 1979)) and, unfortunately, its limited regenerative ability following injury (Frank 2004; Fini and Stramer 2005; Lotz and Kim 2005).

It has long been known that collagen monomers extracted from native tissue will spontaneously self-assemble at neutral pH and 37ºC and form disorganized networks of collagen fibrils with morphologies similar to the native collagen fibrils (D-periodic banding) (Gross and Kirk 1958). However, self-assembled collagen gels used as degradable tissue engineering scaffolds are generally low in density and randomly organized. The absence of highly anisotropic, aligned and dense collagen fibrils has limited scaffold mechanical strength (relative to native load-bearing collagenous ECMs) and has motivated researchers to attempt to organize collagen *de novo* (Dip-pen lithography (Wilson, Martin et al. 2001), magnetic force (Torbet and Ronziere 1984; Torbet, Malbouyres et al. 2007), electro-spinning (Matthews, Wnek et al. 2002), fluid flow (Lee, Lin et al. 2006), combination of flow and magnetic field (Guo and Kaufman 2007), chemical nanopatterning (Denis, Pallandre et al. 2005), etc). The *de novo* methods

which have been designed to gain control over the local and long-range organization of self-assembled collagen gels typically involve the use of significant physical forces or direct manipulation. Unfortunately there has been little success in controlling fibril organization simultaneously over both long and short length scales while propagating that organization into 3 dimensions.

In this chapter a simple approach to the problem of generating local, long-range and 3-dimensional fibril organization is demonstrated. The method entails concentrating, confining and inducing the polymerization of collagen monomers between two parallel flat surfaces. The method, which takes advantage of the natural organizational information encoded into the collagen triple helix, was inspired during our attempts to induce primary human corneal stromal cells (PHCSCs) to reproduce the organized, lamellar matrix of native corneal stroma (Guo, Hutcheon et al. 2007). It was observed that PHCSCs initially formed orthogonal sheets of elongated, confluent cells which appeared to separate over time, while producing a cell-bounded, stratified construct comprising organized, alternating lamellae of collagen fibrils (Figure 3-6 A,B,C) (Ren, Hutcheon et al. 2008). In addition, if corneal fibroblasts are unable to form bounding monolayers and do not stratify, collagen is deposited, but it is not organized (unpublished data). Thus it seems that bounding layers of cells or confinement of collagen could be instrumental in the production of organized, lamellar matrix. We hypothesized that fibroblastic cells export collagen monomers into confined extracellular spaces at high concentration (which are effectively in the liquid crystalline regime) prior to condensation of fibrils. If so, matrix forming cells would not have to directly stitch the orthogonally-organized collagen arrays (as has been suggested to explain corneal

development (Birk and Trelstad 1984)). Instead, fibroblasts would need only to arrange themselves to produce an appropriate confining geometry and then concentrate the collagen monomers. The rate of monomer production has been estimated to be 1-3x10^6 monomers per hour per cell during chick corneal development (from day 11 to 16 of development) which suggests that a single cell could produce ~10-20 cubic microns per hour of collagen concentrated enough to be in the liquid crystalline regime. Given high enough concentrations, collagen monomers will spontaneously produce organized, liquid crystalline patterns (Giraud-Guille 1992) which are readily influenced by both local and confining geometric surfaces. The confined, patterned arrays of monomers would condense into organized arrays of fibrils upon enzymatic cleavage of collagen propeptides. Figure 3-6A demonstrates that primary human corneal fibroblasts do, in fact, naturally form confluent and generally orthogonal sheets on two-dimensional surfaces (this occurs in 3-dimensional gels as well (Doane, Babiarz et al. 1992).

Bouligand showed that collagen fibrils self-assembled *in vitro* demonstrate the twisted structures similar to the ones in cholesteric liquid crystal materials (Bouligand, Denefle et al. 1985). In a series of careful experiments, the laboratory of Dr. Giraud-Guille demonstrated that dehydrating monomeric solutions of tropocollagen and procollagen results in the formation of pre-cholesteric and cholesteric patterns (Giraud-Guille 1989; Martin, Farjanel et al. 2000). The dehydrated monomeric solutions can produce nested arc-shape fibrillar patterns similar to the patterns seen in compact bone (Mosser, Anglo et al. 2006). However, the method does not appear to consistently produce the lamellar organization similar to that found in un-calcified load-bearing tissues such as anulus fibrosus or cornea. This could be due to the effects of the very

strong local dehydration gradients or by the absence of bounding surfaces. Further, and more limiting, the method of Giraud-Guille induces collagen polymerization via toxic ammonium vapour and thus may not be suitable to use in cell culture or for tissue engineering protocols. To address these limitations, Gobeaux *et al*. (Gobeaux, Mosser et al. 2008) did attempt to dehydrate collagen and fibrilize solutions in a manner somewhat similar to that used in this work, however, electron microscopy of the constructs did not demonstrate convincing fibrillar organization over any length scale.

The methods in this investigation entail working with concentrated solutions of atelo type I collagen molecules which are gently concentrated (allowing better control over local pH and ionic strength). The method also permits confinement of the solution in variety of the geometries (e.g. parallel plates, thin-walled cylinder, or nested hemispheres) similar to geometries seen in load-bearing tissues. Further, the constructs produced by the methods proposed herein are readily suitable to be used as organized 3-dimensional scaffolds for cell culture and tissue engineering and have the potential to be formed around embedded cells (which cannot be done if toxic ammonium is used as a neutralization agent). Finally, the simple method of confinement and concentration presented in this investigation results in the persistence of fibrillar organization over long length scales and may provide insight into how cells can readily synthesize anisotropic load-bearing tissues during development.

If a confining, concentrating strategy is a successful method used to produce collagen organization, it greatly simplifies the assumed role of the synthetic fibroblast during matrix production. In addition, with current nano- and MEMS technology, engineers could employ a similar strategy to produce organized collagen lamellar arrays

de novo (provided the length scales over which liquid crystalline collagen organization persists are not too short).

First defined in 1888 (Reinitzer 1888), the term liquid crystal (LC) is applied to a group of substances which exhibit phase of matter that is intermediate between an isotropic liquid and a crystalline solid (Woltman, Crawford et al. 2007). The materials that show the liquid crystalline (or mesogenic) phases exhibit a high degree of shape anisotropy: rod-like (calamitic) or disc-like (discotic). In general there are two classes of liquid crystals: temperature driven (thermotropic) or concentration driven (lyotropic). While thermotropic LCs are of a great interest in industrial applicatons (e.g. eletro-optic displays, temperature and pressure sensors), the lyoptic LCs are of an interest biologically. Many organic molecules including DNA (Yevdokimov Yu, Salyanov et al. 1983), phospholipids and cholesterols (Chapman 1966), Microtubules (Hitt, Cross et al. 1990), and collagen (Giraud-Guille 1989) exhibit lyotropic mesophases and it is hypothesized that it plays a great role in the living cells (for review (Stewart 2003; Stewart 2004)).

In addition to the classification of the liquid crystals based on their origin (i.e. thermotropic or lyotriopic), Friedel distinguished them into the three major classes of nematic, smectic, and cholesteric upon on their symmetry (Friedel 1922). Figure 3-1 is a schematic of the molecular organization in each of different liquid crystalline phases.

The nematic phase is the simplest among all the phases of the liquid crystals. It differs from an isotropic fluid phase in that the molecules exhibit a long range

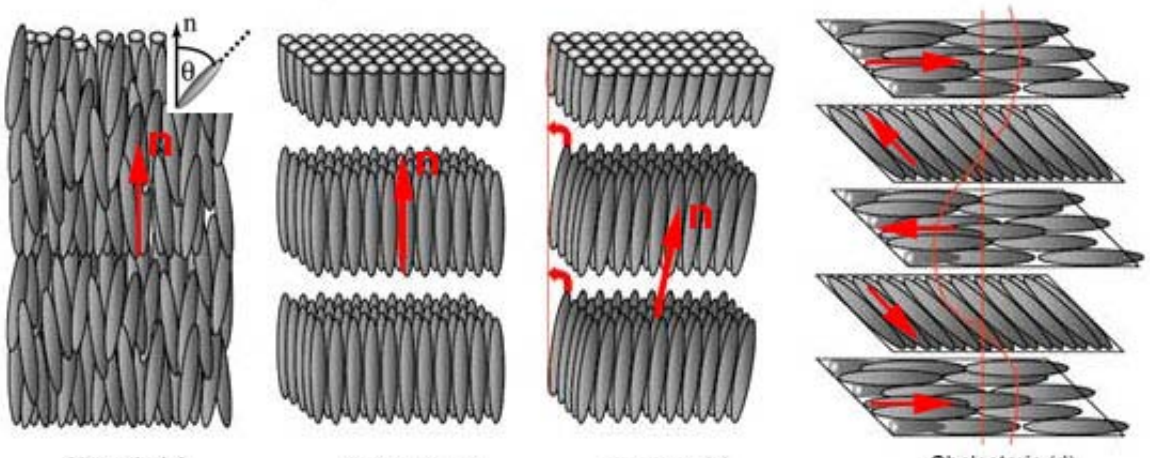

Figure 3-42: (a-d), illustration of the molecular organization indifferent LC phases

orientational order. However, it is still a fluid phase in which molecules do not have any positional order and there is no long range correlation of the molecular center of mass position. The principal axis, n̂, is defined as the average direction of the ensemble of the molecules. In the smectic phase the molecules are arranged into layered structures within which they exhibit one degree of translational ordering. Although eight smectic phases have been identified, smectic A and C are the best well known and identified among them. The main difference between the smectic A and C is the orientation of the molecules with respect to the layer's normal. In the smectic A, the director n̂ is parallel to the layer normal and over a larger scale, the orientation of the molecules are uncorrelated with respect to the center of mass position which results in the fluidity within each layer. As revealed with the X-ray diffraction experiments, the layer thickness is usually the same as the length of the molecules. In smectic C however, the director is tilted with respect to the layer normal which consequently results in a layer thickness which is

significantly smaller than the full length of the molecules. Similar to smectic A, the individual layers are fluid and there is probability of the inter layer diffusion (although less probable in smectic C). Figure 3-1d is a schematic of the molecular organization in the cholesteric (or chiral nematic) LC phase at equilibrium. In a short scale, the cholesteric phase is composed of the stacks of molecules and within each layer the molecules form a nematic phase. In the large scale, the cholesteric director n̂ follows a helix with a spatial period of:

$$L = \frac{\pi}{|q_0|} \tag{1}$$

And the equation:

$$n_x = \cos(q_0 z + \varphi) \tag{2}$$

$$n_y = \sin(q_0 z + \varphi) \tag{3}$$

$$n_z = 0 \tag{4}$$

Where both the magnitude of the phase angle φ and the direction of the helix axis are arbitrary. Based on the Maier-Saupe theory the order parameter for the nematic phase is defined as (Maier and Saupe 1960):

$$\langle P \rangle = \frac{1}{2}(3\langle \cos^2 \theta \rangle - 1) \qquad \begin{cases} \langle P \rangle = 1 & \textit{if perfectly ordered} \\ \langle P \rangle = 0 & \textit{if completely disordered} \end{cases} \tag{5}$$

Diffraction is one the most powerful tools to reveal the internal structure of the materials. Among different radiation (i.e. X-ray, neutron, and electron), X-ray diffraction is the

most widely used method. The biggest advantage of the X-ray diffraction, other than being more readily available, is that it can be performed on samples with dimensions of the order of millimeter. The diffraction patterns cased by the scattering of the of the X-ray by the molecules provide invaluable quantitative information about the molecular organization of the material such as long and short range organization, intermolecular spacing, and most importantly, the order parameter S. In principal, the relationship between the diffraction patterns and the molecular organization is based on the Bragg equation (eq.1) for an incident wavelength λ (Figure 3-2A):

$$n\lambda = 2d \sin\theta_B \tag{6}$$

where n is order of diffraction, d is the normal distance of the diffracting planes, and θB is the diffracting angle. When the diffracting material is composed of multi-directional crystals the diffraction patterns will appear in a form of concentric circles (Figure 3-2B). By measuring the radius of each circle and using eq. 1, it would be possible calculate the normal spacing between the diffracting planes. In the case of non-crystalline materials, the diffraction maxima are diffuse (due to the loss of diffracting planes) however the distance between the peaks is proportional to the average intermolecular spacing.

Figure 3-2D is a schematic of X-ray diffraction patterns from a hypothetical smectic C liquid crystal material (Figure 3-2C). As it is pointed out in the figure, the distance between two diffused diffraction maxima on the equator is equal to the inverse of the intermolecular spacing and the radius of arcing are equal to the inverse of the layer's thickness. While the diffused patterns of arcs on the equator indicate that there is only a sort range molecular organization, the thin and concentric arcs indication of

ordered layers (i.e. long range positional order). The degree of the arcing is also related to the order parameter, S.

As explained before, the liquid crystal materials molecules must have high degree of shape anisotropy which consequently results in the optical anisotropy. Since LC molecules have the ability to align over large distances they exhibit birefringence properties. The birefringence is in fact the result of the optical symmetry with two principal refractive indices (i.e. ordinary, n_o, and extraordinary, n_e, Figure 3-3). The

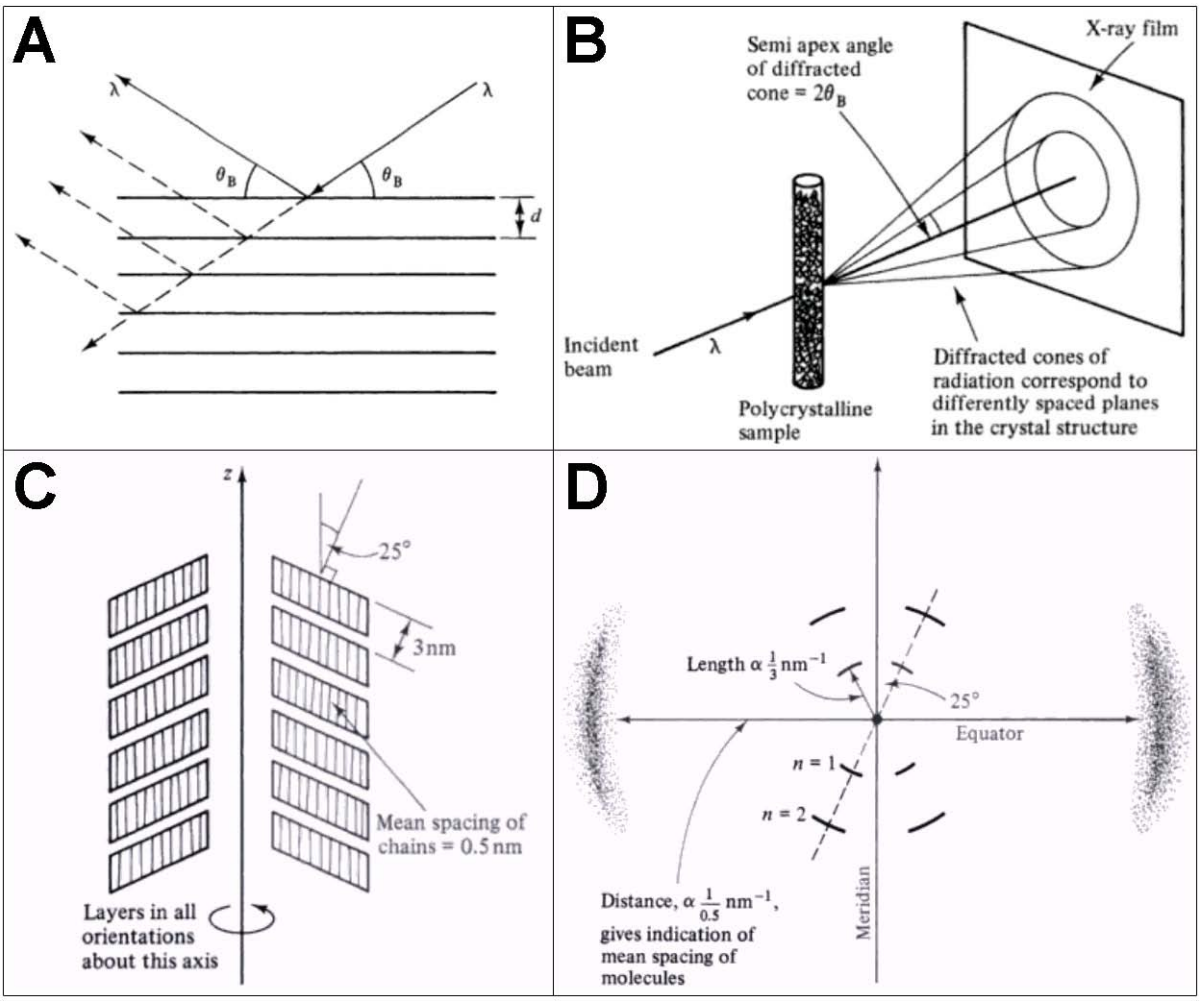

Figure 3-43: Schematics of the X-ray diffraction from a totally organized crystal (A), a crystal with short range organization (B) and smectic C liquid crystal (C and D0). Adopted from (Donald and Windle 1992)

birefringence is defined as:

$$\Delta n = n_e - n_o \tag{7}$$

Due to the birefringence nature of the liquid crystals, polarized light microscopy (PLM) has been widely used to provide information, mainly qualitatively, about the large scale organization of the molecules in liquid crystal materials. This method mainly relies on placing the LC sample between two cross polarizers (i.e. their axes of polarization are orthogonal, Figure 3-4A). In this configuration, when the local director n̂ (i.e. direction of molecular alignment) is parallel to the polarization axes, φ=0º or 90º, they will appear black and when the director is at φ=45º with respect to the polarizers' axes they will appear bright. Figure 3-4B is a demonstration of the different molecular organization and their resulting appearances using two crossed-polarizers. For polarized light microscopy on a LC material at angle θ to the long axis of the molecules the birefringence can be

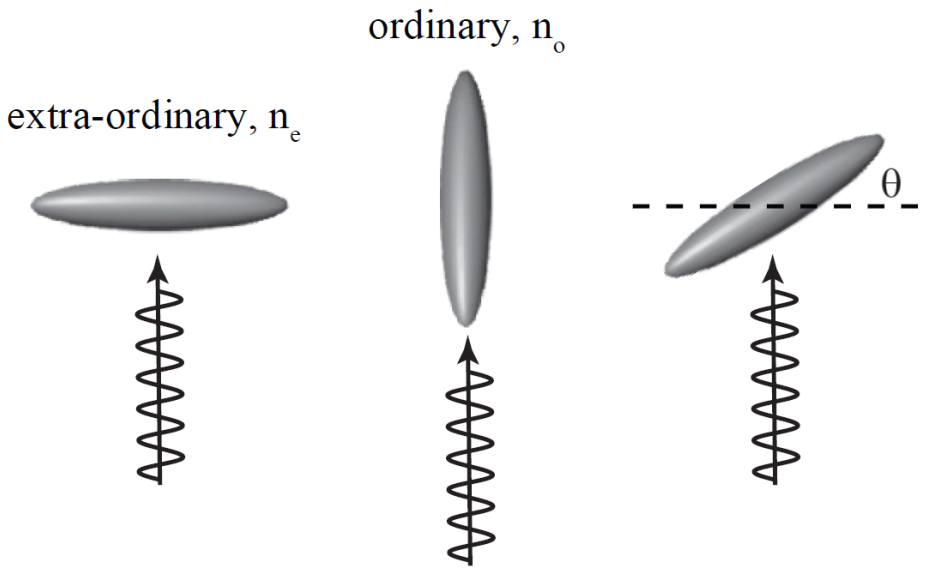

Figure 3-44: A schematic of optical anisotropy (Woltman, Crawford et al. 2007)

calculated according to:

$$n(\theta) = \left[\frac{\cos^2 \theta}{n_e^2} + \frac{\sin^2 \theta}{n_0^2} \right]^{1/2} \tag{7}$$

Figure 3-5 is a typical PLM image of collagen fibrils found both *in vivo* (e.g. osteons) and *in vitro* (i.e. precipitated from a high concentration solution of collagen molecules). The polarization image shows a banded pattern which is an indication of the abrupt changes in direction of the molecules within the samples. Figure 3-5C is a translation of the banded

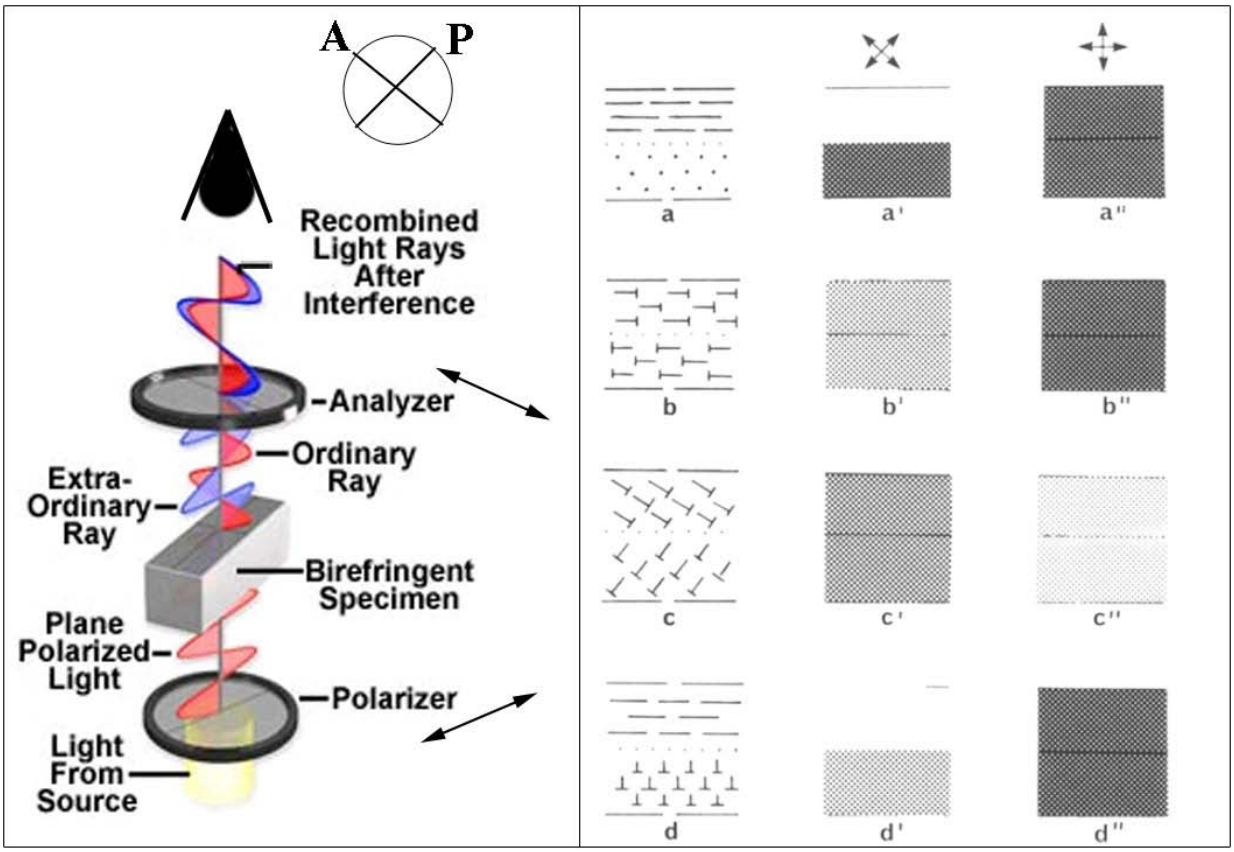

Figure 3-45: (A), A typical Polarized light microscopy (Nikon www.microscopyu.com) and (B), schematic representation of the appearance of molecules with different orientation placed between two crossed-polarizers (Giraud-Guille 1988)

patterns into the molecular organization which clearly shows that the molecules follow a helical twist representative of cholesteric liquid crystal phase. Based on these observations, a plywood model has been proposed to explain the organization of the collagen fibrils in the native tissues. In addition, reproduction of the same fibrillar patterns *in vitro* from reconstituted collagen fibrils (at high concentrations) suggest the liquid crystalline collagen self- assembly as a method employed by the nature to produce organized tissues (during development) (Hulmes 2002).

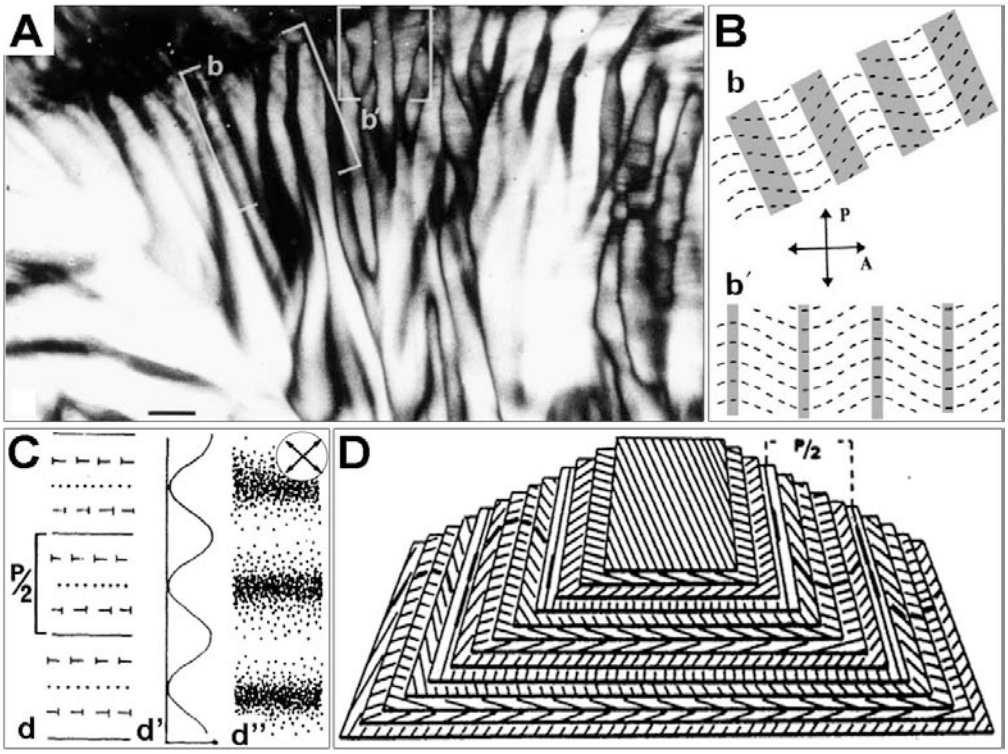

Figure 3-46: (A and B) Collagen fibrils precipitated at high concentrations appear show banded patterns in PLM (Giraud-Guille, Besseau et al. 2000). Bar=10 microns.(C), a schematic showing the molecular organization that produce the banded patterns in (A) (Giraud-Guille 1996). (D), the proposed plywood organization of the collagen fibrils proposed to describe the PLm patterns seen in collagenous matrices both *in vivo* and *in vitro* (Besseau and Giraud-Guille 1995).

3.1. Materials and Methods

To test the hypothesis that confinement and concentration of monomers leads to the production of organized arrays of collagen fibrils, triple helical domains of type I collagen (atelo-collagen monomers extracted from bovine dermis, PURECOL®, Inamed, Freemont, CA) were concentrated to liquid crystalline levels. The collagen monomers in the resulting viscous solutions were then "precipitated" by neutralization and warming to form fibrillar structures while confined between two surfaces. In addition, effects of the collagen concentration, confining heights, buffer reagents, and time required for a complete fibrillogenesis was investigated.

3.1.1. Production of the Collagenous Constructs

Dialysing against polyethylene glycol (PEG) solution (due to its high osmotic pressure) was used in this investigation. When at high concentration, collagen molecules also have high osmotic pressure and the balance of the two osmotic pressures determines the final concentration of collagen molecules. Due to the high viscosity of collagen molecules, it was not possible to measure the osmotic pressure of the solutions at concentrations above 20 mg/ml. Therefore, it is not possible to predict the final concentration of collagen and as the result finding the targeted concentration was more of a trial and error process. The goal in this investigation was to reach three ranges of concentration; 80mg/ml, ~ 150 mg/ml (similar to cornea), and ~350 mg/ml. Once the accurate concentration of PEG was found for each collagen concentration range, the thickness of the samples was controlled by the amount of molecules present in each experiment.

- **Preparation of LC Collagenous Constructs**. 3 mg/mL monomeric solution of collagen was injected into a 3.5 kMWCO dialysis cassette (Thermo scientific, Rockford, IL) and left in the PEG solution for one week at 4ºC to reach concentrations in the range of 60-80 mg/ml. Neutralization of collagen was achieved by neutralizing the PEG solution. The samples were then again reduced and kept at 4ºC for 2 weeks to allow for the complete diffusion of the ions into the dense collagen solution. To initiate fibrillogenesis, samples were transferred into a 37 ºC-100% RH incubator. It should be mentioned that at very high concentrations collagen molecules (and procollagen) undergo the self-assembly process even at the very low temperatures. We acknowledge the possibility that during the concentration process some of the molecules self-assemble and form aggregates. Although this spontaneous process is not desired, it is not avoidable either.
- **Preparation of MC Collagenous Constructs**. 3 mg/mL solution of collagen dialyzed against 40% solution of PEG (20 kMWCO, Sigma) at 4ºC to reach the concentrations in the range of 175±25 mg/mL (low concentration). The collagen solution was neutralized (pH 7-7.4), confined between two coverslips, transferred into a 37 ºC incubator.
- **Preparation of HC Collagenous Constructs**. A medium concentration solution of collagen (method described above), was transferred into a 3.5 kMWCO dialysis cassette and left in PEG solution for one week at 4ºC to reach

concentrations in the range of 375±25 mg/mL. In order to neutralize the collagen solution, the cassettes were transferred into a neutralized PEG solution.

3.1.2. Primary Human Corneal Stromal Cell (PHCSF) Derived Constructs

Cell-derived constructs were produced as described in (Guo, Hutcheon et al. 2007) on disorganized collagenous mats as described in (Ren, Hutcheon et al. 2008). Briefly, after the epithelium and endothelium were removed, corneal stroma were cut into small pieces and left into culture plates. After adhering to the surface of the culture plate, Eagle minimum essential medium (EMEM; Sigma-Aldrich, St. Louis, MO) containing 1% antibiotic/antimycotic (Sigma, St. Louis, MO) and 10% fetal bovine serum (FBS; ATCC, Manassas, VA) was added. Explants were cultured at 37ºC and 5% CO_2 for 1-2 weeks prior to passage. Fibroblasts were seeded at the density of 0.5 x 10^6 onto a bare polycarbonate membrane (no scaffold) or disorganized pepsin extracted reconstituted collagen fibrils (disorganized scaffold). Cells were cultured in EMEM containing 1 mM 2-O-a-D-glucopyanosyl-Lascorbic acid (Wako Chemicals USA, Inc., Richmond, VA).

3.1.3. Effects of Buffers on Collagen Organization: PBS vs. Trizma

Each buffer contains different types and amounts of reagents and therefore, result in collagen solutions with different ionic strength (since collagen self-assembly is very sensitive to the ionic strength of the solution). Based on the previous studies conducted in our lab, titration of collagen solution with both Phosphate Buffer Saline (PBS) and Trizma base results in collagen fibrillogenesis with different morphologies. When the collagen solution is prepared using PBS, collagen fibrils are smaller in diameter where

the number of fibrils per unit volume is significantly larger. To investigate the effects of these buffers on the self-assembly of collagen molecules at high concentrations, MC collagen constructs were titrated using PBS, trizma base buffers, or a solution of 0.1M sodium hydroxide (NaOH)-calcium chloride ($CaCl_2$).

3.1.4. Study the Time Required for Complete Fibrillogenesis

The preliminary ultrastructural assessments of the collagen fibrils self-assembled under liquid crystalline conditions revealed that fibrils do not show the 67nm D-banding characteristics. Collagen self-assembly is an entropy driven process. Upon increasing the temperature collagen molecules spontaneously self-assemble into fibrils. By incorporating into a fibril, molecules also reach to a lower energy landscape (i.e. becoming more stable) (Kadler, Hojima et al. 1987). The D-banding of the fibrils is the result of precise lateral and longitudinal arrangement of the molecules within each fibril (Sec. 1.1). It is possible that the unique gap-overlap arrangement that results in the formation of striation is the lowest energy possible to the molecules.

In vitro studies have shown that at physiological conditions, collagen molecules self-assemble into D-banded fibrils. These studies however were performed at collagen concentrations well below concentrations found in native adult tissues. It is therefore possible that when at high concentrations, due to the high viscosity and close interaction of collagen molecules, the time it takes for the monomers to rearrange and find their lowest energy would be much longer than when at low concentrations. To investigate the required time for complete fibrillogenesis (i.e. formation of D-banded fibrils), the ultra-

structures of the collagenous constructs were investigated after 6 hrs, 24 hrs, 1, 2, and 4 weeks.

3.1.5. Effects of the Confining Geometries on the Organization of the Collagen Fibrils

Another goal of this investigation was to systematically study the effects of the distance between the confining surfaces on the thickness of the layers, angle between the layers and organization of the fibrils within layers. The concentration of PEG solution was adjusted such that it produced HC collagenous constructs with the thicknesses of ~250, 150 and 50 microns. In addition, for each thickness three targeted concentrations of ~300, 200, and 100 mg/ml were studied.

3.1.6. *Concentration Measurements*

A Sircol photometric collagen assay kit (Biocolor Ltd, Carrickfergus, UK) and dry weight measurements (in a vacuum oven at 80ºC) were used to measure the concentration of the collagen solution.

3.1.7. Transmission Electron Microscopy (TEM)

Constructs were fixed overnight in modified Karnovsky fixative (2.5% glutaraldehyde, 2.5% paraformaldehyde, 0.1M cacodylate buffer, pH 7.2), washed with 0.1M buffer, post fixed in 1% osmium tetroxide in 0.1M cacodylate buffer, and dehydrated in a graded series of ethanol. The samples were infiltrated and embedded in a mixture of Spurrs resin and Quetol according to Ellis (Ellis 2006). 60-80nm cross

sections and *en face* sections were cut on an Ultracut E microtome (Reichert, Depew, NY) using a diamond knife. Thin sections were stained with 5% uranyl acetate and Reynolds lead citrate. The sections were viewed with a JEOL JEM 1010 transmission electron microscope (JEOL, Tokyo, Japan) and images were digitally captured on an AMT XR-41B CCD camera system (Advanced Microscopy Techniques Inc., Danvers, MA).

3.1.8. Scanning Electron Microscopy (SEM)

To prepare for SEM, samples were fixed and dehydrated similar to the methods described for TEM. Following the dehydration, constructs were critically point dried using a Samdri Pvt 3 (Tousimis Research Corp., Rockville, MD). The specimens were coated with platinum-palladium (80-20%) by thermal evaporation in a Denton DV 502 vacuum evaporator (Denton Vaccum Inc., Cherry Hill, NJ) and examined with a Hitachi S4800 SEM.

3.1.9. Differential Interference Contrast (DIC) Microscopy

The long range organization of the collagen fibrils was investigated using DIC (Guo, Hutcheon et al. 2007). The collagenous constructs were transferred between two coverslips and placed on the stage of an inverted microscope (TE2000E; Nikon). The alignment of collagen fibrils was studied using a series of in-plane and Z-stacks.

It should be mentioned that DIC is a directional method. Due to the nature of DIC, contrast in an image is maximal along the shear direction of the DIC prism and falls off to a minimum in the orthogonal direction. Consequently, there is a ± 5 degrees bias

along the direction of the shear axis within which the fibrils aligned in that direction will not be distinct. However, due to the small diameter of the collagen fibrils, DIC microscopy is the only light microscopy method capable of resolving collagen fibrils. Therefore, considering the limitations of DIC and our desire to investigate the large scale organization of the collagen fibrils, DIC microscopy was employed to investigate the fibrillar organization.

3.2. Results

Figure 3-6D shows the cross-section of the lamellar-like stratification of a typical LC *de novo* construct produced by confinement and concentration of monomer followed by fibrillogenesis. Differential interference contrast (DIC) z-scan optical imaging was in agreement with the thick section data and revealed that the *de novo* constructs possessed multiple "lamellae" within which the fibrillar matrix was uniformly aligned over long distances in the x-y plane (100s of microns Figure 3-7A). For the LC experiments, the spontaneously formed lamellae were 16.6±6.3 microns thick and their constituent fibrils changed direction *en masse* at an average angle of 50±24 degrees. Because of the high-density of collagen fibrils in the HC experiments, it was difficult to measure lamellar thickness and angle changes optically with DIC. Thus DIC images of the LC constructs were *qualitatively* compared with constructs produced by fibroblasts *in vitro*. In general, the lamellar organization in the LC *de novo* constructs compared favourably with the matrix alignment found in our PHCSC-derived stromal constructs (Figure 3-7). In PHCSC-derived constructs, the synthesized lamellae are generally 2-5 microns thick and appear to change direction by 90º (when direction changes are clearly observable by DIC

(Figure 3-7D and 2F) (Guo, Hutcheon et al. 2007). In the normal human cornea, collagen lamellae are approximately 2 microns thick and the angle between successive lamellae is also generally 90º (Meek and Boote 2004). Thus it appears that our LC *de novo* constructs comprise thicker aligned lamellar structures which change direction more arbitrarily than native tissue, subject to the limitation of DIC microscopy.

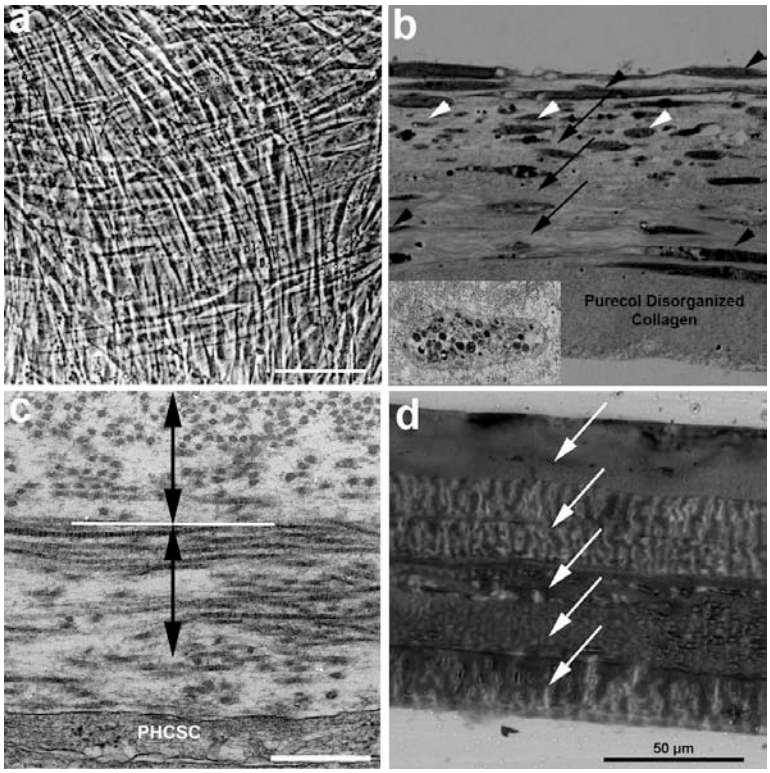

Figure 3-47: Light and Standard Transmission Electron Micrographs (sTEM). (A) Phase contrast image of two week old *in vitro* model of stromal development. PHCSCs form "orthogonal" confining cell sheets. Bar is 50 microns (Guo, Hutcheon et al. 2007) (B) Optical thick section of 8 week old PHCSC-derived, stratified construct comprising PHCSCs with "orthogonal" orientation changes (white and black arrowheads) and layers where aligned collagen lamellae are typically observed (black arrows). (inset: sTEM of single PHCSC in cross-section surrounded by collagen fibrils *aligned* with cell long axis). (C) sTEM of cell-synthesized collagenous matrix comprising alternating layers of small diameter collagen fibrils. Bar is 500 nm. (D) Optical thick section of LC liquid-crystal-collagen-derived *de novo* construct showing 5 morphologically distinct layers.

Standard transmission (sTEM) and scanning (SEM) electron microscopy of the *de novo* constructs in cross-section corroborated the results of the DIC imaging by revealing alternating arrays of aligned fibrils in ersatz "lamellae". Low magnification sTEMs of the constructs produced from LC (Figure 3-8B) and HC (Figure 3-8C) collagen bear a striking resemblance to sTEMs of the normal human cornea (Figure 3-8A). Cross-sectional SEM also confirms the high fibril density, high-degree of fibril alignment and lamellar structure in constructs produced from HC collagen (Figure 3-10A). However, the sTEMs also show that the spontaneously formed lamellae can vary in thickness significantly (Figure 3-8D). Taken together, the low magnification sTEM, SEM and DIC confirm that dense, aligned fibrillar structures spontaneously precipitate from confined, concentrated monomers, however, neither the angle between lamellae nor the precise lamellar thickness exhibits consistency.

Nonetheless, it appears that concentrated, confined collagen is cooperative in that lamellae appear to be spontaneously formed parallel to the confining surfaces. It is quite possible that the role of the fibroblasts is to provide additional "guidance cues" to direct the forming collagen lamellae.

Fibroblasts in the bounding confluent layers may provide external guidance cues (e.g. elongated cell shape) while embedded fibroblasts could control local directionality of the monomers via internal guidance cues (e.g. elongated cell shape and filipodial extensions). In the PHCSC derived constructs, the collagen fibrils were often seen in co-alignment with the long axis of the fibroblast body. Figure 3-9A shows two adjacent lamellae produced by PHCSCs where direction of the fibrils and of the embedded cells (which are co-aligned) changes abruptly. Figure 3-9B demonstrates that the direction of

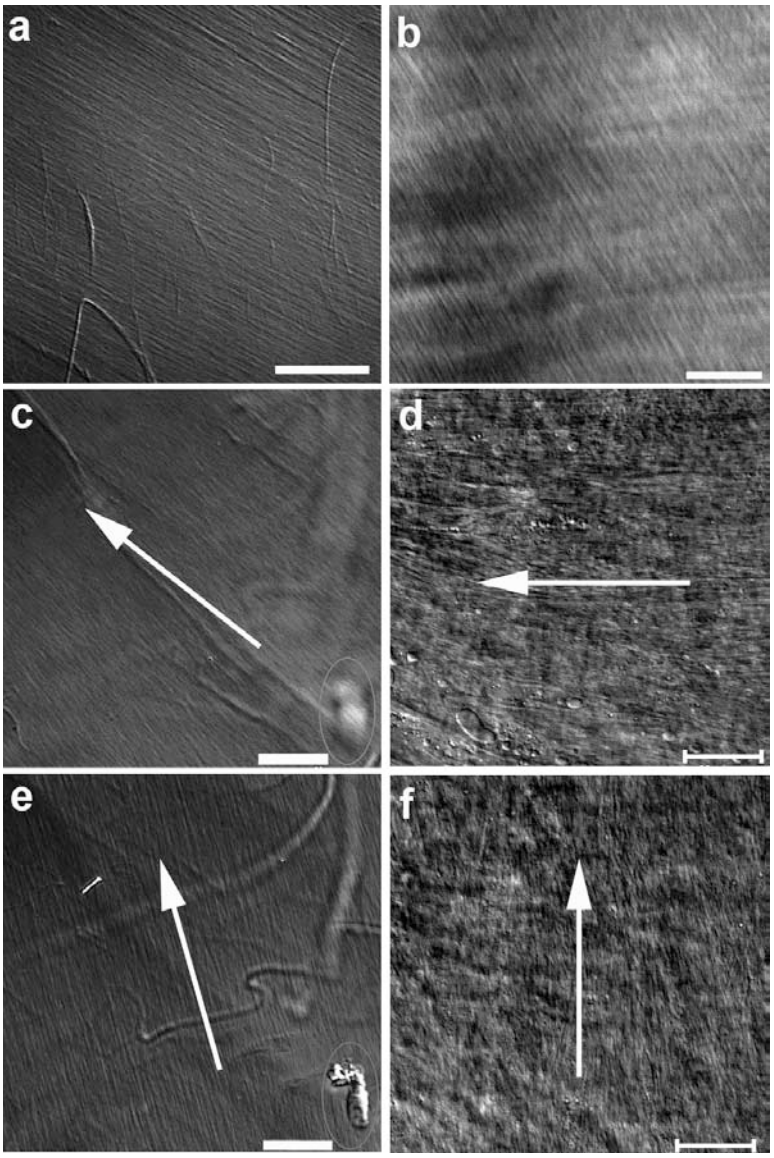

Figure 3-48: DIC optical micrographs of *de novo* and PHCSC-derived collagenous matrix alignment. (A and B) DIC images of typical matrix alignment in the low concentration (A) and high concentration (B) *de novo* constructs. (C-F), DIC images extracted from z-scans demonstrating the change in direction of the matrix in the low concentration *de novo* construct (C,E) and in the cell-derived construct (D-F). The matrix alignment angle changes 30º over a depth of 30 microns in (C,E) while the change is 90º over a depth of 7 microns in (D,F). Bars are 20 microns.

collagen fibrils can be locally modified by the presence of a high-aspect-ratio object (in

this case a glass microcylinder). It is thus possible that the combination of geometric confinement and internal guidance cues (spaced appropriately) can be used to fully control the orientation of collagen fibrils precipitated from dense solutions of collagen

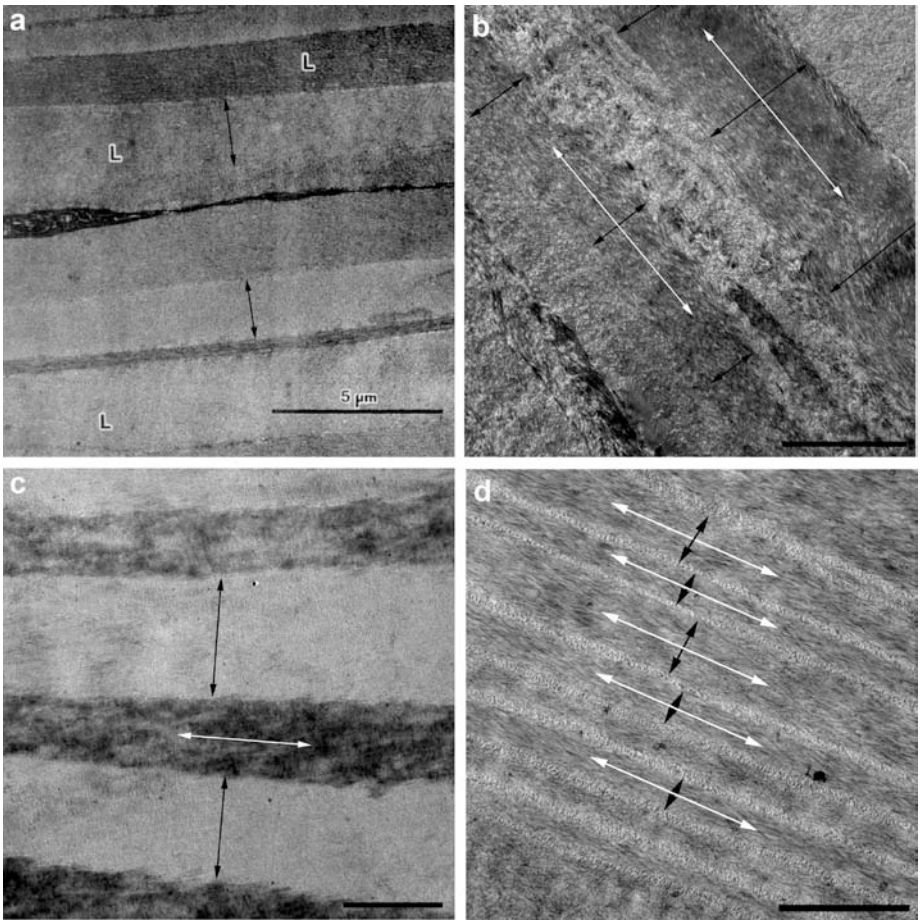

Figure 3-49: Cross-section low magnification sTEM micrographs of collagen "lamellae". (a) Human corneal lamellar structure (from Komai *et al* (Komai and Ushiki 1991)). (b) Lamellar structures spontaneously formed in *de novo* construct at lower concentration of collagen (~150 mg/ml). Lamellae comprising aligned collagen fibrillar arrays are visible (black arrows indicate width of a lamella, white arrow indicates general direction of fibril alignment in a lamellar plate. Bar is 2 microns. (c, d) Lamellar structures spontaneously formed *de novo* constructs at high collagen concentration. Lamellar width is quite variable across samples with those in (c) approximately 5 microns while those shown in (d) are approximately 1 micron. Bar in c is 5 microns. Bar in (d) is 2

monomers.

Though the alignment and lamellar structure of collagenous matrix are readily observed by optical microscopy and by low magnification sTEM and SEM, it is important to examine the morphology of precipitated fibrils. Figure 3-10A and B are low magnification and high magnification sTEMs of an array of collagen fibrils in cross-section which have precipitated from HC collagen monomer solutions. The higher magnification image of the *de novo* construct fibrils reveals generally small diameter, highly polydisperse and irregular "fused" fibrils.

We do not expect to see uniform diameter or circular fibrils without the aid of auxiliary ECM molecules such as proteoglycans, glycosaminoglycans or other collagens. Interestingly, the fibrils have an appearance similar to collagen fibrils produced by a

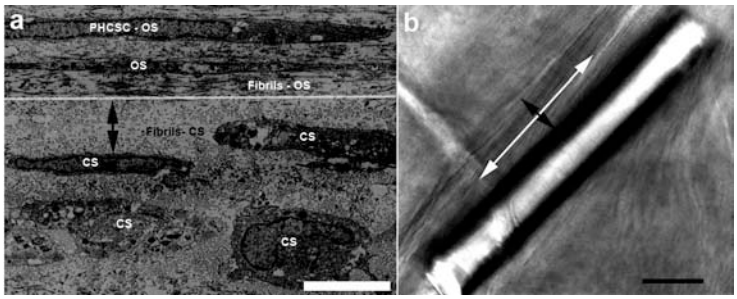

Figure 3-50: Co-alignment in PHCSC constructs and in liquid crystal collagen – internal templating (A) PHCSC Cells in 4 week construct co-aligned with collagen fibrils. Collagen fibrillar arrays change direction at the white line. Below the white line, collagen fibrils and cells are in cross-section (CS). Above the line cells and fibrils are in oblique section (OS). Black double arrow indicates distance over which cell orientation could be influencing the fibril orientation. Bar is 4 microns. (B) Glass microcylinder embedded in fibrils precipitated from liquid crystalline collagen monomers. The long axis of the glass appears to locally influence the collagen fibrils. Black double arrow indicates maximum distance glass "guides" collagen. White double arrow indicates direction of fibrils. Bar is 20 microns.

proteoglycan (lumican) knock-out mouse (Chakravarti, Zhang et al. 2006). This raises the interesting possibility of using the liquid crystal collagen system to test the effect of "knocking-in" matrix controlling molecules.

In the plane of the *de novo* constructs, TEM generally confirmed the DIC images by demonstrating large areas of complete fibril alignment parallel to the confining surfaces (Figure 3-11A and B). In LC constructs, fibrils would sometimes adopt a "wavy pattern" which suggests the production of open space as monomers are incorporated into

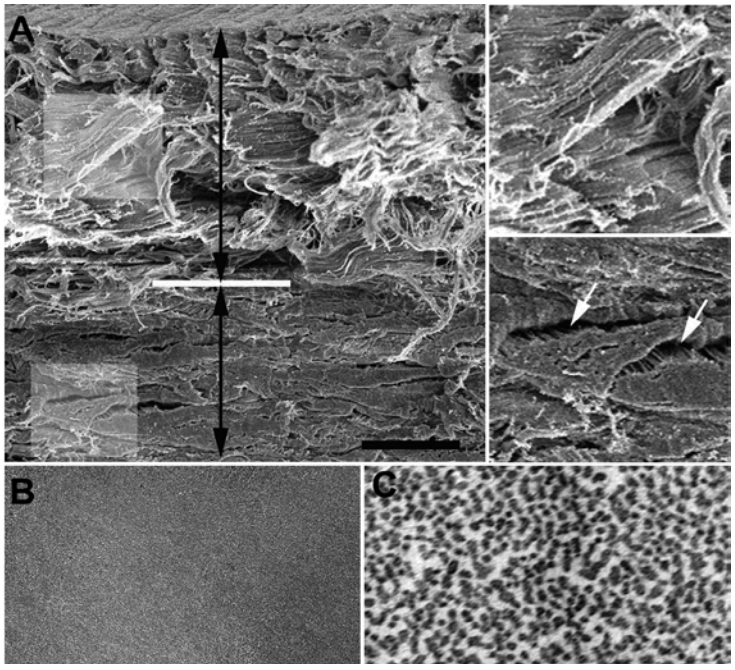

Figure 3-51: SEM and sTEM micrographs of collagen in high-concentration *de novo* constructs in cross-section. (A) SEM of fractured cross-section of construct where a clear change of direction in highly-aligned collagen fibrils in lamellae may be discerned (insets). Fibrils which are cut in cross-section are so densely packed that the construct appears to be "solid" (region indicated by lower black arrow). Bar is 10 microns (B) Low magnification sTEM of large uniform area in cross-section confirming the high-density and uniformity of the fibrillar array. Bar is 2 microns. (C) High-magnification sTEM of collagen in cross-section demonstrating the presence of individual fibrils. In general, fibrils are small and have a polydisperse diameter distribution. Bar is 500 nm.

the aggregating fibrils (Figure 3-10A). In HC constructs, the collagen fibrils appeared to be generally more tightly packed and highly-aligned parallel to the confining surface (Figure 3-10B).

At high magnification, collagen fibrils in longitudinal section are thin (~20 nm), dense and highly-aligned (Figure 3-10C). However, direct comparison to PHCSC-synthesized collagen (Figure 3-11D) demonstrates that the fibrils in the *de novo* construct

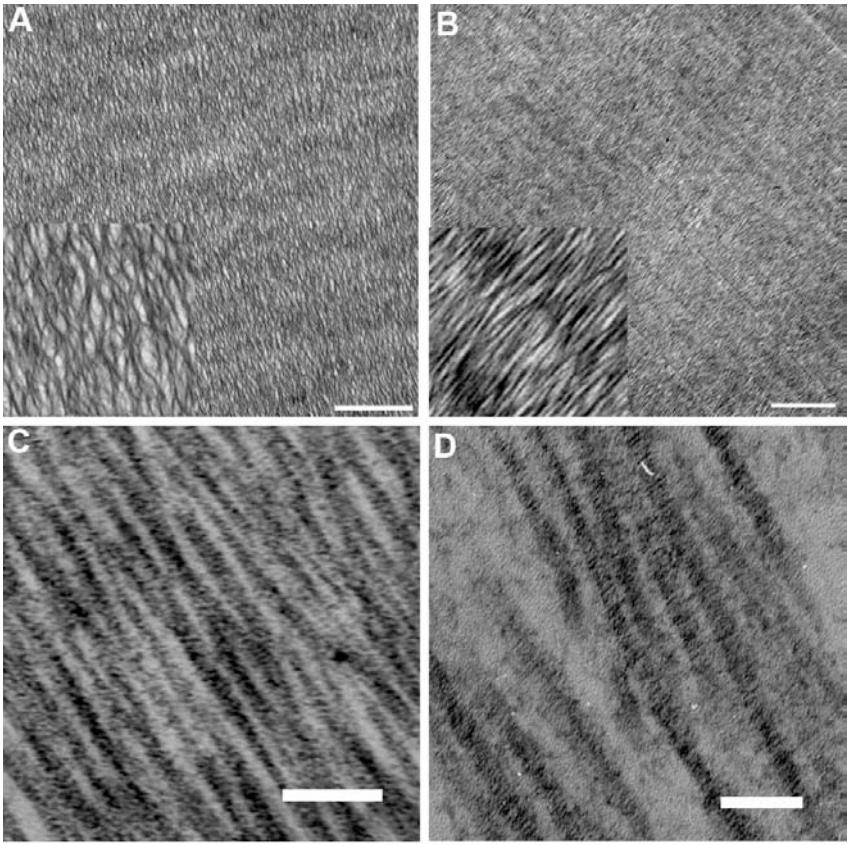

Figure 3-52: sTEM micrographs of collagen in *de novo* and PHCSC derived constructs. (A,B) En face sTEMs of fibril organization produced from low (A) and high (B) concentration collagen monomers. Over large distances fibrils were completely in alignment. Higher magnification insets represent direction and morphology of fibrils. Bars are 2 µm. (C,D) Comparison of the high-concentration *de novo* construct fibrils (C) with cell-synthesized collagen (D). The fibrils derived from concentrated collagen monomers were smaller, denser and did not display prominent D-banding. Bars are 100 nm.

are smaller and do not have clear D-periodic banding (though some striations can be appreciated). Though fibrils formed at low concentration can possess native like D-periodic banding, fibrillogenesis at high concentration likely requires the aid of other auxiliary ECM molecules such as proteoglycans (which are co-secreted during collagen synthesis in developing tissue).

The QFDE images of the construct confirmed the observations previously made by TEM and DIC microscopy methods. The images show the multilamellar structure of the collagenous constructs (Figure 3-12a) composed of small diameter collagen fibrils (Figure 3-12C and D). Low magnification QFDE images show aligned collagen fibrils aligned over large areas which are mimetic of native tissues (Figure 3-12B). The QFDE images reveal that these collagenous constructs are more complex than what was presiously seen in the TEM micrographs. The constructs seem to consist of three groups of fibrils with different diameter range: small diameter (5.5 nm ±1) that don't show any alignment, medium diameter (9.3 nm ±1) that are aligned, and large diameter (17.5 nm ±1) that are aligned and show alternating layers. It appears that medium and large diameter fibrils are embedded in a randomly assembled, interconnected, matrix of small diameter fibrils. It is possible that the small fibrils are evolving into the medium size and eventually large diameter fibrils. During this transformation they also adopt the direction of alignment and produce highly aligned and multilamellar with alternating directions.

Similar to the DIC images, there are also striking similarities between the QFDE images of the collagenous matrices in the liquid crystalline samples and cell-drived collagen fibrils (Figure 3-12 E-H). Both systems show the existence of disorganized, small-diameter network of collagen fibrils (Figure 3-12 G and H) and also the larger

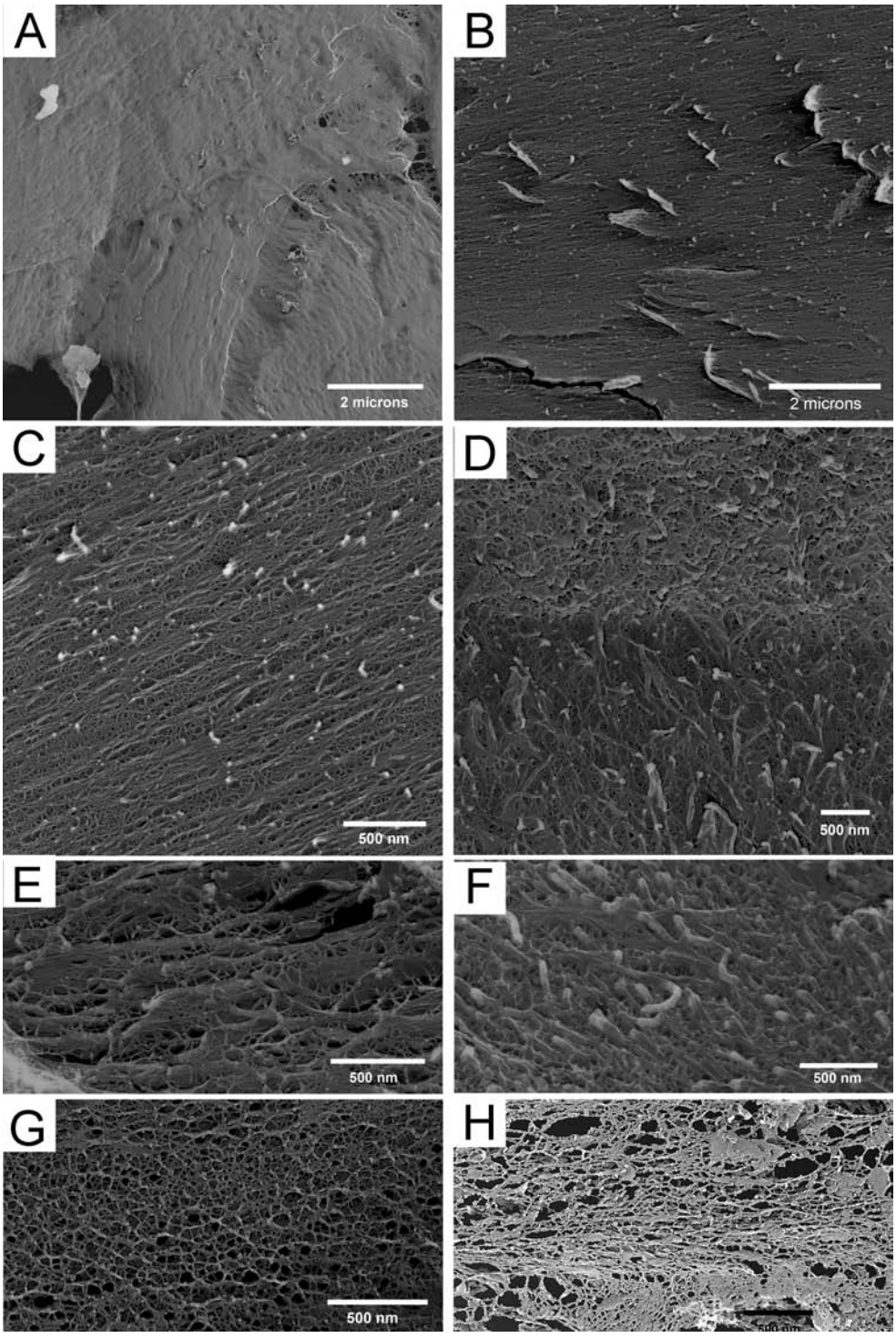

Figure 3-53: The QFDE micrographs of liquid crystalline collagenous constructs. Collagen fibrils form stacks of aligned collagen fibrils with alternating lamellae (A-D). Note the similarities between the *de novo* collagen fibrils (E and G) and cell-synthesized collagen fibrils (F and H).

diameter collagen fibrils that are embedded in a disorganized matrix (Figure 3-12 E and

F).

3.2.1. Investigation of the Time Required for Complete Fibrillogenesis

The ultra-structural studies using transmission electron microscopy revealed that even after 4 weeks collagen fibrils did not exhibit clear D-banding patterns. In addition, no apparent changes in the organization of the fibrils were observed after one week. Considering the results of this study, we decided to keep the constructs at 37ºC for two weeks to allow for complete fibril formation.

3.2.2. Effects of Buffer on the Organization of the Collagen Fibrils

Figure 3-13A and B are DIC images of collagen fibrils self-assembled in the presence of PBS and NaOH, respectively (pH 7.2). As the images show, PBS buffer often

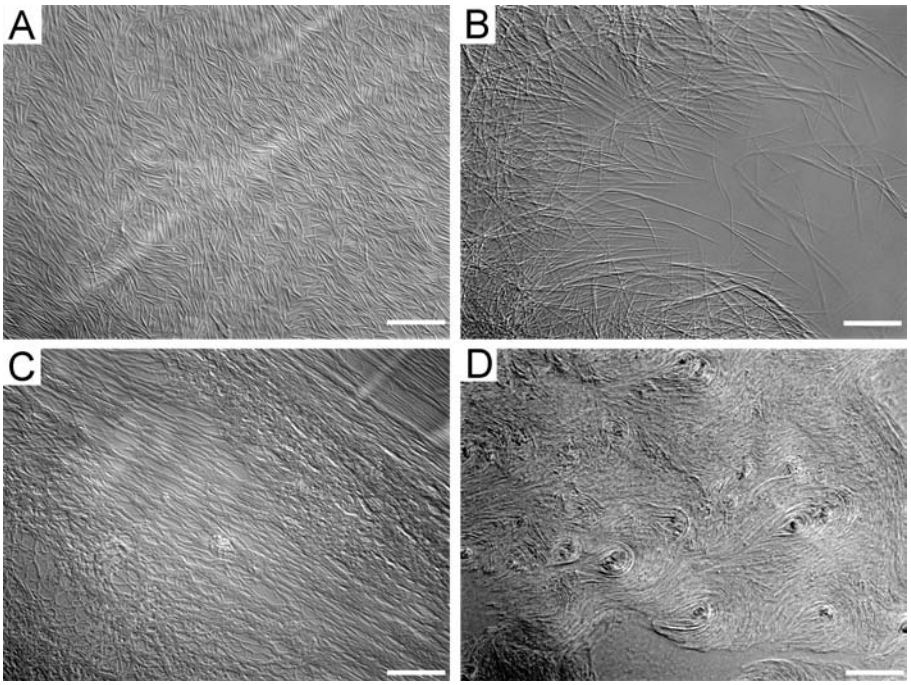

Figure 3-54: DIC images of MC collagen fibrils self-assembled in the presence of PBS (A), NaOH and $CaCl_2$ (B), HA (C), and plasma treated surfaces (D).

resulted in the formation of short, granular aggregates. Fibrils were generally aligned and the lamellar structure was also observed. In contrast, NaOH usually resulted in the formation of long but interrupted collagen fibrils. Unlike fibrils formed in the presence of trizma, fibrils were not packed and did not show organization which might be due to the differences in the ionic strengths of PBS and trizma. Since the energetically driven interactions between collagen molecules play a critical role in fibrillogenesis, using trizma buffer with an ionic strength different from PBS would screen charges on the surface of the collagen molecules in a different way, resulting in the fibrillar organizations.

3.2.3. Effects of Exogenous Molecules on the Organization of the Collagen Fibrils

In addition to the buffer, presence of exogenous co-nonsolvent molecules during the fibrillogenesis could enhance the organization of the collagen fibrils. As mentioned before, collagen self-assembly is an entropic driven process which spontaneously proceeds by loss of the water molecules from the surface of the collagen monomers. Therefore, addition of high osmotic pressure, co-nonsolvent molecules (e.g. Hyaluronic acid, HA, or PEG) to collagen solution would extract water from collagen molecules, while packing them closer to each other, forcing them into self-organization. In fact, it has been shown that decreasing the intermolecular distances (i.e. distance between triple helices) to the range of 2nm results in the attraction force between the molecules which are responsible for collagen fibrillogenesis (Leikin, Rau et al. 1995). Therefore, we hypothesize that the addition of high osmotic pressure molecules to collagen molecules would promote the self-assembly and enhance the global organization of the fibrils. To

test this hypothesis, medium concentration solution of collagen and 1% HA or PEG was prepared (1% was based on the concentration of HA that occur *in vivo* (Comper and Laurent 1978)). Figure 3-13C is a DIC image of collagenous constructs in the presence of 1% HA. Collagen molecules self-assembled into clumps of disorganized collagen fibrils. Similar results were observed when 1% PEG was used as the auxiliary molecule.

In these studies collagen molecules were confined between two coverslips and therefore fibril formation occurs within close apposition of the surfaces. As was discussed before, collagen self-assembly is an energy driven process. Therefore, surface chemistry and surface energy could potentially play a critical role in the organization of collagen fibrils formed at high concentration. To investigate the effect of the surface energy, a low energy surface (i.e. ultrasonically cleaned) or a high energy surface (i.e. oxygen plasma treated after ultrasonically cleaning) were used as the confining surfaces. The surface treatments were chosen based on the contact angle measurements. The collagen solution formed 160º and 180º contact angle with the ultrasonically cleaned and plasma cleaned surface, respectively (which indicates that the latter has a higher surface energy). Figure 3-13D is a DIC image of collagen fibrils self-assembled between two high energy surfaces. Although collagen fibril formation appeared normal, fibrils did not exhibit any organization. Collagen molecules mostly self-assembled into circular arrangements with no apparent liquid crystalline organizations.

3.2.4. Effects of the Confining Geometries on the Organization of the Collagen Fibrils

One of the biggest challenges in this investigation was the observation of the collagen fibrils and lamellar structures using a light microscopy technique. Unfortunately, due to the high concentration and tight packing of the collagen fibrils it was not possible to use DIC microscopy to image the fine organization of the fibrils (except the 100 mg/ml constructs). However, when densely organized, collagen molecules exhibit strong birefringence patterns and this property make the PLM an attractive method to provide some qualitative information about the organization of the collagen fibrils in large scales. Figure 3-14 is a series of PLM images of the collagenous constructs at various thicknesses and concentrations.

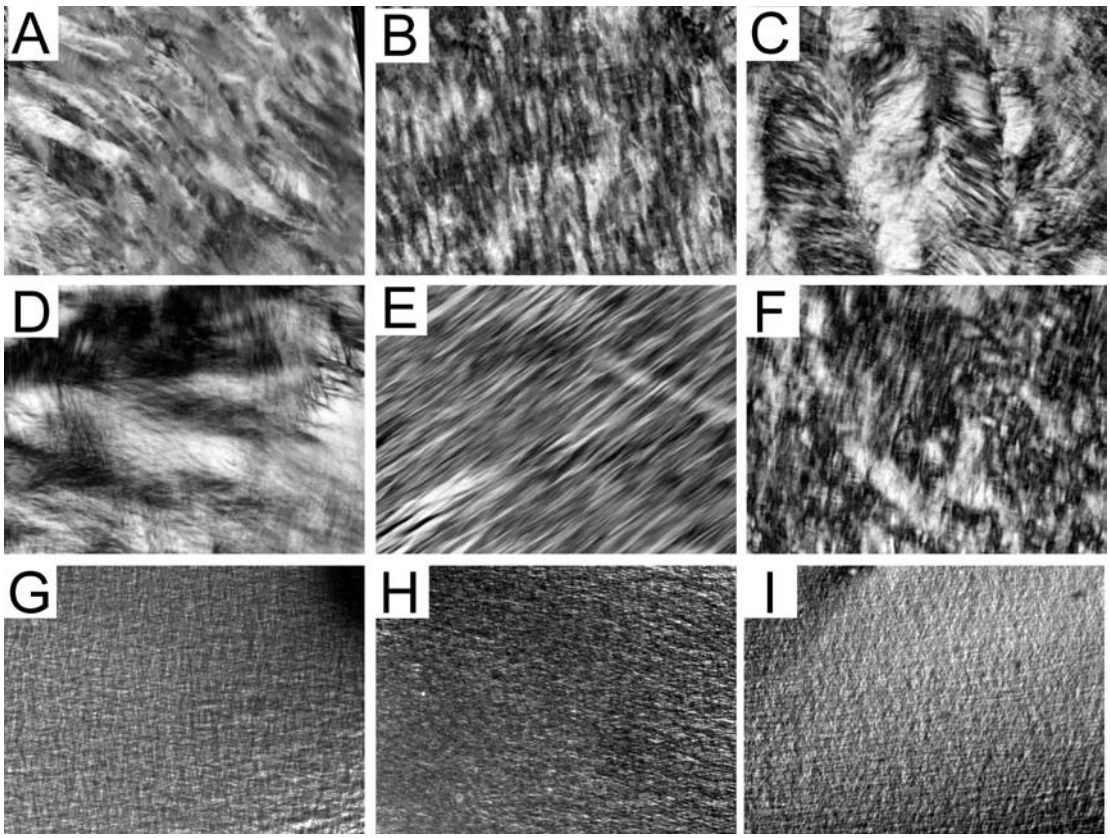

Figure 3-55: Phase microscopy images of HC collagenous constructs with the thicknesses of 250±15µm (A-C), 150±15µm (D-F), and 50±15µm (G-I) and concentrations of 300±25 mg/ml (A,D,G), 200±25µm, 250 mg/ml (B,E,H), and 100±25 mg/ml (C,F,I)

Figure 3-15A-C is a series of SEM micrographs showing the organization and ultra-structure of the collagen fibrils in the same constructs as Figure 3-14A, D, and G, respectively. The insets are the magnified images from the different regions of the cross sections.

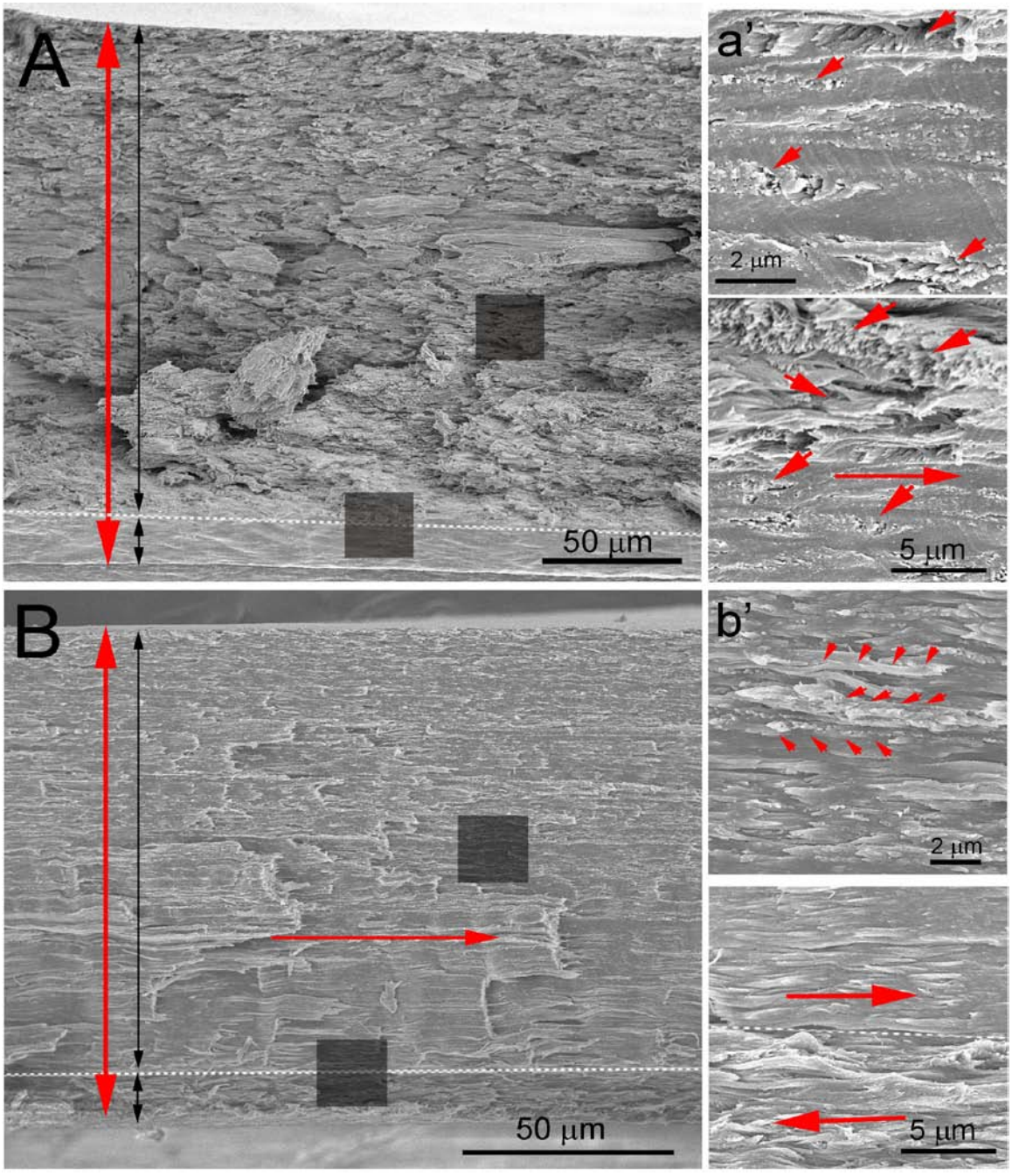

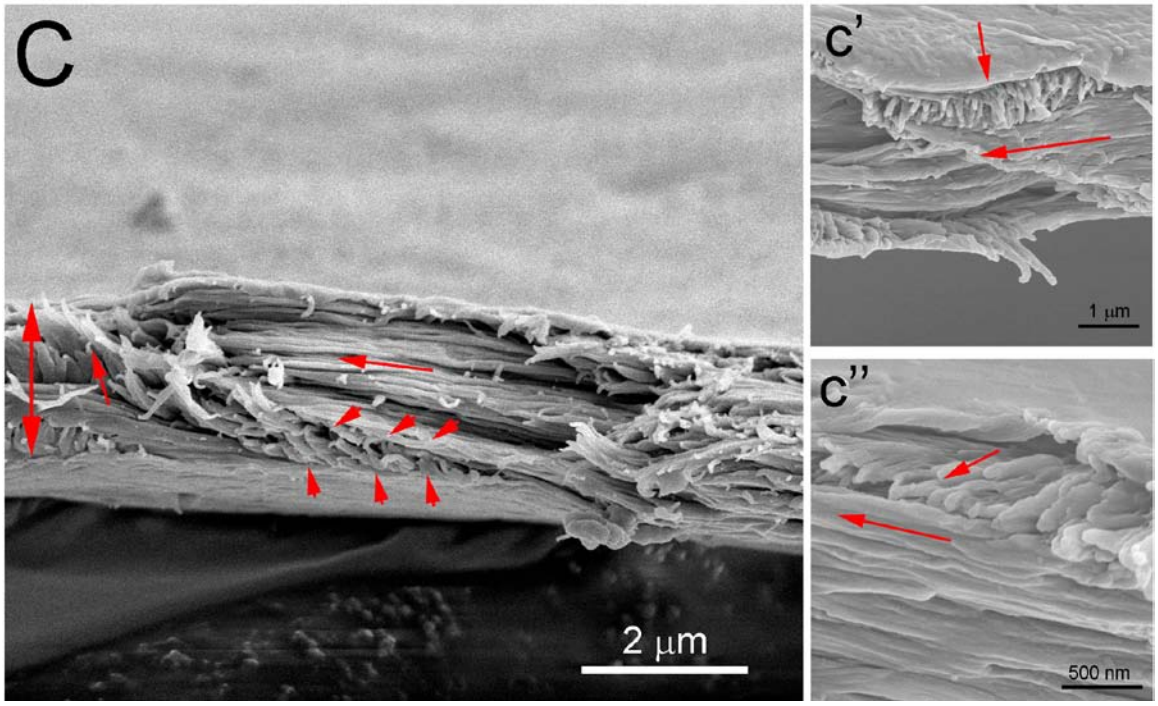

Figure 3-56: SEM micrographs showing the organization and ultra-structure of the collagen fibrils in samples with 250±15μm (A), 150±15μm (B), and 50±15μm (C) thicknesses

These observations confirm the previous TEM and DIC results indicating that the collagenous constructs are composed of the highly aligned layers of collagen fibrils with the alternating directions in the adjacent layers. The SEM images show that the constructs are composed of at least two distinct layers (unequal thicknesses) with an abrupt change of direction between the two layers (Figure 3-15A-C and a'-c'). The collagen fibrils in the thinner layer (~ 15 μm) were completely aligned in the same direction. Although the fibrils in the thicker layer were generally aligned, the higher magnification images show that this layer is also contains very thin layers (1-3 collagen fibrils thick). The direction of the thin layers are at nearly a right angle to the general organization.

The PLM images also show that degree of the organization and the distance over which the collagen fibrils are organized are functions of the thickness of the constructs

such that in the thicker constructs collagen fibrils tend to change direction much rapidly (Figure 3-14A- C). As the thickness of the constructs decreases the area over which the collagen fibrils are aligned in the same direction (Figure 3-14D- F).

Interestingly, when the thicknesses of the constructs were reduced to the range of 50 μm, the collagen fibrils spontaneously self-organized into two equal thickness layers. As revealsed with the PLM images, the fibrils in each layer were completely aligned in the same direction across the area of the samples and the orientation of the fibrils rotated 85±5º.

Discussion

In this study, we investigated the concentration/confinement strategy to produce organized scaffolding in a hybrid approach to the engineering of tissue such as the corneal stroma (a very difficult structure to reproduce). Previous investigators have used high concentration collagen and produced cholesteric phases of collagen molecules and fibrils, but in a system which uses toxic ammonium and air drying in a very thin collagen film (Mosser, Anglo et al. 2006; Gobeaux, Mosser et al. 2008). Although the results were similar to the packing of collagen fibrils in bone (e.g. series of arching patterns) they did not produce large scale lamellar organization required for corneal tissue engineering. This is the first study which has produced such a highly organized collagenous arrays (as demonstrated by TEM) with a simple fibril forming buffer solution and no air drying. Classical tissue engineering approaches to produce ersatz corneas have generally utilized a “degradable” disorganized scaffolding into which stromal cells are seeded. However, during corneal development in mammals, there is no discernible pre-existing provisional

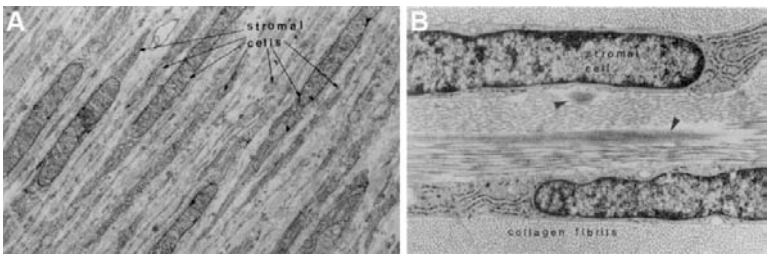

Figure 3-57: Transmission electron micrographs of developing rabbit corneal stroma. (A) In a 21 day gestational rabbit, the stromal fibroblastic cells are elongated, densely packed in organized in layers parallel to the corneal surface. There is no organized provisional primary stromal matrix as there is in the developing chick. (B) At birth (32 days), highly-organized, orthogonal arrays of stromal collagen have "filled" in the spaces between the cells. Interestingly there are fibril directional changes often midway between the fibroblasts. Reproduce from Cintron et al. 1981 with permission (Cintron, Covington et al. 1983). Original magnifications were (A) x5690 and (B) x22,140

scaffolding. Instead, the mesenchymal cells infiltrate the prospective stromal space at very high density, self-organize and then produce the aligned collagen arrays (Hay and Revel 1969; Trelstad and Coulombre 1971; Cintron, Covington et al. 1983). We have seen similar behavior with primary human corneal stromal cells in a scaffold-free system (Guo, Hutcheon et al. 2007). When a provisional or primary matrix *is* present in the developing cornea (as in the chick and zebrafish), it is synthesized by the epithelium and is already highly-organized (Hay and Revel 1969; Zhao, Yee et al. 2006). Thus is has been generally regarded as a "template" which guides the organization of the subsequently secreted secondary stroma (Trelstad and Coulombre 1971). The only time a provisional and disorganized "scaffolding" is found in the cornea is during wound healing (Cintron, Covington et al. 1983; Jester, Petroll et al. 1999; Fini and Stramer 2005). It is interesting to note that even in a fairly regenerative animal such as the rabbit, a full thickness fibrin plug requires over two years to remodel to clarity (yet the resulting

matrix is still distinct from normal cornea - (Cintron, Hong et al. 1981)). These facts are consistent with the idea that to produce highly-anisotropic tissues such as the corneal stroma, some level organization or guidance cues (in the form of cell alignment or a template matrix) should already be in place prior to the secretion of the organized collagen. We thus *suggest* that if tissue engineers are to effectively (and rapidly) reproduce corneal structure, it is important to either allow/induce the cells to provide the initial organization (as in a scaffold-free system or on an aligned template) or impart organization into the system exogenously via a pre-organized scaffolding (such as that produced in the present study).

Conclusion

In closing, it is important to point out two of the major concerns with this work. First, we are aware that the use of atelo-collagen will preclude functional native cross-linking because there are no telopeptides. Thus, these constructs will be organized but cannot be appreciably strengthened naturally. Examining the effect of having the two short non-helical telopeptides present on the collagen will be one of the next steps. Interestingly, the telopeptides have been shown to affect the organization of the collagen molecules within the fibrils. Therefore, using tropocollagen may enhance the overall organization or morphology of the fibrils. Second, since our system is produced in the absence of molecules thought to control fibril morphology (proteoglycan cores, glycosaminoglycans, type V collagen, etc), fibril banding and uniform fibril diameter was not expected (though there is clear banding in many of our TEM images). We are currently adding ECM molecules directly to this system to control fibril morphology spacing and optical properties (transparency).

Our goal in producing organized tissue *de novo* requires that we first solve the more difficult problem of controlling both the local and long-range organization of collagen molecules to produce lamellar structures that are reasonably mimetic of structures found in native load-bearing tissues. What we found was a very cooperative molecule which exhibited a natural tendency to form load-bearing structures in the form of alternating lamellar sheets of fibrils. It is difficult to imagine that biology would not take advantage of this intrinsic property of collagen when producing the complex structures necessary to successfully negotiate a world replete with mechanical challenges.

References

Besseau, L. and M. M. Giraud-Guille (1995). "Stabilization of fluid cholesteric phases of collagen to ordered gelated matrices." J Mol Biol **251**(2): 197-202.

Birk, D. E. and R. L. Trelstad (1984). "Extracellular compartments in matrix morphogenesis: collagen fibril, bundle, and lamellar formation by corneal fibroblasts." J Cell Biol **99**(6): 2024-33.

Birk, D. E. and R. L. Trelstad (1985). "Fibroblasts create compartments in the extracellular space where collagen polymerizes into fibrils and fibrils associate into bundles." Ann N Y Acad Sci **460**: 258-66.

Birk, D. E. and R. L. Trelstad (1986). "Extracellular compartments in tendon morphogenesis: collagen fibril, bundle, and macroaggregate formation." J Cell Biol **103**(1): 231-40.

Bouligand, Y., J. P. Denefle, et al. (1985). "Twisted architectures in cell-free assembled collagen gels: study of collagen substrates used for cultures." Biol Cell **54**(2): 143-62.

Canty, E. G., Y. Lu, et al. (2004). "Coalignment of plasma membrane channels and protrusions (fibripositors) specifies the parallelism of tendon." J Cell Biol **165**(4): 553-63.

Chakravarti, S., G. Zhang, et al. (2006). "Collagen fibril assembly during postnatal development and dysfunctional regulation in the lumican-deficient murine cornea." Dev Dyn **235**(9): 2493-506.

Chapman, D. (1966). "Liquid crystals and cell membranes." Ann N Y Acad Sci **137**(2): 745-54.

Cintron, C., H. Covington, et al. (1983). "Morphogenesis of rabbit corneal stroma." Invest Ophthalmol Vis Sci **24**(5): 543-56.

Cintron, C., B. S. Hong, et al. (1981). "Quantitative analysis of collagen from normal developing corneas and corneal scars." Curr Eye Res **1**(1): 1-8.

Comper, W. D. and T. C. Laurent (1978). "Physiological function of connective tissue polysaccharides." Physiol Rev **58**(1): 255-315.

Coulombre, A. (1965). "Problems in corneal morphogenesis." Advances in Morphogenesis **4**: 81.

Denis, F. A., A. Pallandre, et al. (2005). "Alignment and assembly of adsorbed collagen molecules induced by anisotropic chemical nanopatterns." Small **1**(10): 984-91.

Doane, K. J., J. P. Babiarz, et al. (1992). "Collagen fibril assembly by corneal fibroblasts in three-dimensional collagen gel cultures: small-diameter heterotypic fibrils are deposited in the absence of keratan sulfate proteoglycan." Exp Cell Res **202**(1): 113-24.

Donald, A. M. and A. H. Windle (1992). Liquid Crystalline Polymers, Cambridge University Press.

Ellis, E. A. (2006). "Solutions to the Problem of Substitution of ERL 4221 for Vinyl Cyclohexene Dioxide in Spurr Low Viscosity Embedding Formulations." Microscopy Today **14**(4): 32.

Exposito, J. Y., C. Cluzel, et al. (2002). "Evolution of collagens." Anat Rec **268**(3): 302-16.

Fini, M. E. and B. M. Stramer (2005). "How the cornea heals: cornea-specific repair mechanisms affecting surgical outcomes." Cornea **24**(8 Suppl): S2-S11.
Frank, C. B. (2004). "Ligament structure, physiology and function." J Musculoskelet Neuronal Interact **4**(2): 199-201.
Fratzl, P., K. Misof, et al. (1998). "Fibrillar structure and mechanical properties of collagen." J Struct Biol **122**(1-2): 119-22.
Friedel, G. (1922). "Les e´tats me´somorphes de la matie`re." Ann. de Phys. **18**: 273-474.
Giraud-Guille, M. M. (1988). "Twisted plywood architecture of collagen fibrils in human compact bone osteons." Calcif Tissue Int **42**(3): 167-80.
Giraud-Guille, M. M. (1989). "Liquid crystalline phases of sonicated type I collagen." Biol Cell **67**(1): 97-101.
Giraud-Guille, M. M. (1992). "Liquid crystallinity in condensed type I collagen solutions. A clue to the packing of collagen in extracellular matrices." J Mol Biol **224**(3): 861-73.
Giraud-Guille, M. M. (1996). "Twisted liquid crystalline supramolecular arrangements in morphogenesis." Int Rev Cytol **166**: 59-101.
Giraud-Guille, M. M., L. Besseau, et al. (2000). "Structural aspects of fish skin collagen which forms ordered arrays via liquid crystalline states." Biomaterials **21**(9): 899-906.
Gobeaux, F., G. Mosser, et al. (2008). "Fibrillogenesis in dense collagen solutions: a physicochemical study." J Mol Biol **376**(5): 1509-22.
Gross, J. and D. Kirk (1958). "The heat precipitation of collagen from neutral salt solutions: some rate-regulating factors." J Biol Chem **233**(2): 355-60.
Guo, C. and L. J. Kaufman (2007). "Flow and magnetic field induced collagen alignment." Biomaterials **28**(6): 1105-14.
Guo, X., A. E. Hutcheon, et al. (2007). "Morphologic characterization of organized extracellular matrix deposition by ascorbic acid-stimulated human corneal fibroblasts." Invest Ophthalmol Vis Sci **48**(9): 4050-60.
Hay, E. D. and J. P. Revel (1969). "Fine structure of the developing avian cornea." Monogr Dev Biol **1**: 1-144.
Hitt, A. L., A. R. Cross, et al. (1990). "Microtubule solutions display nematic liquid crystalline structure." J Biol Chem **265**(3): 1639-47.
Hulmes, D. J. (2002). "Building collagen molecules, fibrils, and suprafibrillar structures." J Struct Biol **137**(1-2): 2-10.
Jester, J. V., W. M. Petroll, et al. (1999). "Corneal stromal wound healing in refractive surgery: the role of myofibroblasts." Prog Retin Eye Res **18**(3): 311-56.
Kadler, K. E., Y. Hojima, et al. (1987). "Assembly of collagen fibrils de novo by cleavage of the type I pC-collagen with procollagen C-proteinase. Assay of critical concentration demonstrates that collagen self-assembly is a classical example of an entropy-driven process." J Biol Chem **262**(32): 15696-701.
Komai, Y. and T. Ushiki (1991). "The three-dimensional organization of collagen fibrils in the human cornea and sclera." Invest Ophthalmol Vis Sci **32**(8): 2244-58.
Lee, P., R. Lin, et al. (2006). "Microfluidic alignment of collagen fibers for in vitro cell culture." Biomed Microdevices **8**(1): 35-41.
Leikin, S., D. C. Rau, et al. (1995). "Temperature-favoured assembly of collagen is driven by hydrophilic not hydrophobic interactions." Nat Struct Biol **2**(3): 205-10.

Lotz, J. C. and A. J. Kim (2005). "Disc regeneration: why, when, and how." Neurosurg Clin N Am **16**(4): 657-63, vii.
Maier, W. and A. Saupe (1960). "A simple molecular-statistics theory of the nematic nematic liquid-crystalline phase." Zeitschrift für Naturforschung **15a**: 15.
Marchini, M., R. Strocchi, et al. (1979). "Ultrastructural observations on collagen and proteoglycans in the annulus fibrosus of the intervertebral disc." Basic Appl Histochem **23**(2): 137-48.
Martin, R., J. Farjanel, et al. (2000). "Liquid crystalline ordering of procollagen as a determinant of three-dimensional extracellular matrix architecture." J Mol Biol **301**(1): 11-7.
Matthews, J. A., G. E. Wnek, et al. (2002). "Electrospinning of collagen nanofibers." Biomacromolecules **3**(2): 232-8.
Meek, K. M. and C. Boote (2004). "The organization of collagen in the corneal stroma." Exp Eye Res **78**(3): 503-12.
Mosser, G., A. Anglo, et al. (2006). "Dense tissue-like collagen matrices formed in cell-free conditions." Matrix Biol **25**(1): 3-13.
Nikon. (www.microscopyu.com). "Polarized light microscopy diagram." from http://www.microscopyu.com/.
Parry, D. A. (1988). "The molecular and fibrillar structure of collagen and its relationship to the mechanical properties of connective tissue." Biophys Chem **29**(1-2): 195-209.
Ploetz, C., E. I. Zycband, et al. (1991). "Collagen fibril assembly and deposition in the developing dermis: segmental deposition in extracellular compartments." J Struct Biol **106**(1): 73-81.
Provenzano, P. P. and R. Vanderby, Jr. (2006). "Collagen fibril morphology and organization: implications for force transmission in ligament and tendon." Matrix Biol **25**(2): 71-84.
Reinitzer, F. (1888). "Beiträge zur Kenntniss des Cholesterins." Monatshefte für Chemie / Chemical Monthly **9**(1): 421-441.
Ren, R., A. Hutcheon, et al. (2008). "Human primary corneal fibroblasts synthesize and deposit proteoglycans in long-term 3-D cultures." Dev Dyn **In Press**.
Stewart, G. T. (2003). Liquid crystals in biology I. Historical, biological and medical aspects. Liquid Crystals, Taylor & Francis Ltd. **30:** 541.
Stewart, G. T. (2004). Liquid crystals in biology II. Origins and processes of life. Liquid Crystals, Taylor & Francis Ltd. **31:** 443-471.
Torbet, J., M. Malbouyres, et al. (2007). "Orthogonal scaffold of magnetically aligned collagen lamellae for corneal stroma reconstruction." Biomaterials **28**(29): 4268-76.
Torbet, J. and M. C. Ronziere (1984). "Magnetic alignment of collagen during self-assembly." Biochem J **219**(3): 1057-9.
Trelstad, R. L. (1971). "Vacuoles in the embryonic chick corneal epithelium, an epithelium which produces collagen." J Cell Biol **48**(3): 689-94.
Trelstad, R. L. (1982). "The bilaterally asymmetrical architecture of the submammalian corneal stroma resembles a cholesteric liquid crystal." Dev Biol **92**(1): 133-4.
Trelstad, R. L. and A. J. Coulombre (1971). "Morphogenesis of the collagenous stroma in the chick cornea." J Cell Biol **50**(3): 840-58.

Wilson, D. L., R. Martin, et al. (2001). "Surface organization and nanopatterning of collagen by dip-pen nanolithography." Proc Natl Acad Sci U S A **98**(24): 13660-4.

Woltman, S. J., G. P. Crawford, et al. (2007). Liquid crystals : frontiers in biomedical applications. Hackensack, NJ, World Scientific.

Yevdokimov Yu, M., V. I. Salyanov, et al. (1983). "A mesophase (liquid crystal) state of DNA complexes with anthracycline antibiotics." Biomed Biochim Acta **42**(7-8): 855-66.

Zhao, X. C., R. W. Yee, et al. (2006). "The zebrafish cornea: structure and development." Invest Ophthalmol Vis Sci **47**(10): 4341-8.

Chapter 4

Investigation of the Mutability of the Collagenous Matrices in the Presence of Proteoglycans

Introduction

Collagen molecules are the building blocks of the extracellular matrix (ECM) of the load bearing tissues. The organization and ultrastructure of the collagen fibrils in these tissues dictates their form and function. The adaptation of form and function is best manifested in the corneal stroma; mechanical strength and transparency. To carry the tensile load exerted by the intraocular pressure (IOP ~15mm Hg in human) cornea is composed of stacks of collagen fibrils with plywood structure. In each layer collagen fibrils are aligned in the same direction and generally form right angles to the fibrils in the adjacent layers (Boote, Dennis et al. 2005). In addition, to accommodate for transparency, the collagen fibrils in the cornea are monodisperse in diameter (32.2±1 nm in human (Daxer, Misof et al. 1998)) and uniformly spaced (61.9±4.5 nm, in human (Gyi, Meek et al. 1988)).

It is well established that the ultrastructure (i.e. diameter and spacing) of the collagen fibrils is mainly controlled via interaction with proteoglycans (PGs) and their associated glycosaminoglycans (GAGs) (Scott 1991). PGs are soluble macromolecules in

the ECM which are composed of a globular protein core that covalently bonds to one or more GAG chains. GAGs are long, sulphated, linear heterogeneous polysaccharides. Due to the their sulphate and carboxyl groups, GAG chains are highly negatively charged which results in the strong repulsion forces between the neighbouring molecules. It has been suggested that when associating with collagen fibrils, PGs control the diameter of the fibrils by inhibiting the lateral fusion of the fibrils (Danielson, Baribault et al. 1997; Chakravarti, Zhang et al. 2006). Similarly, the repulsion force between the GAG chains of the neighboring fibrils results in the control of the fibril-to-fibril spacing. Interestingly, it has been shown that the length of the GAG chains in the cornea is similar to the interfibrillar spacing (Scott 1995).

The effects of proteoglycans on the diameter of the collagen fibrils were also confirmed by *in vitro* studies. Several investigations showed that collagen molecules are self-assembled in the presence of PGs, both the diameter of the collagen fibrils and lateral fusion of the fibrils reduces significantly (Rada, Cornuet et al. 1993; Neame, Kay et al. 2000). These results primarily suggest that PGs are passively involved in the control of collagen fibrils ultrastructure.

In a series of experiments, primary human corneal fibroblastic cells (PHCFCs) were seeded on (a) bare polycarbonate membranes or (b) disorganized reconstituted collagen scaffold (RCS) (Guo, Hutcheon et al. 2007; Ren, Hutcheon et al. 2008). In both systems cells stratified and produced organized layers of collagen fibrils after four weeks. In the RCS system cells continued producing and maintaining a healthy construct for a period of 11 weeks. In contrast, the appearance of the collagen fibrils in the scaffold-free system started to decline significantly after 8 weeks.

Considering that the presence of the scaffold in the RCS system was the only difference between the two, it is possible that that the existence of the exogenous reconstituted collagen fibrils in the RCS system fibrils resulted in stabilization of the cell-derived ECM. One of the mechanisms that RCS could help the cells to maintain a healthy construct is by providing a source of collagen monomer which could be incorporated into newly synthesized fibrils or act as a "sink" for matrix metalloproteinase and therefore, decrease the rate of the cell synthesized ECM degradation.

The electron microscopy investigations also revealed that the reconstituted collagen fibrils in the scaffold system undergone an extensive remodeling over the period

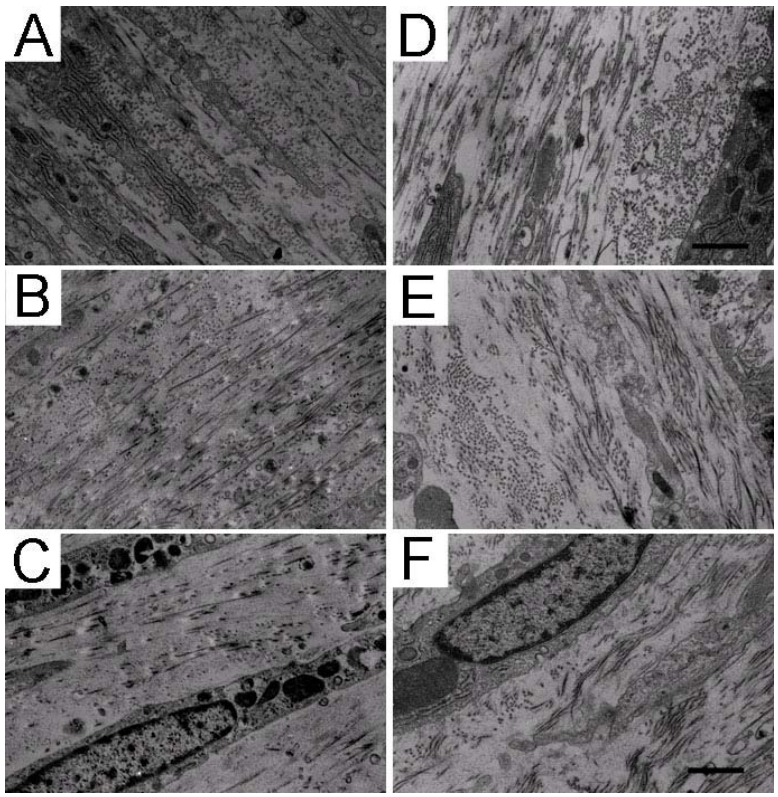

Figure 4-58: The TEM micrographs of cell-drived collagenous constructs in the scaffold-free (A-C) and RCS (D-F) systems after 4 weeks (A & D), 8 weeks (B & E), 11 weeks C, and 12 weeks (F) (Guo, Hutcheon et al. 2007; Ren, Hutcheon et al. 2008).

of 11 weeks (Figure 4-2). The QFDE micrographs show that prior to the cell seeding the RCS was composed of a dense network of large diameter fibrils (Figure 4-2A). After 4 weeks the RCS was transformed into a loose network of collagen fibrils (Figure 4-2B). More interestingly, transmission electron micrographs show that during this transformation very small diameter, satellite fibrils appear next to the large diameter RCS collagen fibrils. It is therefore possible that due to interaction with cell-synthesized macromolecules the large diameter fibrils are branched into fibrils with smaller diameters. These results point out the possibility that collagen fibrils are mutable.

In addition to this evidence from our cell culturing systems, two recent publications have also provided substantial support for the mutability properties of collagen fibrils. The studies showed that resumption of lumican synthesis by targeted expression of this PG (Du, Carlson et al. 2008) or injection of the human corneal stem cells (Meij, Carlson et al. 2007) partially restores abnormally formed collagen fibrils in the lumican knock-out mice corneas. It is therefore possible that expression of lumican in the knock-out mouse results in the recovery of the abnormal collagen fibrils. The results of these studies not only provides evidence for the mutability of the collagen fibrils but also suggest that proteoglycans could be potentially involved in the remodeling of the collagen fibrils.

Indeed the reconstituted collagen fibrils in the RCS were decorated with the cell-synthesized proteoglycans and their associated GAG chains at 4, 8 and 11 weeks and the interaction between the two appears to increase over time. Therefore, we hypothesize that collagen fibrils are mutable in which interaction with proteoglycans results in the transformation of the larger diameter fibrils into smaller fibrils. The mutability is also an

energy driven process by which the interaction with proteoglycans results in the formation of a more stable (i.e. smaller diameter) collagenous construct.

To test this hypothesis, keratin sulfate proteoglycans (KSPGs) were added to the reconstituted type I collagen fibrils. Transmission Electron (TEM) and Differential Scanning Calorimetry (DSC) techniques were used to investigate the changes in the diameter and thermal stability of the collagen fibrils as the result of interaction, respectively.

4.1. Materials and Methods

4.1.1. Sample Preparation

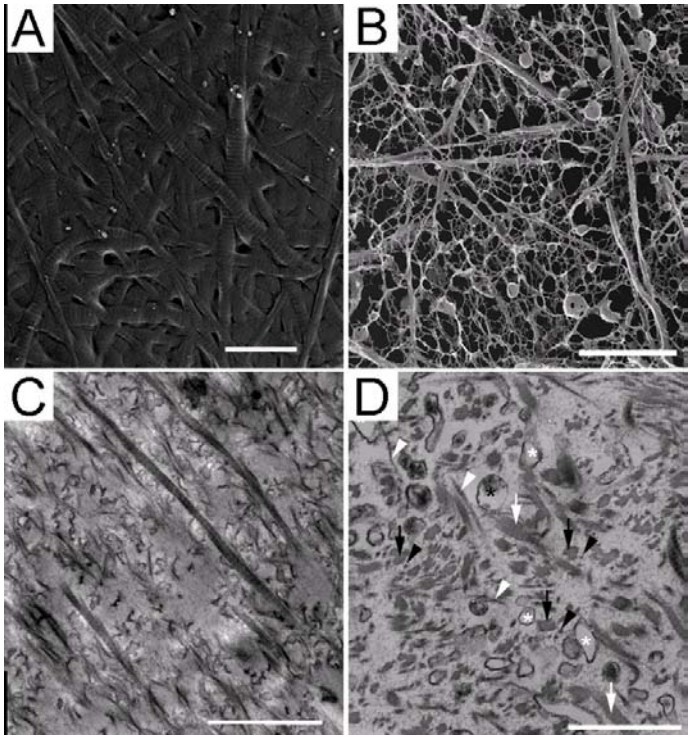

Figure 4-59: QFDE (A & B) and sTEM (C & D) images of collagen fibrils prior (A & C) and after (B & D) cell seeding. The QFDE images also show that the fibrils are densely packed prior to the cell-seeding (A and B). Note the existence of the small diameter, satellite fibrils next to the larger fibrils in (A).

The type I collagen solution (pepsin extracted from bovine dermis, Cohesion Technologies, Palo Alto, CA, 3 mg/mL) was neutralized by mixing with 10X trizma in a 9:1 ratio. The solution was kept overnight at the 37ºC-100% RH prior to the addition of KSPGs.

The KSPGs solution (extracted from bovine cornea, K0198, United States Biological, Swampscott, MA) was dispensed onto the collagen gels in the ratio of 1:15 (dry weight collagen:dry weight KSPG) and transferred back into the incubator.

4.1.2. Differential Scanning Calorimetry (DSC)

Thermal analysis was performed using a METTLER DSC822e differential scanning calorimeter (Mettler-Toledo, Columbus, OH). Approximately 20 µL collagen samples were loaded into the 40µL aluminum crucible pans, hermitically sealed and placed into the DSC chamber. After equilibration at 25ºC, temperature of the samples was ramped up to 80ºC at the rate of 10ºC/min. For each sample, an empty crucible was used as the reference point.

Data gathering and post-processing was performed using the Starre software provided with the instrument. Temperature of the denaturation (T_m) was the peak of the endotherm and the enthalpy of denaturation was the integral of the power over time between the peek's onset and endset points using a spline integration tool (Figure 4-3).

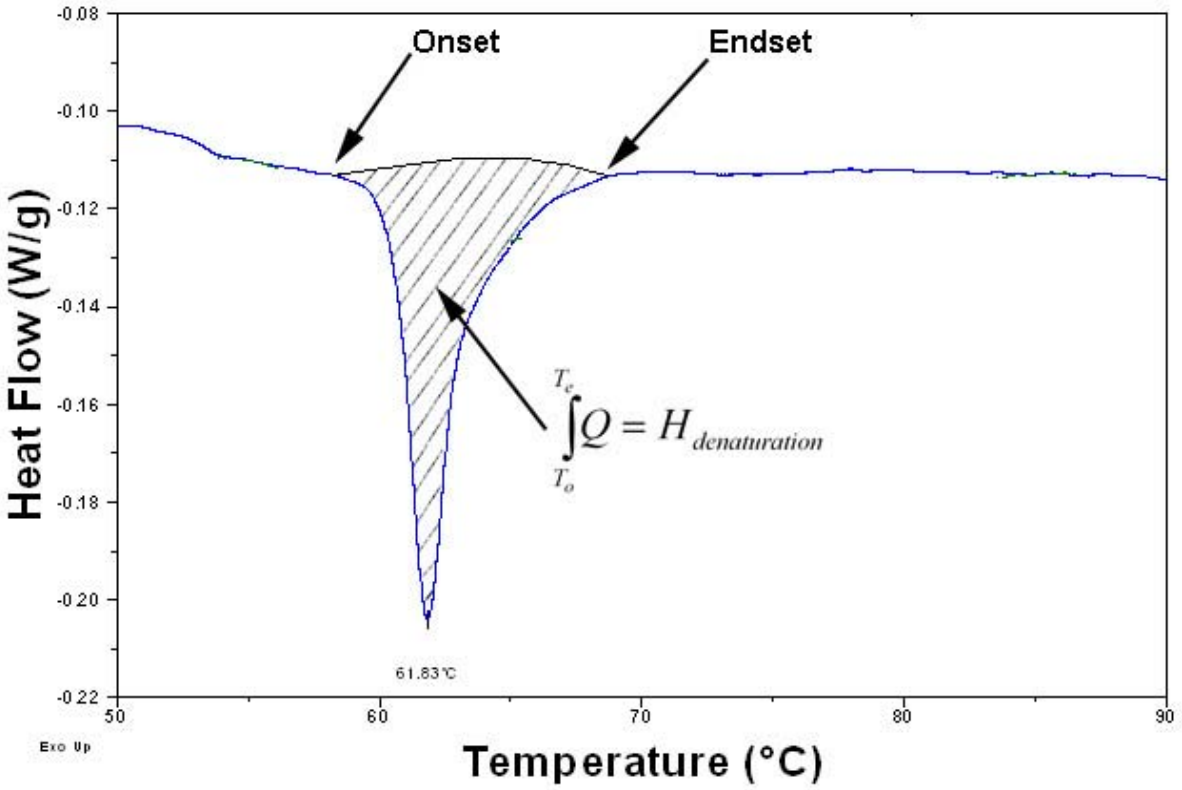

Figure 4-60: Representative DSC plots

4.1.3. Transmission Electron Microscopy (TEM)

Standard TEM and Cuprolinic blue staining TEM were used to investigate the morphology of the collagen fibrils and sulphated GAG chain-collagen interaction, respectively.

For sTEM, the constructs were fixed overnight in modified Karnovsky fixative (2.5% Glutaraldehyde, 2.5% Paraformaldehyde, 0.1M Cacodylate buffer, pH 7.2), washed twice with 0.1M buffer, post fixed in 1% osmium tetroxide in 0.1M Cacodylate buffer, and dehydrated in a graded series of ethanol. The samples were infiltrated and embedded in a mixture of Spurrs resin and Quetol according to Ellis (Ellis 2006).

For the cuprilinic blue staining, after primary fixation in 2% Paraformaldehyde, 2.5% Glutaraldehyde, and 40% Phosphate Buffer Saline (PBS) the samples were transferred into the mixture of 1% Cuprolinic blue, 0.3 M $MgCl_2$, and 2.5 % Glutaraldehyde and stained for 20-24 hr at room temperature (Gong, Freddo et al. 1992). Samples were rinsed in PBS, dehydrated and embedded in eponaraldite.

60-80nm *en face* sections were cut on an Ultracut E microtome (Reichert, Depew, NY) using a diamond knife. Thin sections were stained with 5% Uranyl acetate and Reynolds lead citrate for sTEM or saturated Uranyl Acetate for Cuprilinic blue. The sections were viewed with a JEOL JEM 1010 transmission electron microscope (JEOL, Tokyo, Japan) and images were digitally captured on an AMT XR-41B CCD camera system (Advanced Microscopy Techniques Inc., Danvers, MA).

4.2. Results

4.2.1. Calorimetry Measurements

Figure 4-4 represents the denaturation temperature ($T_{m,}$ red) and enthalpies ($\Delta H_{m,}$, blue) of the collagen fibrils in the absence and presence of the KSPGs. Although there is a minimal increase in the average value of the fibrils' denaturation temperature as a result of interaction with KSPGs, the differences are not significant. In contrast, the ΔH_m results show significant increases in the denaturation enthalpies of collagen fibrils when associated with KSPGs.

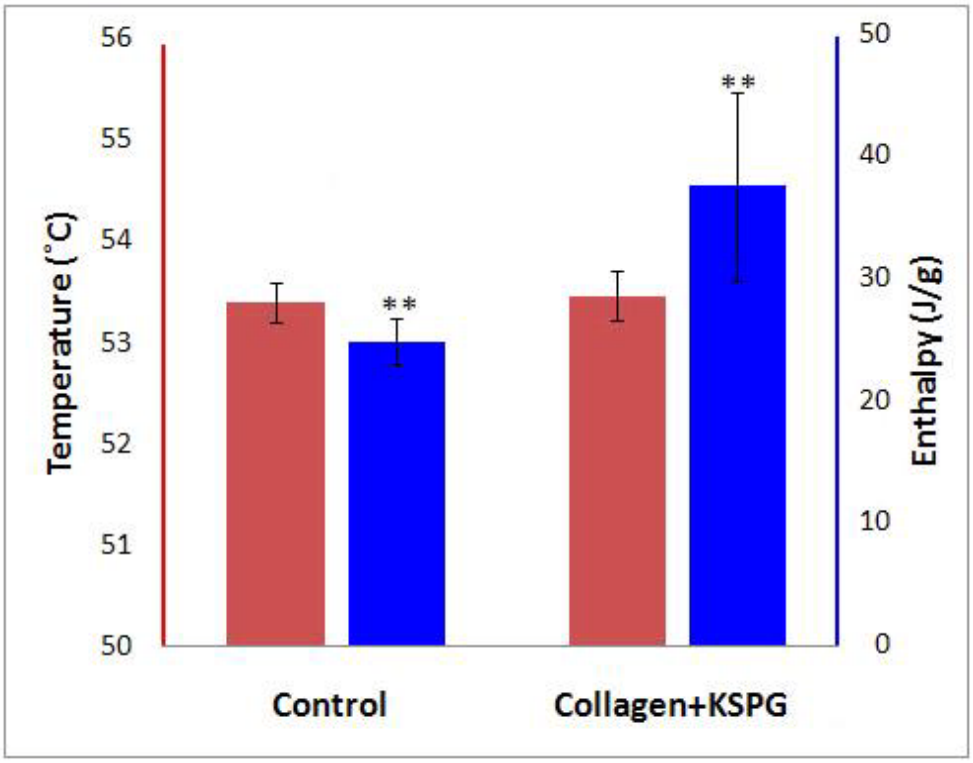

Figure 4-61: The DSC results of the denaturationtemperature (red) and enthalpy (blue) of the collagen fibrils in the absence (control) or presence (collagen+KSPG) of the proteoglycans.

4.2.2. Transmission Electron Microscopy

Figure 4-5 is representative standard TEM micrographs of the collagen fibrils in the absence (A) or and after interaction with KSPGs (B). As was discussed before, it has been shown that the proteoglycans with collagen molecules results in regulation of fibril's morphology, prevention of lateral fusion, and reduction of fibril's diameter. Indeed the TEM images show that the number of the fibrils with circular cross sections was increased by two fold in the presence of the KSPGs.

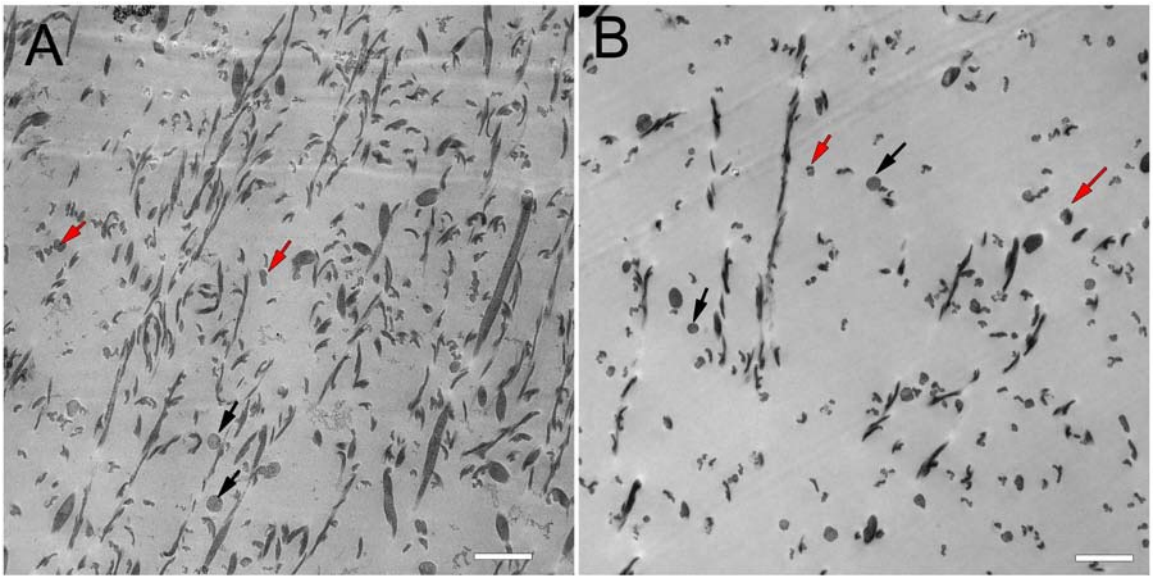

Figure 4-63: sTEM micrograph of collagen fibrils in the absence (A) and presence (B) of KSPGs. Bars are 1µm.

Collagen fibrils associated with KSPGs also had smaller diameter. Figure 4-6 shows the diameter distribution of the fibrils in the absence (red) or presence (blue) of the KSPGs. The diameter distribution of the fibrils shows a significant shift toward smaller range after interaction with KSPGs (Figure 4-6). While in the absence of KSPGs the

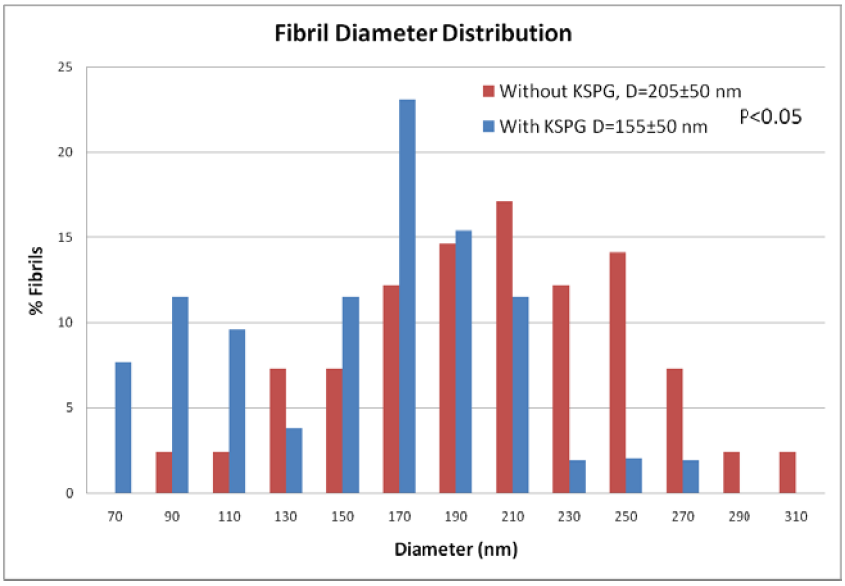

Figure 4-62: Diameter distribution of the fibrils

average diameter of the fibrils was 205 ± 50 nm, the fibrillar diameter was reduced to 155 ± 50 nm when collagen fibrils interacted with KSPGs. Therefore, addition of KSPGs to the collagen fibrils significantly reduced the diameter of the fibrils.

4.2.3. Cuplrolinic Blue Staining

The cuprolinic blue staining was performed to reveal the interaction of the collagen fibrils with the sulfated GAG chains of the proteoglycans. Figure 4-7 is composite Cuprolinic blue stained collagen fibrils in the absence (A) and presence, (B), of the KSPGs. While there is no staining in the absence of KSPGS (as expected), the Cuprolinic blue stained appears in the form of black spots along the collagen fibrils. Interestingly, more often the stain appeared in the D-band regions of the fibrils. In addition, while in the absence of the KSPGs the D-banding striations were very faint

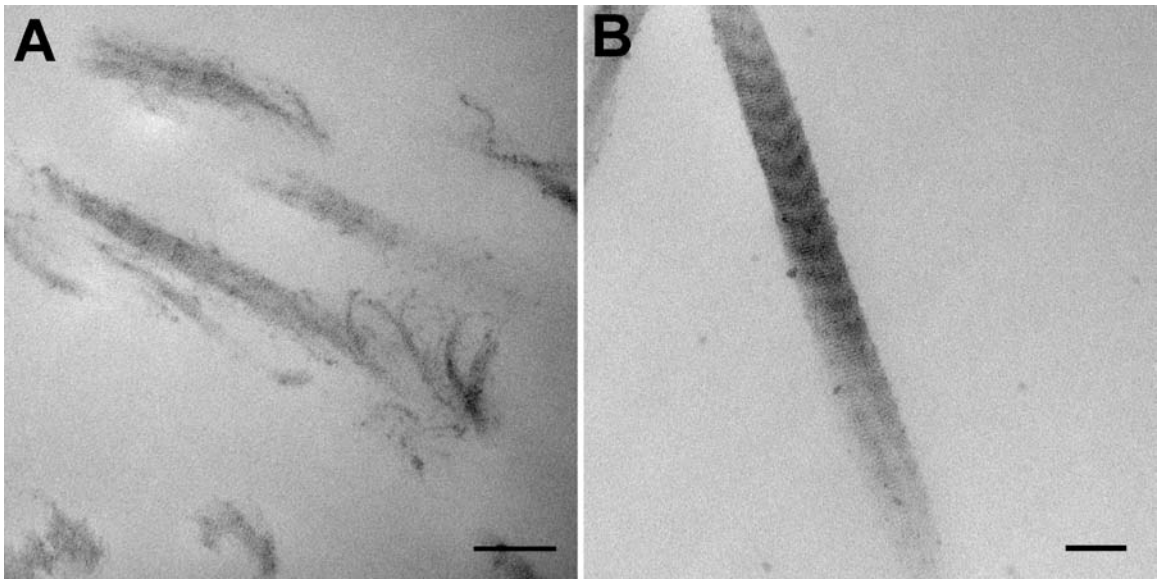

Figure 4-64: Cuprolinic blue stained collagen fibrils in the absence (A) and presence (B) of the KSPGs. Collagen fibrils associated with the proteoglycans show globular stains and have distinct D-banding patterns. Bars are 100 nm.

Figure 4-7A, after interaction with KSPGs are more distinct and significant Figure 4-7B.

It should be mentioned that when a native cornea is stained with proteoglycans the staining appears in the form of long, linear chains. In contrast, the staining in these experiments appeared in the form of small globular patterns. The native keratan sulfate proteoglycans have a molecular weight of 37,000 kDa and the KSPGs used for these experiments have a molecular weight of 13,000 kDa. Therefore less that 2/3 of the molecules size have been lost during the processing. This difference in the size of the molecules size could explain the differences between the staining patterns seen in these experiments and in the native tissues.

4.3. Discussion

Both *in vitro* and *in vivo* knock-out studies has previously shown that self-assembly of the collagen molecules in the presence of the proteoglycans results in the formation of collagen fibrils with smaller diameter, round cross-sections, and fewer number of lateral fusions. It has been suggested that due to their high negative charges, the GAG chains of the proteoglycans inhibit the lateral fusion of the fibrils resulting in the control of the fibril diameter and spacing.

These interactions however could not explain the results of two recent studies showing the recovery and remodeling of fibrils (Meij, Carlson et al. 2007; Du, Carlson et al. 2008). The results of the present investigation show, for the first time, the effects of proteoglycans on the remodeling of collagen fibrils after complete gelation. The sTEM results indicate that interaction of the proteoglycans with collagen fibrils play a similar role as the interaction with collagen molecules prior to the fibrillogenesis. Even after

fibril formation, proteoglycans and their associated glycosaminoglycans are able to reduce the diameter of collagen fibrils. Two mechanisms could potentially explain the diameter reduction of the fibrils. The first scenario is that after binding to a fibril, the interaction between the GAG chains of the neighboring PGs result in the compaction of the monomers within the fibril. In this situation the PGs act like a belt surrounding the perimeter of a fibril resulting in a smaller diameter fibril. Second scenario explains the mechanism based on the energy landscape of the molecules (Gibb's free energy). It is well established that collagen self-assembly is an energy driven process in which self-assembly spontaneously proceeds by monomers losing their surface associated molecules (e.g. water molecules). This results in reaching a lower energy landscape (i.e. lower Gibb's free energy) and therefore by incorporating into a fibril, molecules reach a more energetically stable state. The change in the Gibb's free energy of a reaction is calculated according to the Eq. 1:

$$\Delta G = \Delta H - T\Delta S \quad (1)$$

Where, T is the temperature of the reaction, ΔG, ΔH, and ΔS are the changes in Gibb's free energy, enthalpy, and entropy of self-assembly, respectively. For collagen self-assembly the changes in the enthalpy and entropy are +56 $kcal/mol$ and +220 $cal/K.mol$ (Kadler, Hojima et al. 1987) . Therefore, the changes in the Gibb's free energy of the molecule's during the self-assembly at 37ºC is -13 $kcal/mol$. The negative sign of the ΔG shows that the molecules loose free energy by incorporating into a fibril (i.e. they have less available energy) and thus, they are more stable.

It is also possible that depending on the lateral and longitudinal arrangements of the molecules within a fibril there are several low energy states available to the monomers (Figure 4-8).

In the absence of proteoglycans the molecules could organize such that they fall in one of the intermediate energy states and not necessary the lowest energy possible. Association with proteoglycans however causes the whole system of collagen fibril-proteoglycan to become unstable (one of the peaks in the Figure 4-7). Instability of a fibril would result in the loss of monomers from the periphery of the fibril and reduction of the fibril's diameter. The loss of molecules will continue until the system of collagen-PG reach a stable state, possibly, the lowest energy state. Unfortunately, the transmission electron microscopy does not have enough resolution to provide any information on the number of collagen molecules in the cross section of the fibrils.

However, if this hypothesis is correct and interaction of the proteoglycans with collagen results in a change to a lower energy state, the collagen-PGs matrix should be also more stable. Indeed, the calorimetry data showed that when exposed to proteoglycans, collagen fibrils have higher denaturation enthalpy which is an indication of more stable fibrils.

Considering the geometry of a KSPG's protein core, horseshoe shape with 2.5nm opening, which is in the same range as a single collagen molecule it seems unlikely that a proteoglycan could act as a belt and compact all the monomers within a fibril. It is more probable that a PG molecule binds a single collagen molecule within a fibril and destabilizes the fibril. This scenario which is in agreement with the data presented in this

study could explain the mutability of the collagen fibrils as the result of the interactions with proteoglycans.

Conclusion

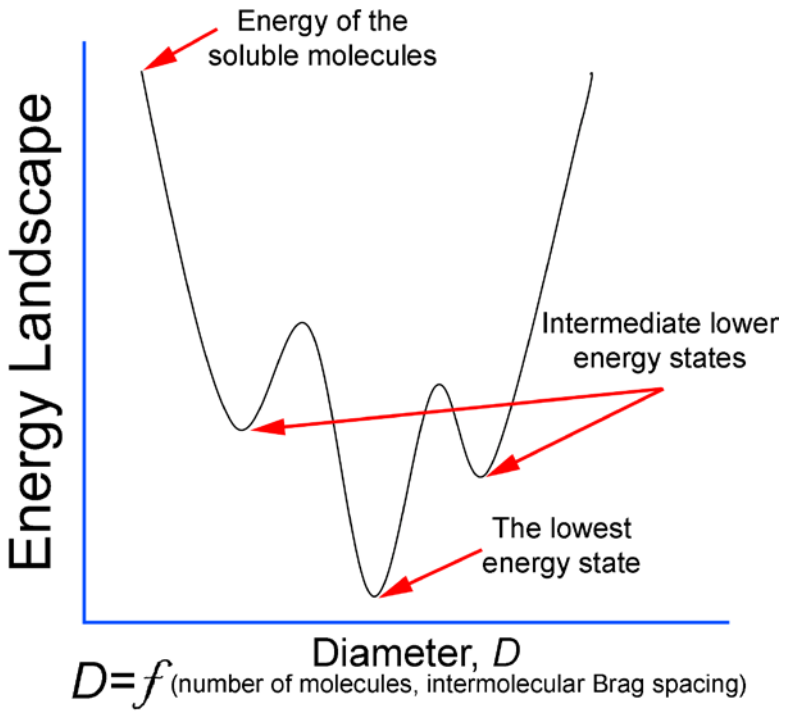

Figure 4-65: Schematic of the energy states of a collagen molecule

This investigation provides the first evidence for the mutability of the collagen fibrils as the result of interaction with proteoglycans. This is a novel concept that could potentially explain many of the reactions seen in the ECM, including the recovery of the collagen fibrils in the knock-out mice corneas following seeding with stem cells (Meij, Carlson et al. 2007; Du, Carlson et al. 2008). This concept changes the mindset that the ECM and ECM macromolecules are passive and the interactions are only facilitated directly guided by the resident cells. In contrast, collagen molecules are actively interacting with the other macromolecules (e.g. PGs) based on physiochemical principals.

The system is thus potentially dynamic. The goal of the ECM molecules is to control the morphology of the local collagen network to suit the needs of the resident cell population. This could be done by making the desired state of the collagen fibrils, the lowest possible energy state. The proteoglycans may help to "set" the lowest energy state to a particular fibril diameter via their specific collagen interaction. Further investigation is required to study the potential involvement of the other ECM macromolecules (e.g. fibronectin, and other types of collagen) in the process.

References

Boote, C., S. Dennis, et al. (2005). "Lamellar orientation in human cornea in relation to mechanical properties." J Struct Biol **149**(1): 1-6.

Chakravarti, S., G. Zhang, et al. (2006). "Collagen fibril assembly during postnatal development and dysfunctional regulation in the lumican-deficient murine cornea." Dev Dyn **235**(9): 2493-506.

Danielson, K. G., H. Baribault, et al. (1997). "Targeted disruption of decorin leads to abnormal collagen fibril morphology and skin fragility." J Cell Biol **136**(3): 729-43.

Daxer, A., K. Misof, et al. (1998). "Collagen fibrils in the human corneal stroma: structure and aging." Invest Ophthalmol Vis Sci **39**(3): 644-8.

Du, Y., E. C. Carlson, et al. (2008). "Rescue of the Stromal Phenotype in Lumican Null Mice by Human Corneal Stem Cell Transplantation." Invest. Ophthalmol. Vis. Sci. **49**(5): 4522-.

Ellis, E. A. (2006). "Solutions to the Problem of Substitution of ERL 4221 for Vinyl Cyclohexene Dioxide in Spurr Low Viscosity Embedding Formulations." Microscopy Today **14**(4): 32.

Gong, H., T. F. Freddo, et al. (1992). "Age-related changes of sulfated proteoglycans in the normal human trabecular meshwork." Experimental Eye Research **55**(5): 691-709.

Guo, X., A. E. Hutcheon, et al. (2007). "Morphologic characterization of organized extracellular matrix deposition by ascorbic acid-stimulated human corneal fibroblasts." Invest Ophthalmol Vis Sci **48**(9): 4050-60.

Gyi, T. J., K. M. Meek, et al. (1988). "Collagen interfibrillar distances in corneal stroma using synchrotron X-ray diffraction: a species study." International Journal of Biological Macromolecules **10**(5): 265-269.

Kadler, K. E., Y. Hojima, et al. (1987). "Assembly of collagen fibrils de novo by cleavage of the type I pC-collagen with procollagen C-proteinase. Assay of critical concentration demonstrates that collagen self-assembly is a classical example of an entropy-driven process." J Biol Chem **262**(32): 15696-701.

Maurice, D. M. (1957). "The structure and transparency of the cornea." J Physiol **136**(2): 263-86.

Meij, J. T., E. C. Carlson, et al. (2007). "Targeted expression of a lumican transgene rescues corneal deficiencies in lumican-null mice." Mol Vis **13**: 2012-8.

Neame, P. J., C. J. Kay, et al. (2000). "Independent modulation of collagen fibrillogenesis by decorin and lumican." Cell Mol Life Sci **57**(5): 859-63.

Rada, J. A., P. K. Cornuet, et al. (1993). "Regulation of corneal collagen fibrillogenesis in vitro by corneal proteoglycan (lumican and decorin) core proteins." Exp Eye Res **56**(6): 635-48.

Ren, R., A. E. Hutcheon, et al. (2008). "Human primary corneal fibroblasts synthesize and deposit proteoglycans in long-term 3-D cultures." Dev Dyn **237**(10): 2705-15.

Scott, J. E. (1991). "Proteoglycan: collagen interactions and corneal ultrastructure." Biochem Soc Trans **19**(4): 877-81.

Scott, J. E. (1995). "Extracellular matrix, supramolecular organisation and shape." J Anat **187 (Pt 2)**(Pt 2): 259-69.

Chapter 5

Conclusions

Collagen is the main structural component of vertebrates and fibril forming collagens provide structural integrity to the metazoans. They are the building blocks of the load-bearing tissues and are essential to their functions. Each year millions of injuries result in need for tissue replacement. In 2002 alone, 200,000 cases of reconstructive ligament surgery were performed in the United Stated which cost more than five billion dollars. In the same year 232,000 cases of Achilles tendon injuries were reported in the United States among which one quarter required surgery. Given the lack of enough donors (in 1999 only 20,000 people became tissue donor in USA), tissues engineering of the load-bearing organs has attracted significant attention in the last few decades. Collagen fibrils in the ECM of the load-bearing tissues are highly organized, providing them the necessary mechanical strength. Therefore to tissue engineer these organs, it is required to find methods to either directly organize collagen fibrils or find ways to guide to produce organized ECMs. Although extensive research has been focused on this topic there is still a little success in organizing collagen fibrils.

The goal of this Ph.D. research was to gain control over the organization and morphology of the self-assembling collagen fibrils. Several different methods were employed to produce aligned arrays of collagen fibrils. Shear induced self-assembly was the first method used for these investigations. During self-assembly collagen molecules

were exposed to the hydrodynamic shear stress produced in a microchamber. During this process the real-time dynamics of collagen assembly was also investigated. The results of this investigation indicate that shear-influenced collagen fibrils are relatively aligned in the flow direction. There is however a complex relationship between the alignment of the fibrils and shear rate. At very high shear rates fibrils are short and curly and at low shear rates the flow not is not strong enough to influence the organization of the collagen fibrils. In addition, the reversal growth of the fibril (i.e. hooks) reduces the strength of the alignment. Spin coating is another method that was used to organize collagen fibrils in shear flow. The advantage of this method over the pure shear flow in a microchamber is that the collagen molecules are confined in a thin film very close to the glass surface. This provides an opportunity to more greatly influence the alignment of the fibrils by reducing the ability of the fibrils to sample space in the z-direction. The collagen fibrils self-assembled using this method had the same characteristic as the fibrils assembled in a microchamber. Fibrils showed the reversal growth features similar to fibrils in the shear flow. In addition, in neither of the methods did the fibrils exhibit the D-banding patterns characteristics of native collagen fibrils. Therefore, the shear-influenced self-assembly data indicate that despite the capacity of this method in aligning collagen fibrils to a good degree, it not a suitable method to produce organizations similar to the ones seen *in vivo* which suggests that different methods should be pursued.

It has been shown that at high concentrations collagen molecules exhibit self-organizing behavior. This phenomenon, which is known as liquid crystalline, has been previously investigated in both molecular and fibrillar levels. The goal of the third chapter of this thesis was to investigate the organization of collagen fibrils self-assembled

at high concentrations and develop method to control and influence the organization. The effects of the parameters like concentration, confinement geometry, ionic strength, time, and auxiliary macromolecules on the organization of the resulting fibrils were investigated. The results of this investigation revealed that despite the previous belief, collagen fibrils formed under these conditions are capable of producing long range planar organizations in the form of highly aligned stacks. More interestingly, the fibrils in the adjacent layers showed a change in direction which was similar to the patterns seen in tissues like cornea or anulus fibrosus. Concentration appeared to have a strong influence on the fibrils. At higher ranges of concentration (~350 mg/ml) collagen fibrils are highly aligned with alternating direction in the adjacent layers. In the lower ranges of concentration fibrils still exhibit the long range organizations but individual fibrils adopt a wavy structure. The confining geometry also played a significant role on the global organization of the fibrils. In the thick samples (~250 microns) the persistence length of organization is very short. Decreasing the thickness (100 microns) resulted in increasing the persistence length to the order of millimeter square. In these investigations no clear relationship between the thickness and number of the layers was found. These results indicate that the information necessary to produce organized lamellae of the collagen fibrils is encoded within the structure of a single collagen molecule.

In the first two chapters the effects of physiochemical conditions on the organization of the collagen fibrils were investigated. *In vivo,* collagen molecules closely interact with other ECM macromolecules like proteoglycans. These interactions have been shown to strongly influence and control the morphology of the collagen fibrils and the ultrastructure of the ECM. These investigations suggest that the interactions are

necessary prior or during collagen fibrillogenesis. There is mounting evidences however that these interactions could take place even after fibril formation and influence the morphology of the fibrils. The goal of the last chapter of this thesis is to investigate the mutability of the collagen fibrils in interaction with proteglycans. The morphological studies of collagen fibrils after interactions with Keratan sulfate proteoglycans (KSPGs) revealed that the KSPGs are capable of reducing the diameter of fully formed collagen fibrils. The calotrimetric measurements also showed that the fibrils are more thermally stable as the result of these PG interactions. These results suggest that collagen fibrils form a dynamic system in which the interaction with proteoglycans would result in the remodeling of the fibrils in order to reach a lower energy state. This is a very enabling concept which enables us to better understand the interactions that occur in ECM and also to produce more stable collagenous matrices.

The idea that the triple helix in atelo-collagen carries both short-range and long-range structural information is both simplifying and empowering. It is simplifying because it changes conceptually the idea that fibroblasts need to "stitch together" complex, highly-organized 2-D+ structures like the cornea. Instead, they would merely need to confine and concentrate collagen monomer while providing low-energy directional cues (which could be active cell attachments to the matrix, filipodia or merely the high aspect ratio "spindle" shape fibroblasts typically employ). It is also empowering because engineers may now be able to envision new ways to produce organized collagenous tissues and scaffoldings which do not entail the use of millions of intelligent, mobile, ~20 micron diameter, collagen extrusion machines operating independently. In

short, if the collagen is a “cooperative” structural material, engineers (and fibroblasts) can more easily exert control over its behavior and ultimately, its final structure.